COLLÈGE DE FRANCE
1530

Chaire de Physique
de la Matière Condensée
Antoine Georges

Fermions en interaction: Introduction à la théorie de Champ Moyen Dynamique(DMFT)

Cours 6

La transition de Mott selon la théorie de champ moyen dynamique

Cycle 2018-2019
11 juin 2019

COLLÈGE DE FRANCE
1530

Chaire de Physique
de la Matière Condensée
Antoine Georges

Interacting Fermions: Introduction to Dynamical Mean-Field Theory (DMFT)

Lecture 6

The Mott transition: a DMFT perspective

Slides will be in English

Please don't hesitate to ask questions in French or English

2018-2019 Lectures
June 11, 2019

Today's seminar (11:30)

Olivier Parcollet

CCQ-Flatiron Institute, Simons Foundation, New York

and Institut de Physique Théorique - CEA Saclay

Unifying spin-fluctuations and DMFT:

TRILEX and vertex-based approaches

Mini-Workshop: 14:00-18:30

14:00-14:45 Manuel Zingl (CCQ, Flatiron Institute). ***Recent insights on Sr_2RuO_4: High-resolution photoemission and Hall effect***

14:45-15:30 Jernej Mravlje (Jožef Stefan Institute, Ljubljana). ***Hund's metals: overview, NRG insights, and the role of spin-orbit coupling***

15:30-16:15 Hugo Strand (CCQ, Flatiron Institute). ***Magnetic response of a Hund's metal within DMFT: Sr_2RuO_4***

16:15-17:00 Break

17:00-17:45 Alessandro Toschi (IFP – TU Wien). ***Fluctuation diagnostics of many-electron systems: how to read between the lines of single-particle spectra***

17:45-18:30 Leonid Pourovskii (CPHT, Ecole Polytechnique and Collège de France). ***A DMFT insight into the Earth's core: many-electron effects in iron under extreme conditions***

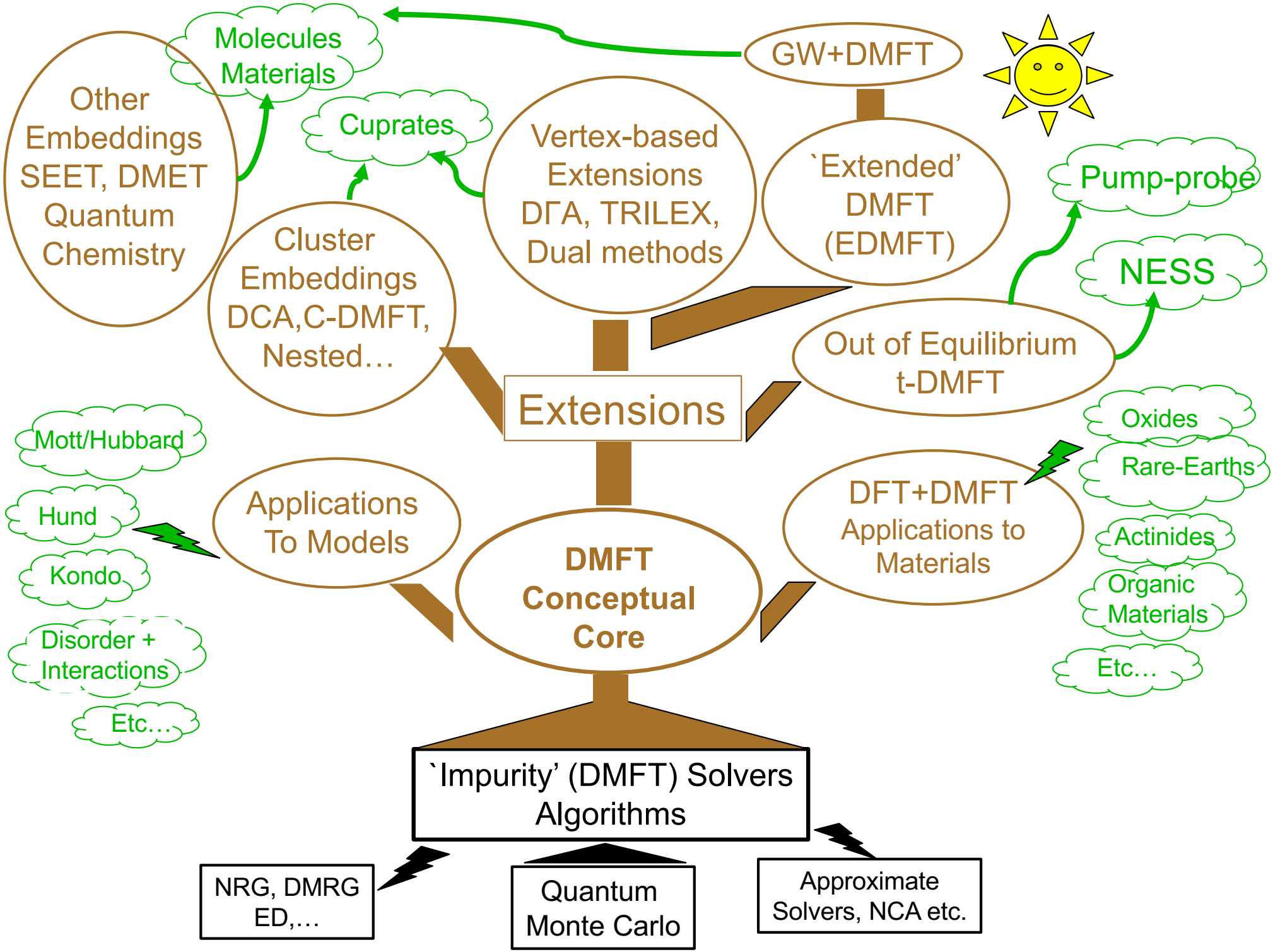
Molecules
Materials
GW+DMFT
Other
Embeddings
SEET, DMET
Quantum
Chemistry
Cuprates
Vertex-based
Extensions
DΓA, TRILEX,
Dual methods
`Extended'
DMFT
(EDMFT)
Pump-probe
NESS
Cluster
Embeddings
DCA,C-DMFT,
Nested…
Out of Equilibrium
t-DMFT
Extensions
Mott/Hubbard
Hund
Kondo
Disorder +
Interactions
Etc…
Applications
To Models
DMFT
Conceptual
Core
DFT+DMFT
Applications to
Materials
Oxides
Rare-Earths
Actinides
Organic
Materials
Etc…
`Impurity' (DMFT) Solvers
Algorithms
NRG, DMRG
ED,…
Quantum
Monte Carlo
Approximate
Solvers, NCA etc.

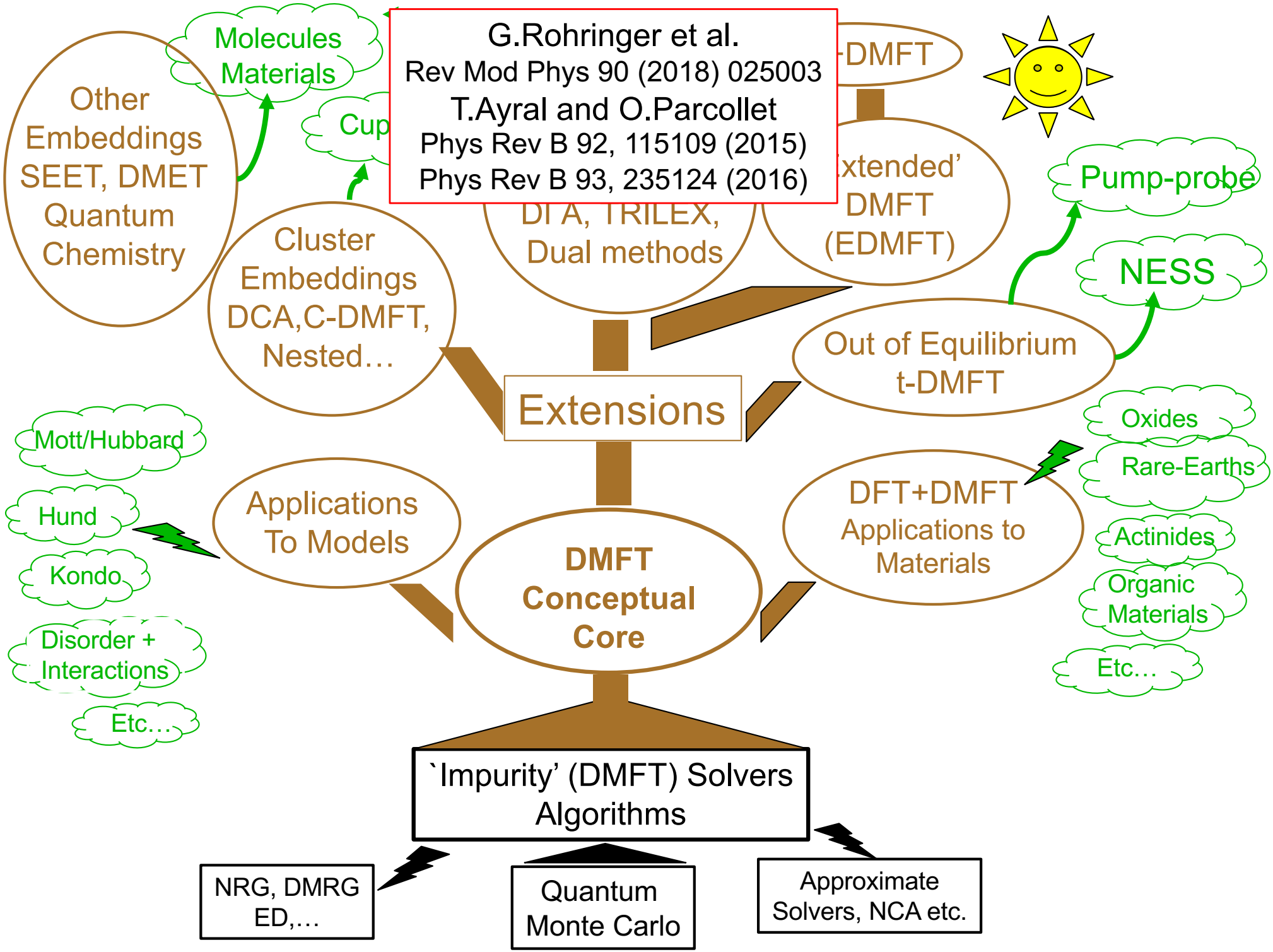
G.Rohringer et al.
Rev Mod Phys 90 (2018) 025003
T.Ayral and O.Parcollet
Phys Rev B 92, 115109 (2015)
Phys Rev B 93, 235124 (2016)
Molecules
Materials
Other
Embeddings
SEET, DMET
Quantum
Chemistry
Cluster
Embeddings
DCA,C-DMFT,
Nested…
DFA, TRILEX,
Dual methods
'Extended'
DMFT
(EDMFT)
Pump-probe
NESS
Out of Equilibrium
t-DMFT
Extensions
Mott/Hubbard
Hund
Kondo
Disorder +
Interactions
Etc…
Applications
To Models
DMFT
Conceptual
Core
DFT+DMFT
Applications to
Materials
Oxides
Rare-Earths
Actinides
Organic
Materials
Etc…
`Impurity' (DMFT) Solvers
Algorithms
NRG, DMRG
ED,…
Quantum
Monte Carlo
Approximate
Solvers, NCA etc.

Crossovers for Hubbard ½ filled, cubic lattice

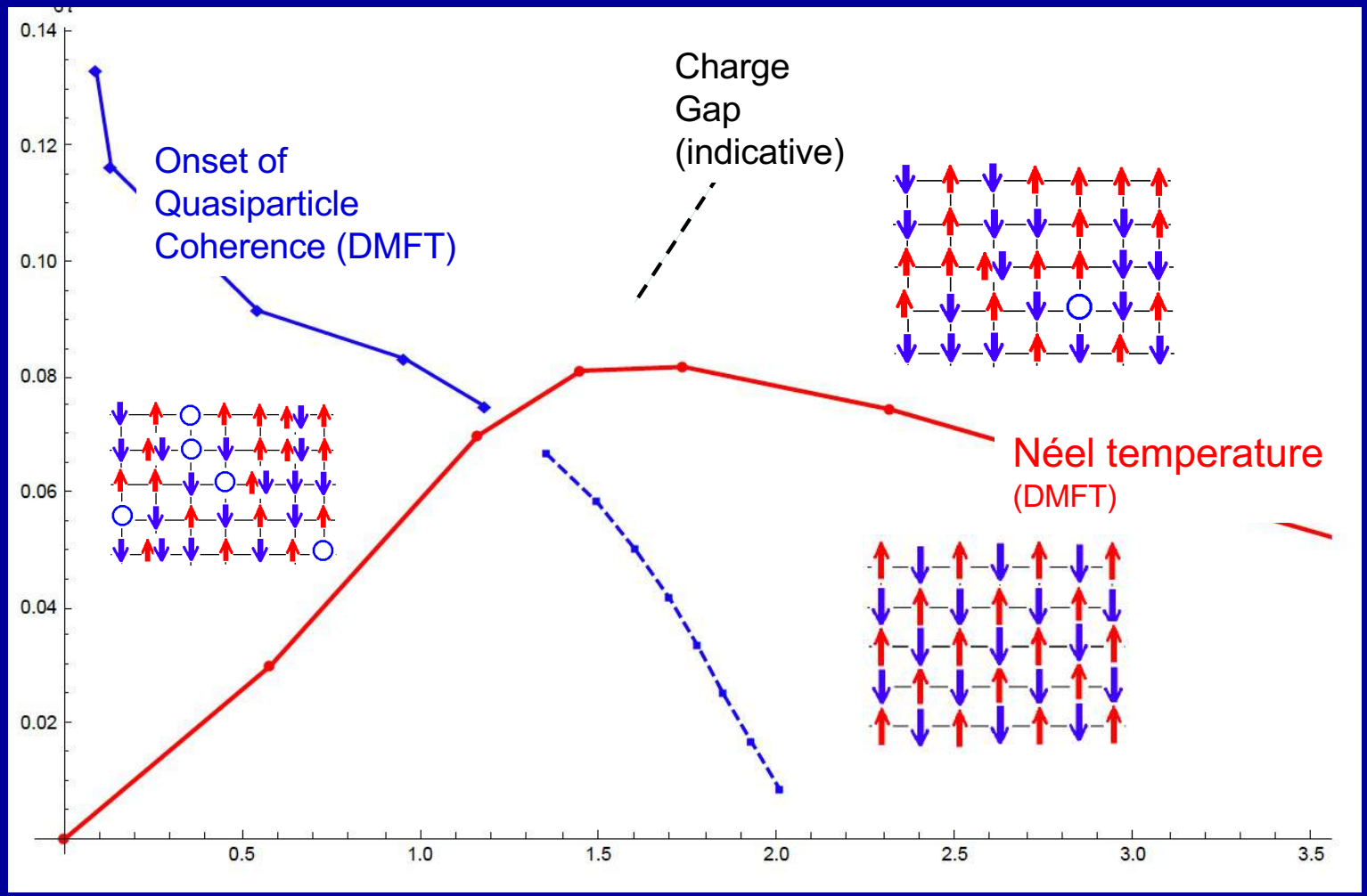

Data for onset of quasiparticle coherence: courtesy Alfred Kirsch

Hence, 6 distinct regimes:

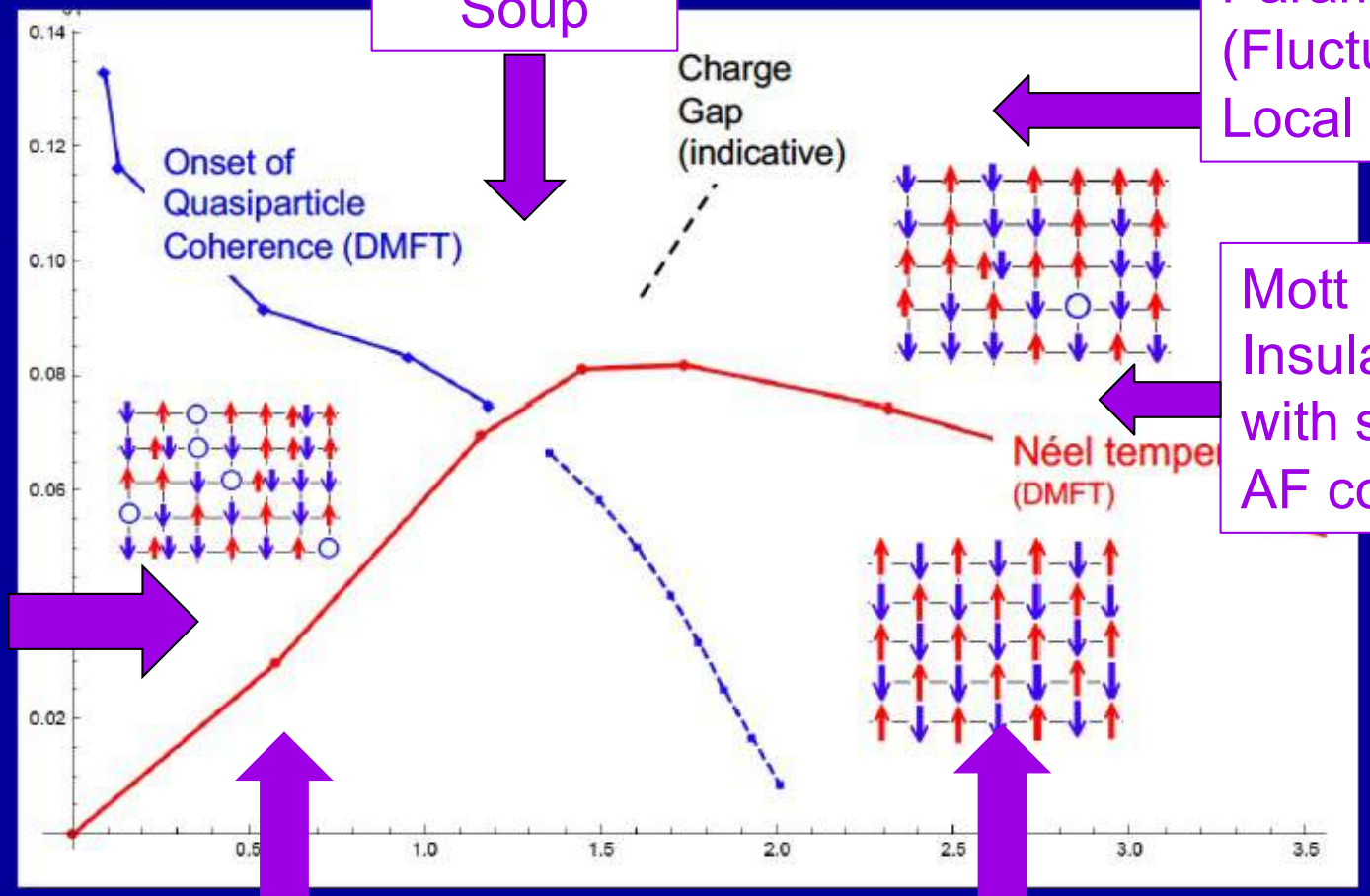

Incoherent Soup

Mott Insulating Paramagnet (Fluctuating Local Moments)

Mott Insulator with short-range AF correlations

~ Fermi Liquid

~ Slater AF

~ Heisenberg AF Ordered Mott Insulator

Frustrating Magnetic Ordering:
Revealing the `genuine' Mott phenomenon

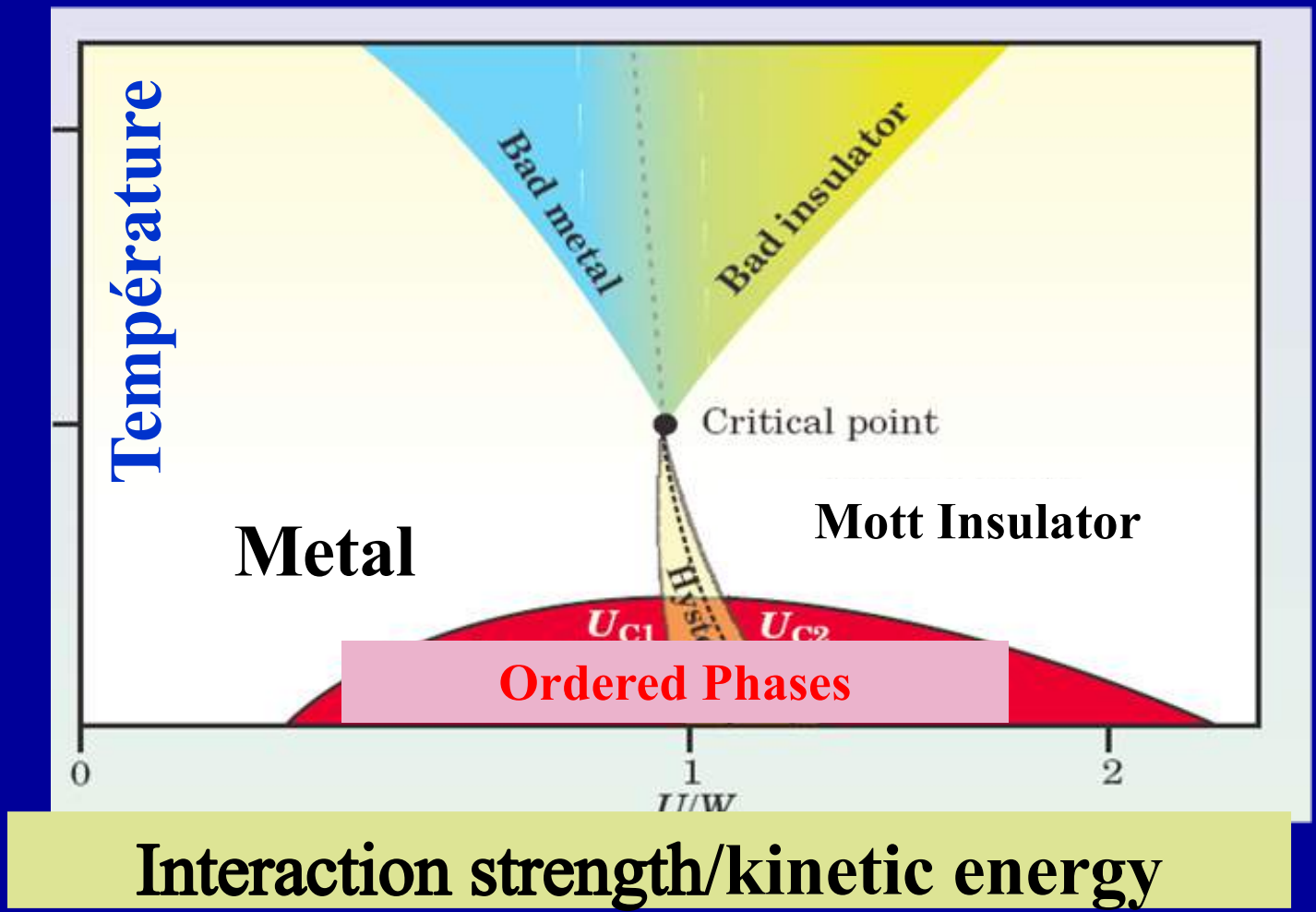

Revealing the `genuine' Mott phenomenon

- Frustrating magnetic ordering (cf. board)
- The basic equations:

$$\boxed{G \;=\; G_{\rm imp}[\Delta] \;\;,\;\; \Delta = t^2\, G} \;\;,\;\; (D = 2t)$$

- NB: General lattice: $\Delta[G] = R[G] - 1/G$
- Do these equations have a solution and if so, is it unique ?
- How does the physical nature of this solution change as U/D, T/D is varied ?

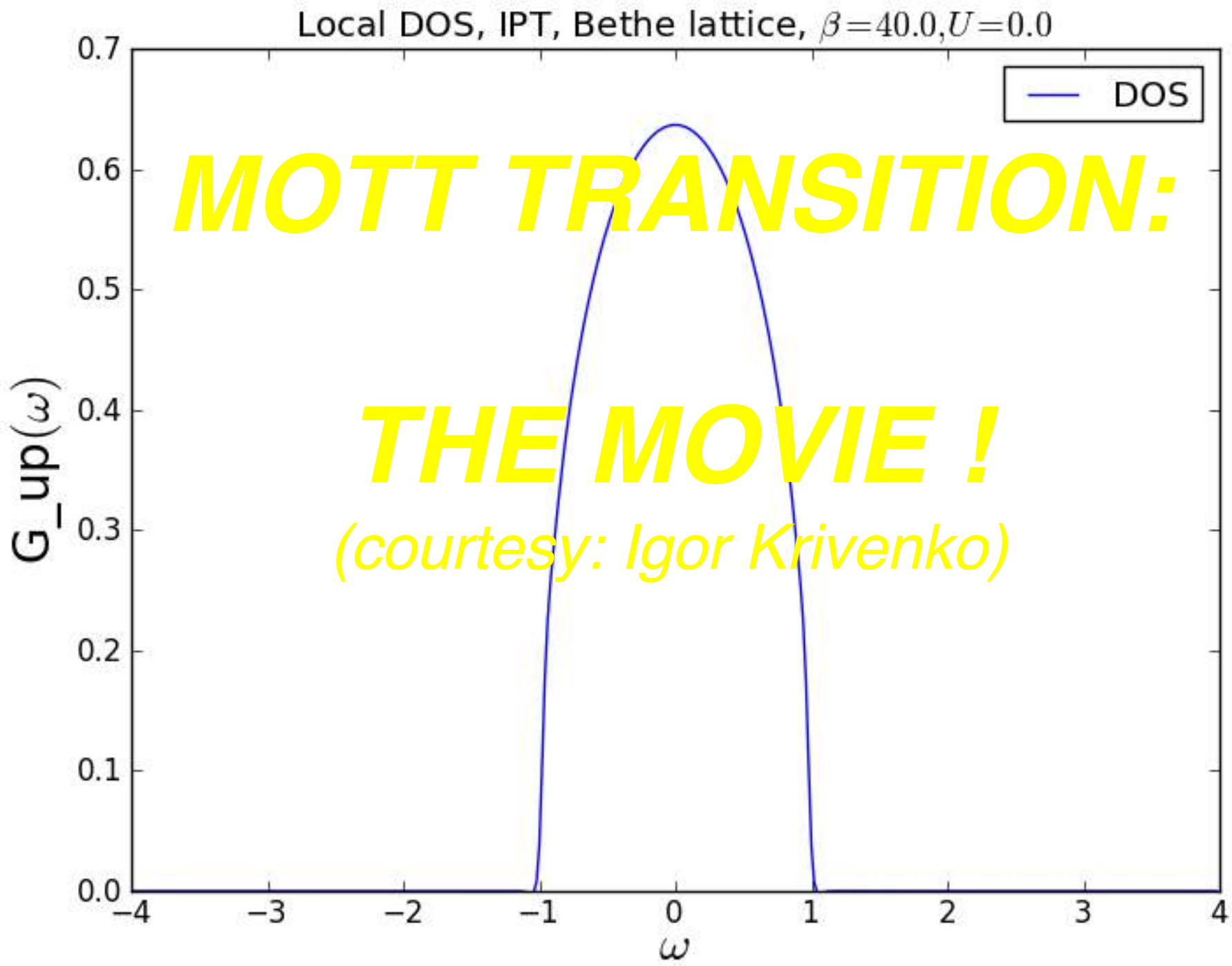

MOTT TRANSITION:

THE MOVIE !

(courtesy: Igor Krivenko)

The movie just shown was obtained with an approximate solver:

Iterated Perturbation Theory (IPT)

- explain on board –

but is qualitatively consistent with exact numerical solvers (QMC, Wilson NRG)

The IPT approximation (G.Kotliar &AG, 1992)

(~ simplest approximate solver)

Motivated by regularity of perturbation theory in U for the AIM

Integral equation easily solved iteratively w/ FFTs

EXACT (at ½ filling for U=0 and in the atomic limit !

IPT approximate solver: $\Sigma(\tau) \simeq U^2 \mathcal{G}_0(\tau)^3$

Iteration scheme: $\mathcal{G}_0 \rightarrow$ $\Sigma(\tau) \simeq U^2 \mathcal{G}_0(\tau)^3$ solver

Dyson

$G(i\omega_n)^{-1} = \mathcal{G}_0^{-1}(i\omega_n) - \Sigma(i\omega_n)$

$\mathcal{G}_{0,\mathrm{new}}^{-1} = i\omega_n - t^2 G(i\omega_n)$ self-consistency

Iterated perturbation theory: a simple DMFT solver

Introduction

IPT solver

We start by writing an IPT solver that implements the weak-coupling perturbation theory for a symmetric single-band Anderson model. All Green's functions in the calculations have just one index because *up* and *down* components are the same.

```
from pytriqs.gf.local import *

class IPTSolver:

    def __init__(self, **params):

        self.U = params['U']
        self.beta = params['beta']

        # Matsubara frequency
        self.g_iw = GfImFreq(indices=[0], beta=self.beta)
        self.g0_iw = self.g_iw.copy()
        self.sigma_iw = self.g_iw.copy()

        # Imaginary time
        self.g0_tau = GfImTime(indices=[0], beta = self.beta)
        self.sigma_tau = self.g0_tau.copy()

    def solve(self):

        self.g0_tau << InverseFourier(self.g0_iw)
        self.sigma_tau << (self.U**2) * self.g0_tau * self.g0_tau * self.g0_tau
        self.sigma_iw << Fourier(self.sigma_tau)

        # Dyson equation to get G
        self.g_iw << inverse(inverse(self.g0_iw) - self.sigma_iw)

 ---Output:---
```

An early success of DMFT (1992-1999)
Complete theory of the Mott transition

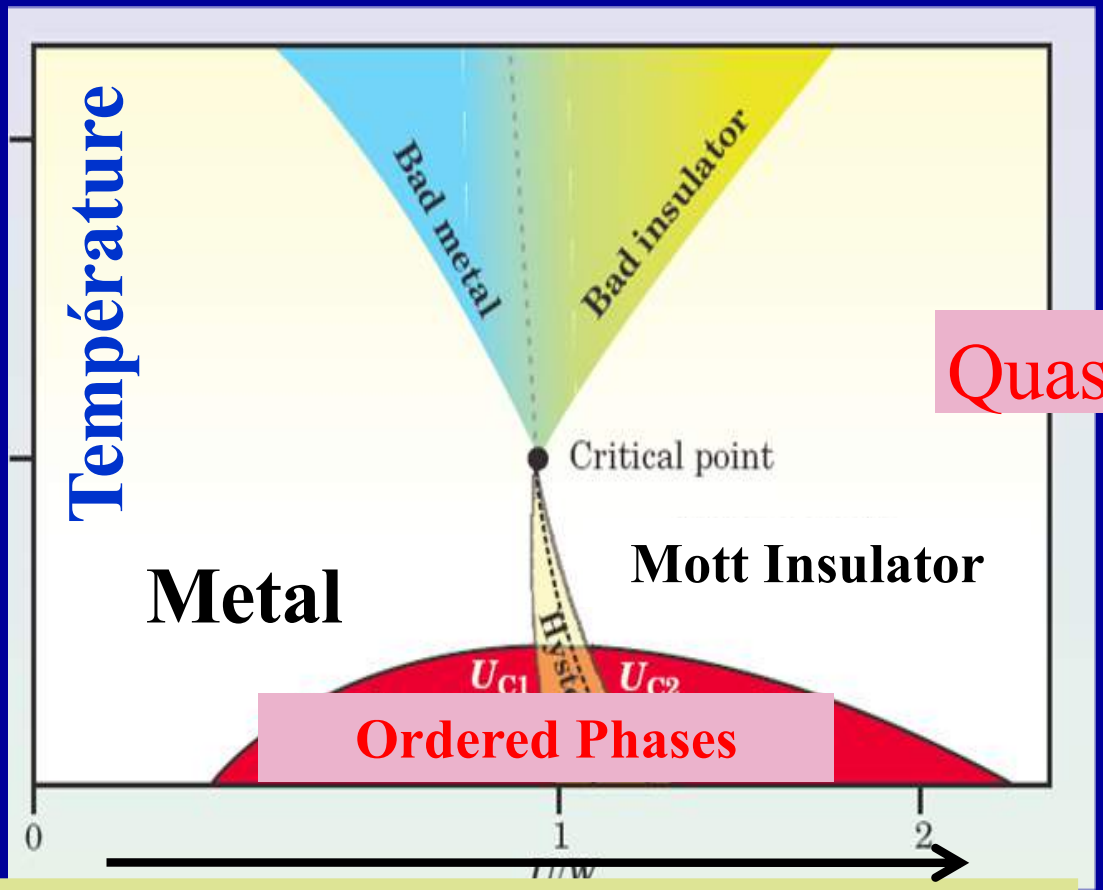

Quasiparticles

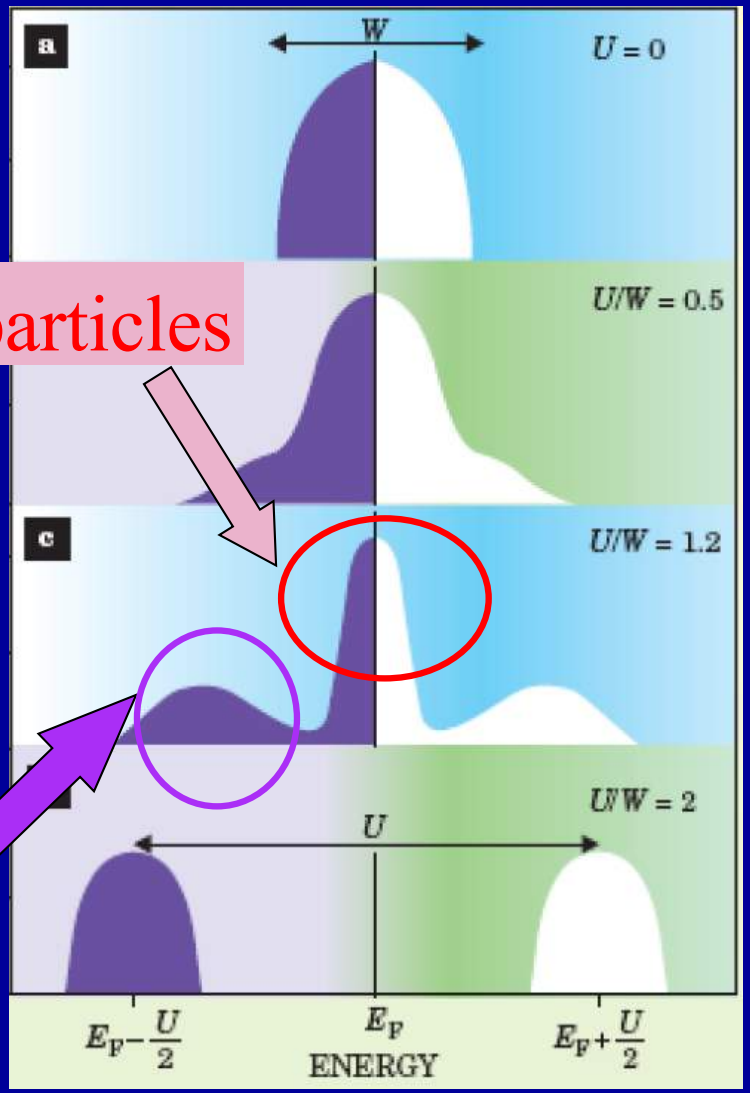

Quasi atomic excitations

Phase diagram : zoom on paramagnetic solutions

Hubbard model, Bethe lattice, homog. phase, $n = 1$, e.g., DMFT(QMC)

[Blümer '02]

Unit:
Bandwidth

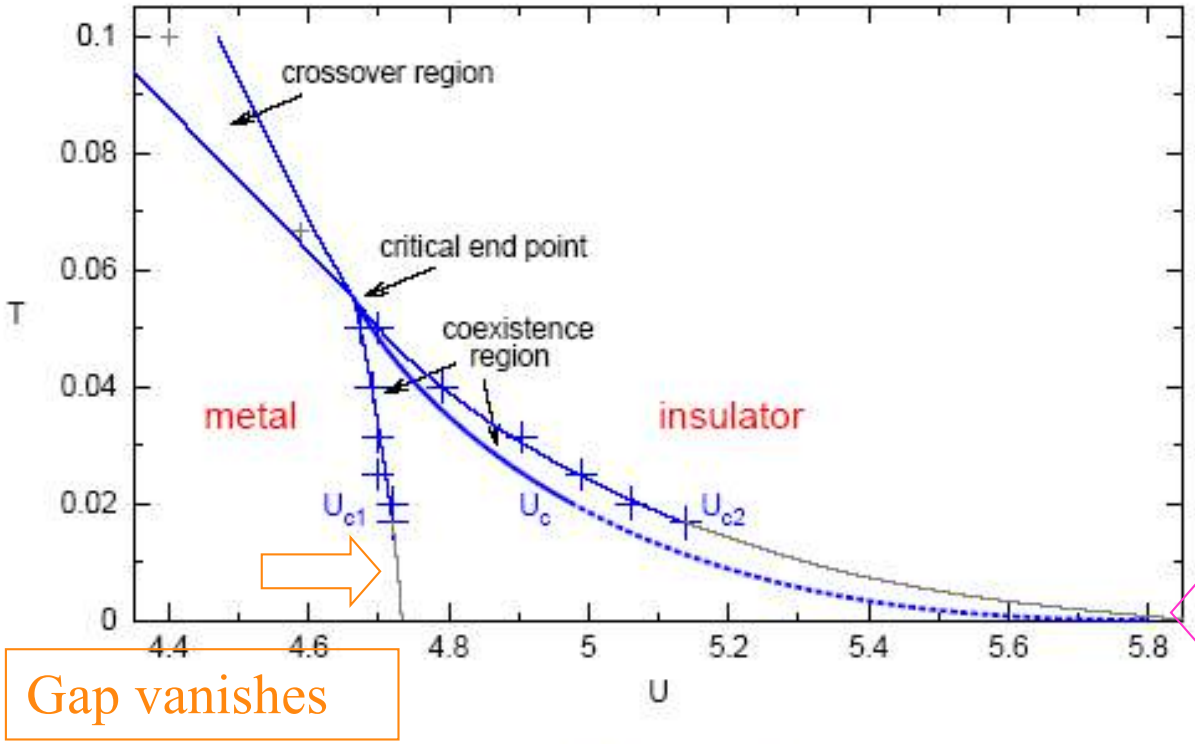

Gap vanishes

Coherence
scale vanishes

- coexistence region $[U_{c1}; U_{c2}]$, first-order transition
- crossover above critical region

57

Blümer et al. Units here are 4D=2*bandwidth

Low-frequency behavior of $\Delta(\omega)$ determines nature of the phase

- $\Delta(\omega \to 0)$ finite → local moment is screened. `Self-consistent' Kondo effect. Gapless metallic state.

- $\Delta(\omega)$ gapped → no Kondo effect, degenerate ground-state, insulator with local moments

Self-consistent structure of the bath

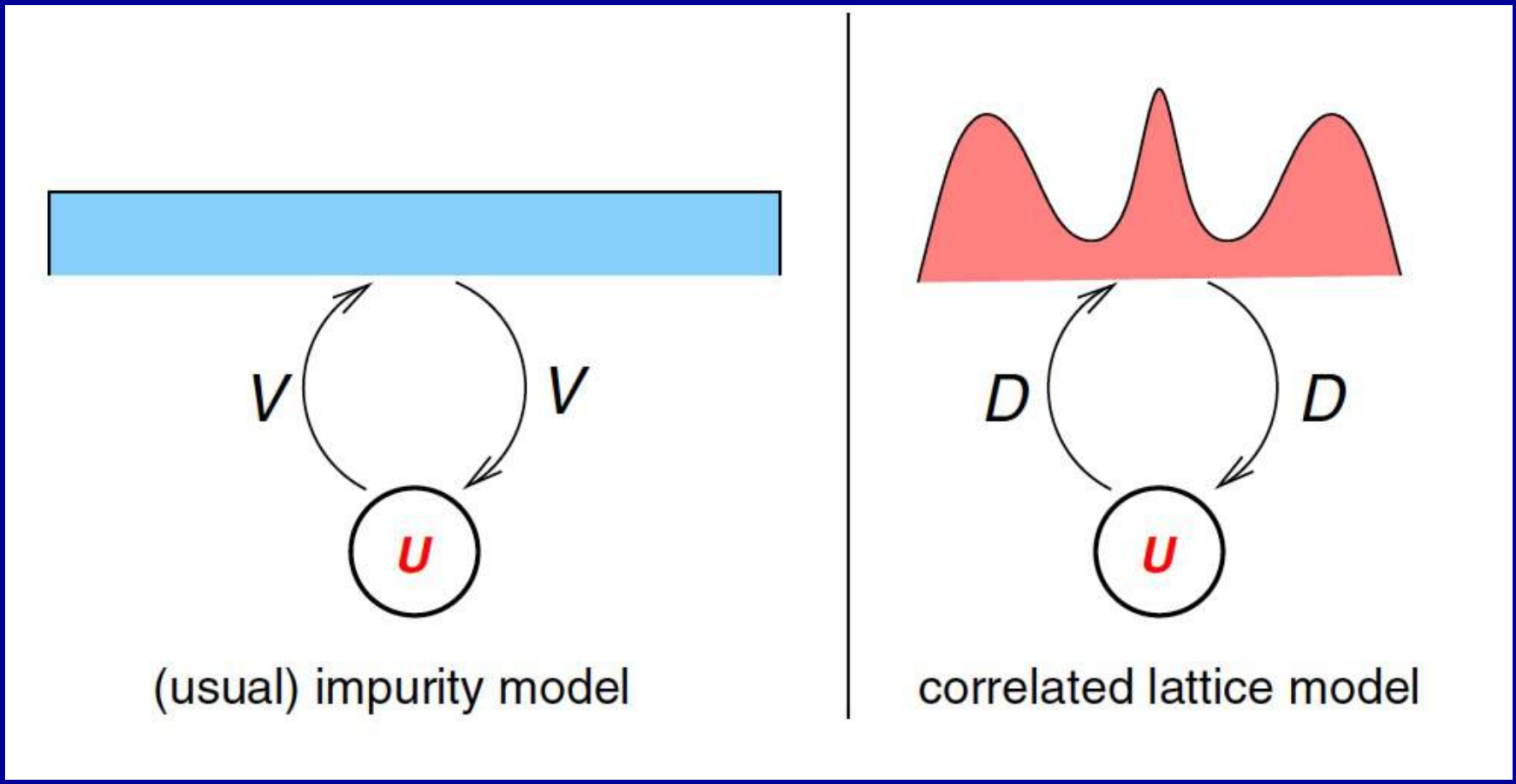

Cartoon from Held, Peters and Toschi PRL 110, 246402 (2013)

T=0 disappearance of the metal: Quantum Critical Point at U_{c2} (`Brinkman-Rice' physics)

The simplest ED:
1-bath site approximation ~ Gutzwiller/BR
Focuses on quasiparticles only

M.Potthoff PRB 64, 165114 (2001)

$$\Delta(\omega) = \frac{V^2}{\omega}$$

$$\Rightarrow \Sigma = \frac{U^2}{8}\left[\frac{1}{\omega - 3V} + \frac{1}{\omega + 3V}\right]$$

$$\Rightarrow Z^{-1} \equiv 1 - \frac{\partial \Sigma}{\partial \omega}|_{\omega=0} = 1 + \frac{U^2}{36V^2}$$

$$V^2 = \frac{U^2}{36}\frac{Z}{1-Z}$$

$$\Delta = \frac{D^2}{4}G \Rightarrow \frac{U^2}{36}\frac{Z}{1-Z} = \frac{D^2}{4}Z$$

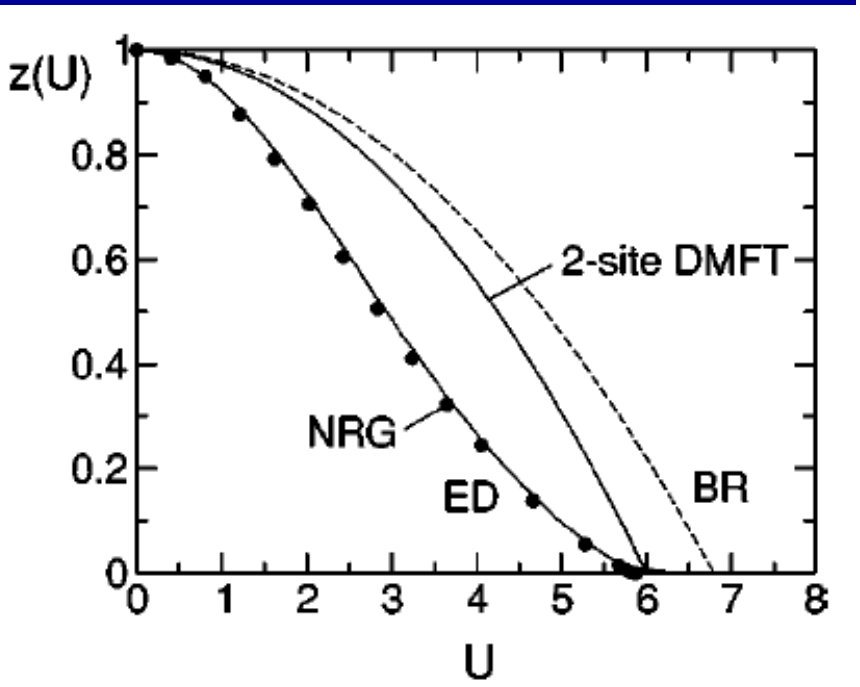

$$Z = 1 - \left(\frac{U}{3D}\right)^2$$

Exact solution for a single site in the bath:

$$H = H_{\rm at} + V \sum_{\sigma} \left(c_{\sigma}^{\dagger} d_{\sigma} + d_{s}^{\dagger} c_{\sigma} \right)$$

Conserved quantum numbers:
N, S, S^z

1+4+6+4+1=16 states

- $N = 0$: one state $|0\rangle$ $(S = S^z = 0)$
- $N = 1$: 4 states, $S = 1/2, S^z = \pm 1/2$
- $N = 2$: $S = 1$ a triplet of states
- $N = 2$: $S = 0$ three singlet states
- $N = 3$: 4 states
- $N = 4$: one states: $|\uparrow\downarrow, \uparrow\downarrow\rangle$

Focus on N=2 (ground-state) sector in LM regime:

- The $N = 2, S = 1$ triplet sector has eigenstates: $|\uparrow,\uparrow\rangle$, $|\downarrow,\downarrow\rangle$ and $\frac{1}{\sqrt{2}}[|\uparrow,\downarrow\rangle + |\downarrow,\uparrow\rangle]$. These states are insensitive to the hybridization V because the Pauli principle does not allow for hopping an electron through. Hence their energy is ε_d.

The $N = 2, S = 0$ sector is more interesting.

Basis set: $|\uparrow\downarrow,0\rangle$, $\frac{1}{\sqrt{2}}[|\uparrow,\downarrow\rangle - |\downarrow,\uparrow\rangle]\ |0,\uparrow\downarrow\rangle$.

The matrix reads:
$$\begin{pmatrix} 2\varepsilon_d + U & \sqrt{2}V & 0 \\ \sqrt{2}V & \varepsilon_d & \sqrt{2}V \\ 0 & \sqrt{2}V & 0 \end{pmatrix}$$

Symmetric case ε_d=-U/2
$$E = 0\ ,\ E_\pm = -\frac{U}{4} \pm \frac{1}{2}\sqrt{\frac{U^2}{4} + 16V^2}$$

The *ground-state* has energy E_-. For $V \ll U$, this reads:
$$E_0 = E_- \simeq -\frac{U}{2} - \frac{8V^2}{U} + \cdots$$

Energy in SINGLET SECTOR is lowered by virtual hops

Double occupancy in intermediate state → energy denominator ~ U

Ground-state wave-function:

$$|\Psi_0\rangle = \sqrt{1-\eta^2}\,|\mathcal{S}\rangle + \eta\,|\mathcal{D}\rangle$$

$$|\mathcal{S}\rangle \equiv \frac{1}{\sqrt{2}}\left[|\uparrow,\downarrow\rangle - |\downarrow,\uparrow\rangle\right]$$

$$|\mathcal{D}\rangle \equiv \frac{1}{\sqrt{2}}\left[|\uparrow\downarrow,0\rangle + |0,\uparrow\downarrow\rangle\right]$$

$$\text{with } \eta \sim \frac{V}{U} \ll 1.$$

Key points:

- Because of virtual hopping and the Pauli principle, a spin-singlet ground-state has been stabilized, in which the impurity spin is screened out by a conduction electron.
- Virtual hopping has induced a (small) admixture of states with $n_d = 0$ and $n_d = 2$ in the wave-function, hence allowing for charge fluctuations on the atom.

- The atomic limit V=0 is SINGULAR in the LM regime
- A non-zero V lifts the ground-state degeneracy
- The ground-state becomes a singlet: the impurity moment is ``screened'' by binding w/ a conduction electron

$$G(z) = \sum_{j=1}^{2} \left(\frac{a_j}{z - \epsilon_j} + \frac{a_j}{z + \epsilon_j} \right),$$

$$\epsilon_1 = \frac{1}{4} \left(\sqrt{U^2 + 64V^2} - \sqrt{U^2 + 16V^2} \right),$$

$$\epsilon_2 = \frac{1}{4} \left(\sqrt{U^2 + 64V^2} + \sqrt{U^2 + 16V^2} \right),$$

$$a_1 = \frac{1}{4} \left(1 - \frac{U^2 - 32V^2}{\sqrt{(U^2 + 64V^2)(U^2 + 16V^2)}} \right),$$

E.Lange
Mod Phys Lett B 12, 915 (1998)
arXiv:9810208
See also Appendix in
Alex Hewson's book

Spectral function for
1site in the bath,
½ filling

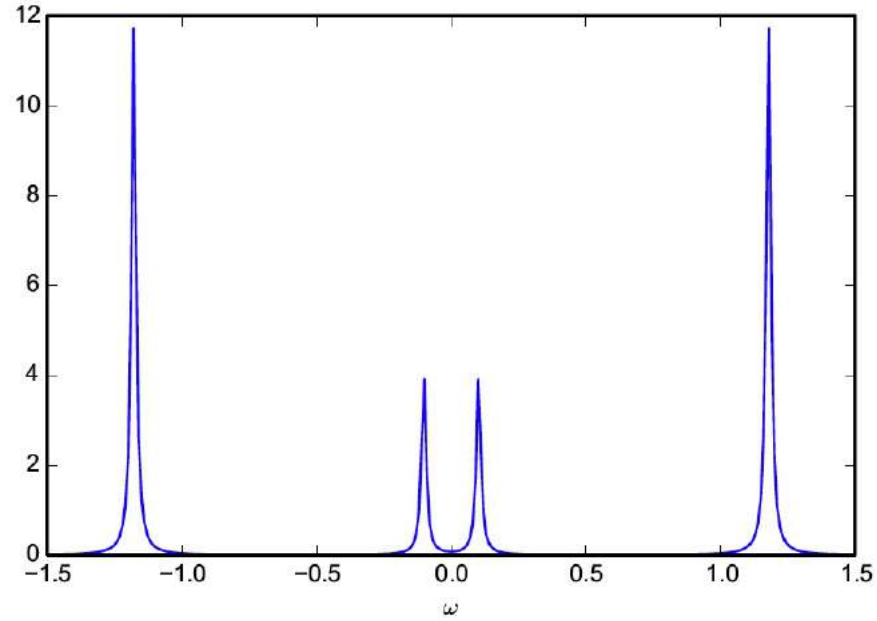

Figure 3: Spectral function for $U = 2.0$, $V = 0.2$

$$G(\omega) \simeq \frac{1}{2}\left[\frac{1}{\omega - \Delta(\omega) - U/2} + \frac{1}{\omega - \Delta(\omega) + U/2}\right]$$

$$\Delta = \frac{D^2}{4} G$$

$$\Rightarrow \boxed{D^4 G^3 - 8D^2 \omega G^2 + 4(4\omega^2 + D^2 - U^2)G - 16\omega = 0}$$

Gap at large-U approximation: Hubbard-like ignore Kondo-like processes/ quasiparticles

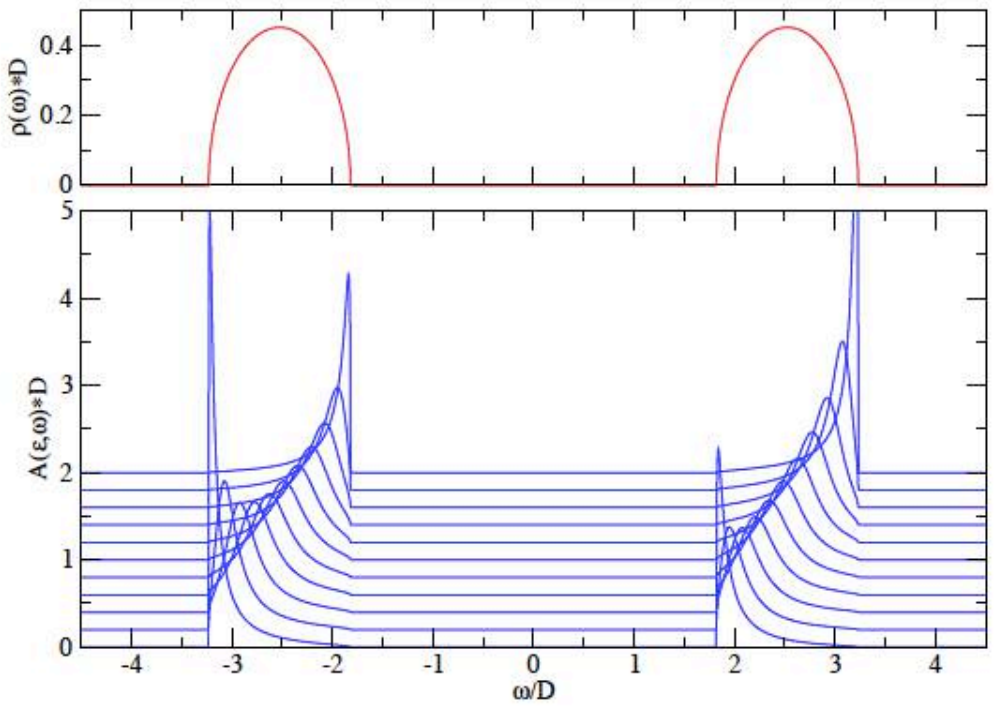

FIG. 10: Spectral density $\rho(\omega)$(a) and ε-resolved spectral function $A(\varepsilon, \omega)$ for several ε (from bottom to the top, $\varepsilon = -D, \ldots D$ with a step 0.2) (b), with $U/D = 4.0$ and $T = 0$. The results are from Hubbard III approximation.

A ``Hubbard satellite'' is nothing but an *atomic transition*

(broadened by the solid-state environment)

Imagine a simplified atom with a single atomic level

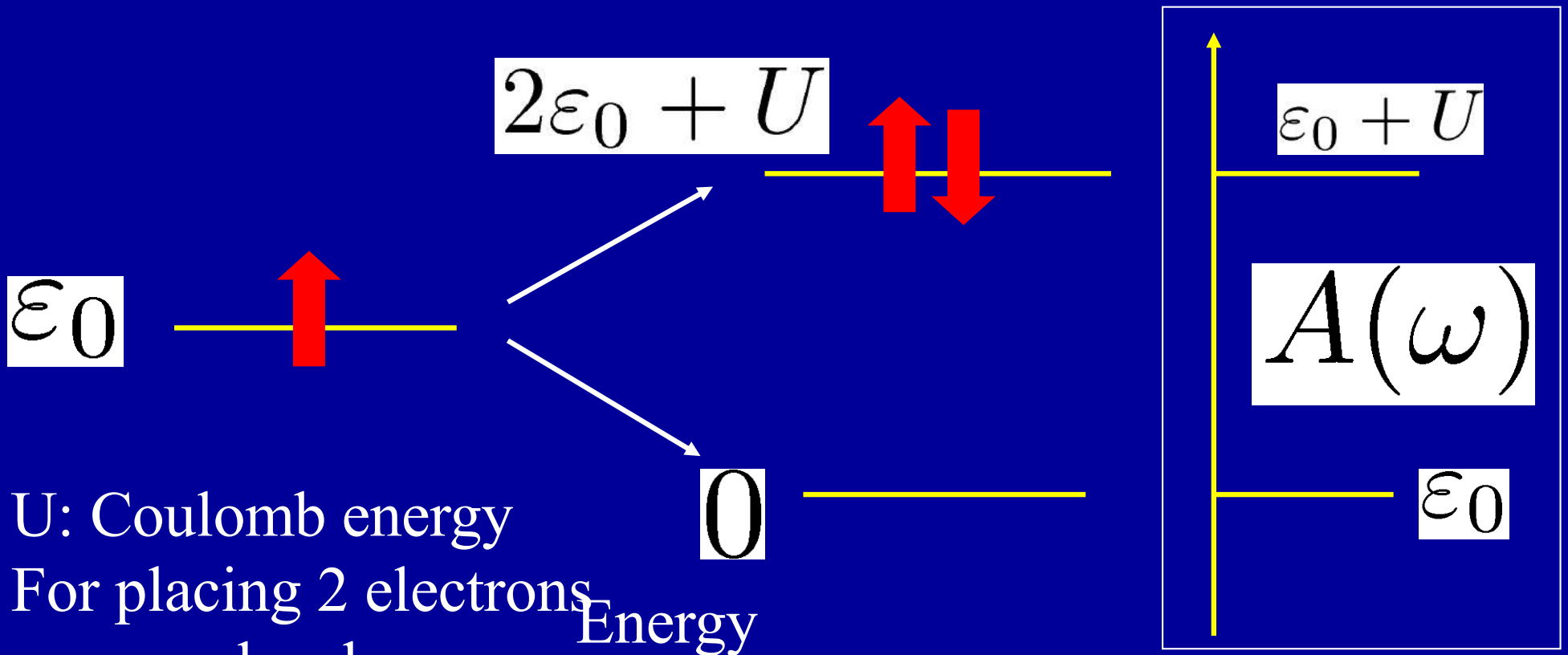

U: Coulomb energy
For placing 2 electrons on same level

The actual k-integrated spectral function has both Hubbard bands and low-energy quasiparticles

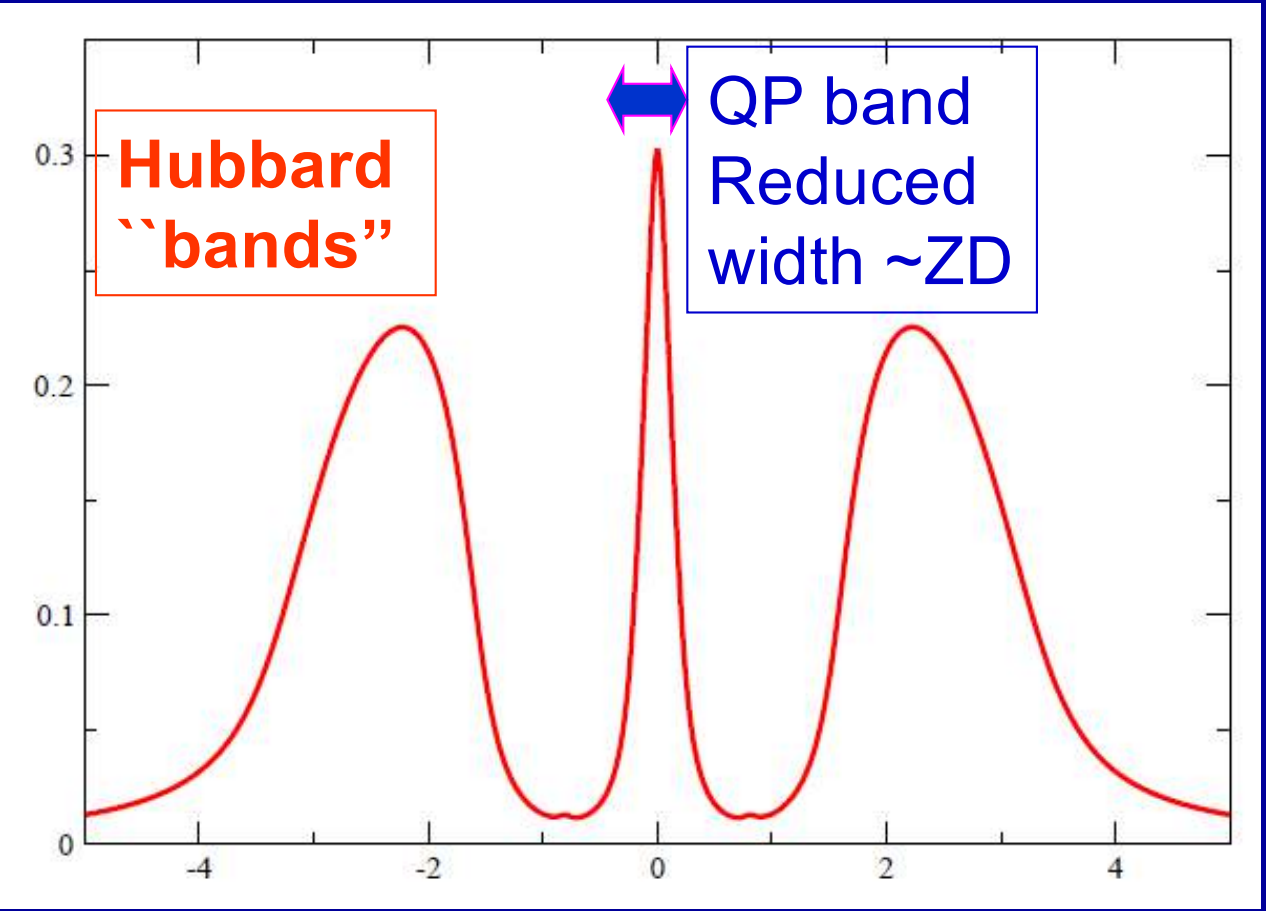

Value of A(ω=0) is pinned at U=0 value due to Luttinger theorem

→ Low-energy quasiparticles and incoherent Hubbard bands Coexist in one-particle spectrum of correlated metal

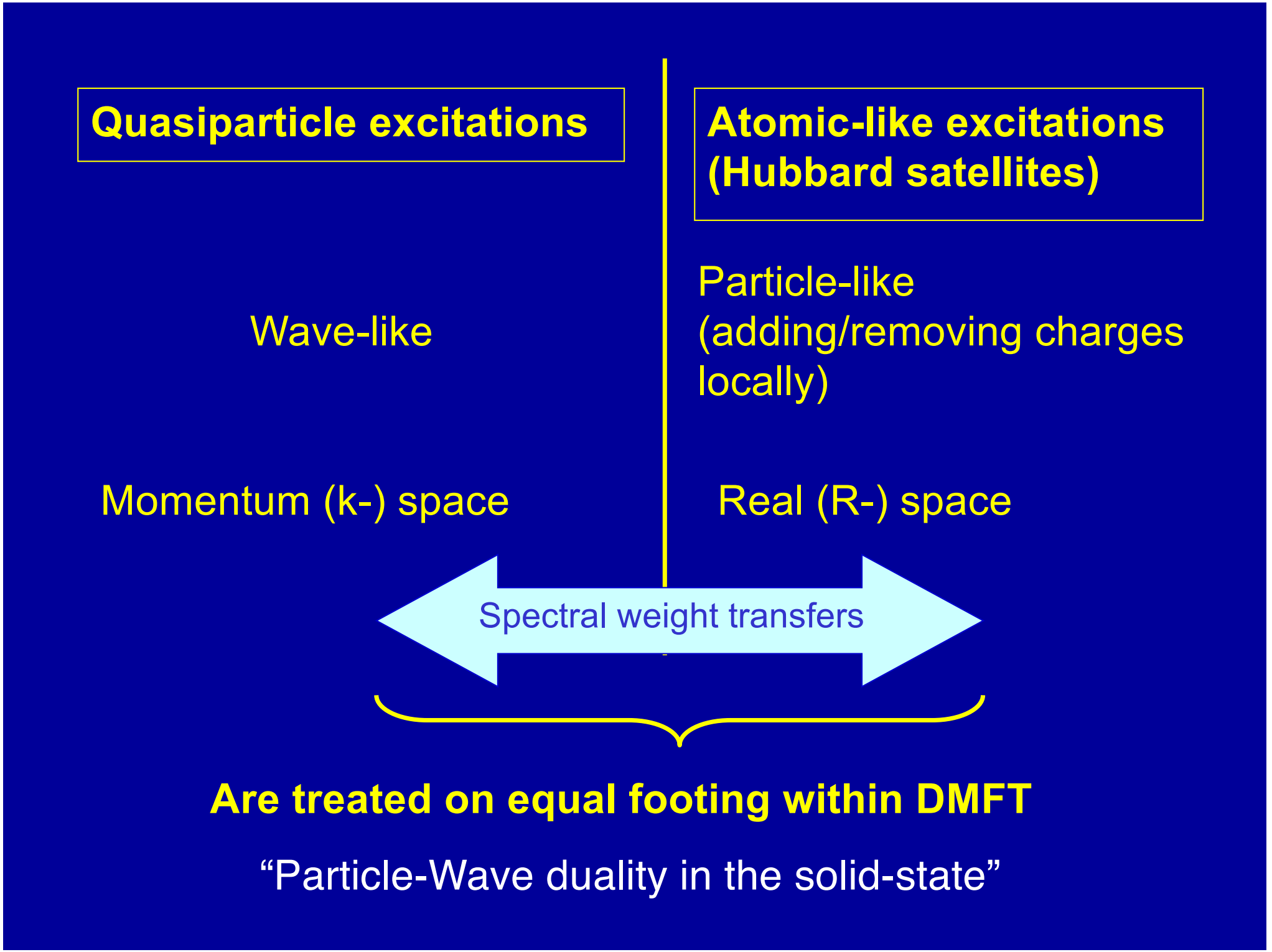
Quasiparticle excitations
Atomic-like excitations (Hubbard satellites)
Wave-like
Particle-like (adding/removing charges locally)
Momentum (k-) space
Real (R-) space
Spectral weight transfers
Are treated on equal footing within DMFT
"Particle-Wave duality in the solid-state"

``Atsushi Fujimori's map of ABO_3 perovskites''

J.Phys Chem Sol. 53 (1992) 1595

Imada, Fujimori, Tokura, Rev.Mod.Phys (1998)

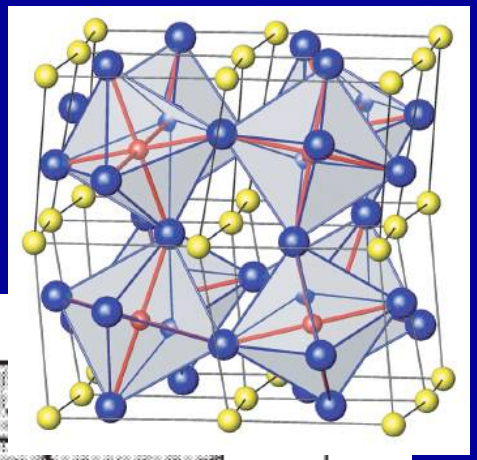

A=rare-earth site (yellow) B=metal site (red)

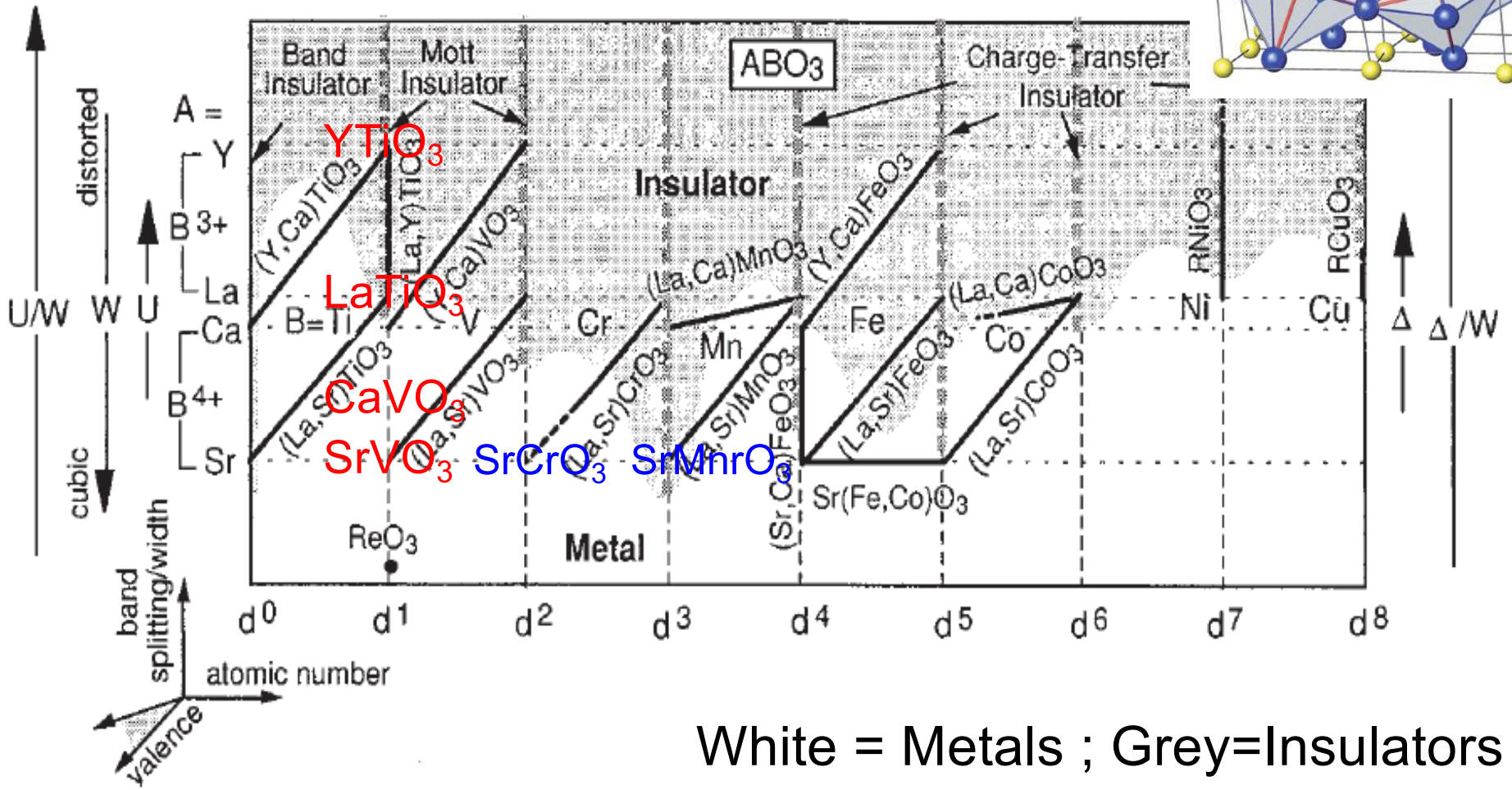

White = Metals ; Grey=Insulators

From weak to strong correlations in d^1 oxides [Fujimori et al. PRL 69, 1796 (1992)]

Puzzle:
Why is $SrVO_3$
a metal
and $LaTiO_3$, $YTiO_3$
Mott insulators ?

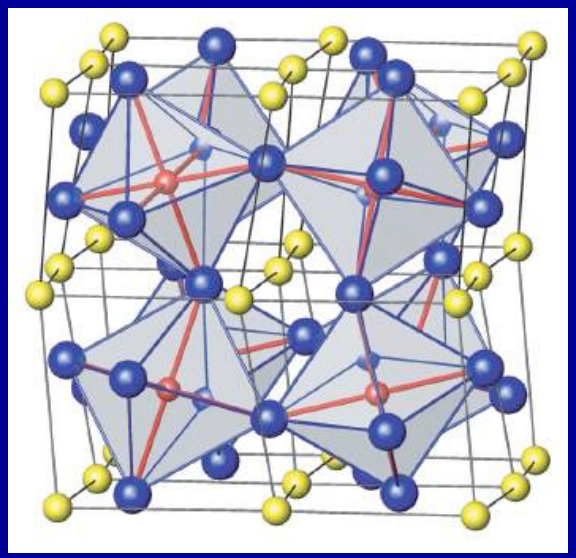

Mott insulators :

Their excitation spectra contain atomic-like excitations

Band structure calculations (interpreting Kohn-Sham spectra as excitations) are in serious trouble for correlated materials !

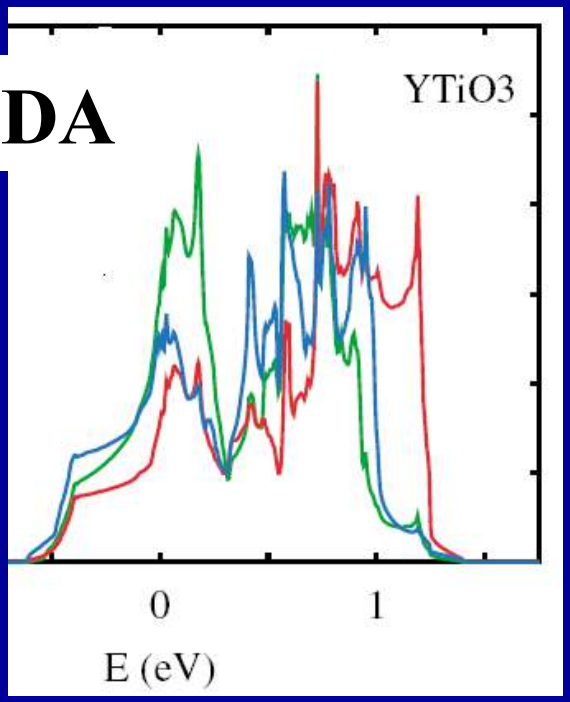

Metallic LDA (KS) spectrum !

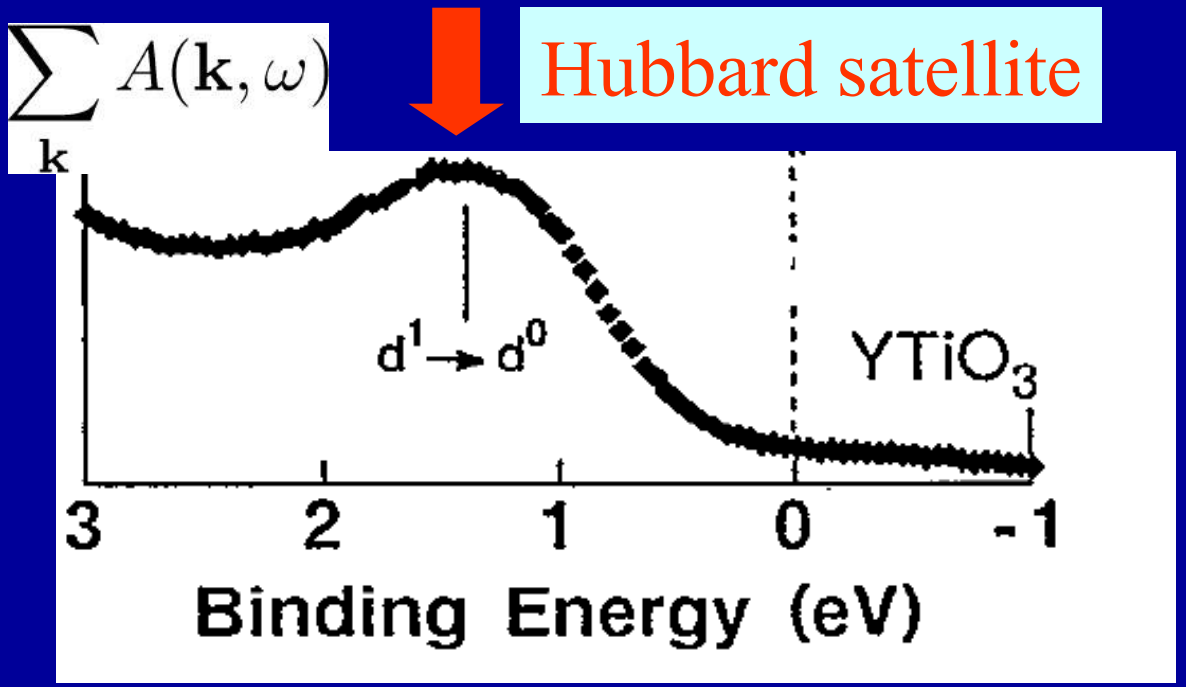

Photoemission: Fujimori et al., PRL 1992

Correlated metals: atomic-like excitations at high energy, quasiparticles at low energy

- **Narrowing of quasiparticle bands** due to correlations (the Brinkman-Rice phenomenon)
- **Hubbard satellites** (i.e extension to the solid of atomic-like transitions)

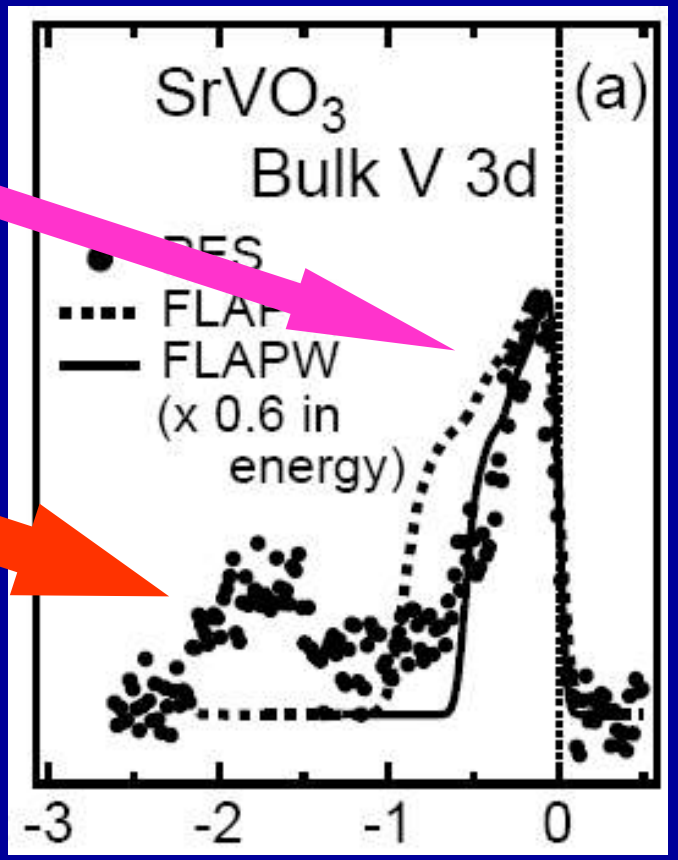

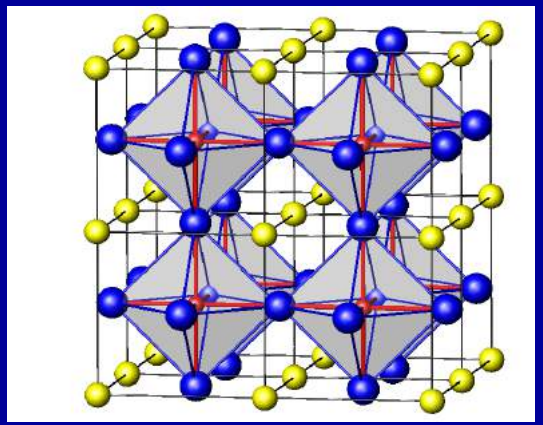

Dashed line:
Spectrum obtained from Conventional band-structure methods (DFT-LDA)

$SrVO_3$

Sekiyama et al., PRL 2004

PHOTOEMISSION…
A 12 years (success) story

Fujimori et al, 1992

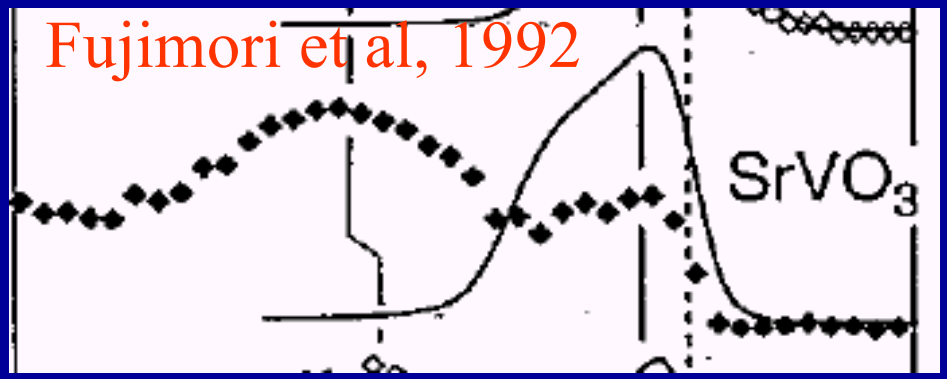

Maiti, Sarma et al., 1999

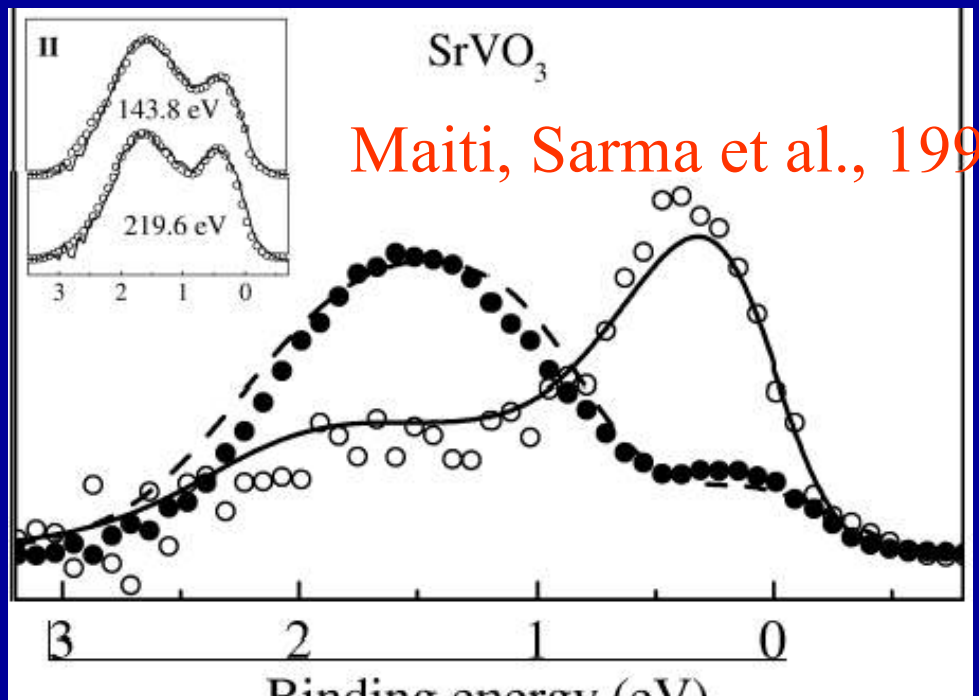

Inoue et al., 1995

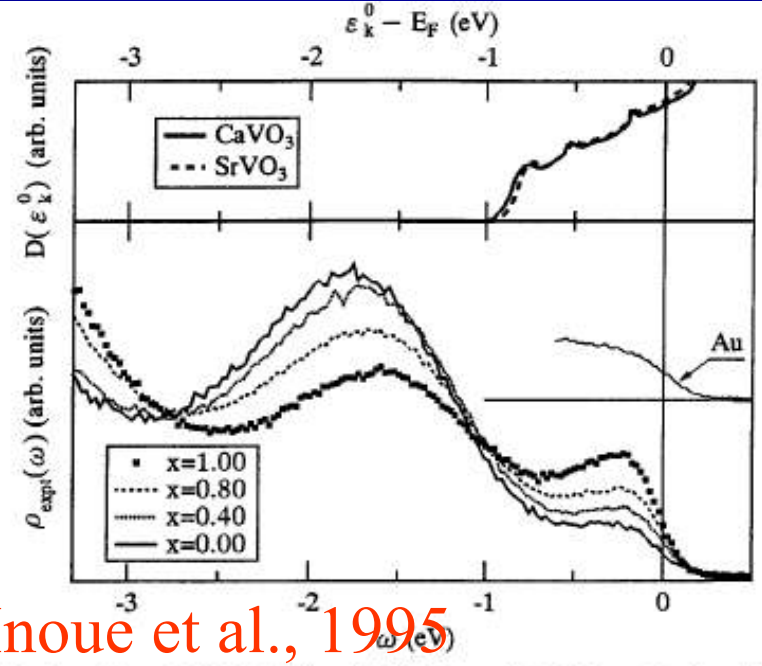

FIG. 1. Top: DOS $D(\varepsilon_k^0)$ of $CaVO_3$ and $SrVO_3$ calculated by the APW method. Bottom: measured photoemission spectra $\rho_{expt}(\omega)$ of $Ca_{1-x}Sr_xVO_3$ taken with $h\nu = 50$ eV. A spectrum of Au is also shown as a reference to E_F and the instrumental resolution.

Sekiyama et al., 2001

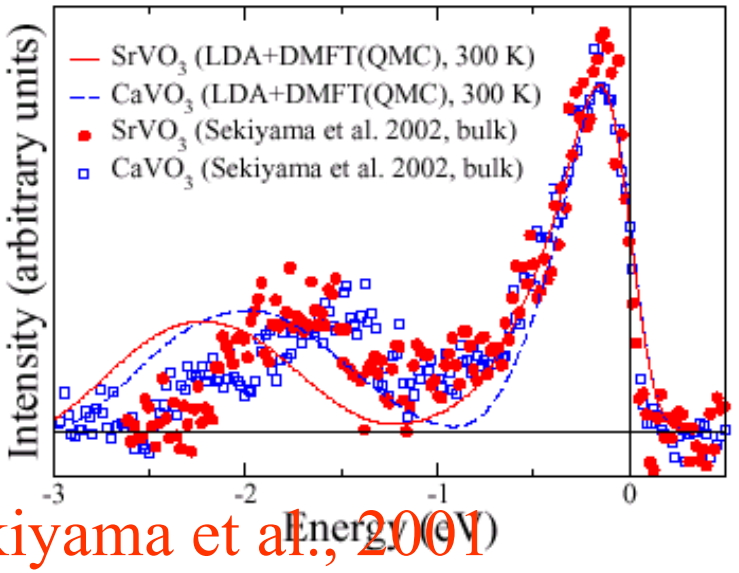

FIG. 4: Comparison of the calculated, parameter-free LDA+DMFT(QMC) spectra of $SrVO_3$ (solid line) and $CaVO_3$ (dashed line) with bulk-sensitive high-resolution PES ($SrVO_3$: circles; $CaVO_3$: rectangles) [4]. Horizontal line: experimental subtraction of the background intensity.

Fermi Liquid nature of the metallic phase

- At (possibly very) low T,ω: a Fermi liquid

$$\mathrm{Re}\Sigma(\omega+i0^+)=U/2+(1-1/Z)\omega+O(\omega^3),$$

$$\mathrm{Im}\Sigma(\omega+i0^+)=-B\omega^2+O(\omega^4).$$

- Fermi surface is unchanged by interactions w/in DMFT for single orbital model. But Drude weight ~Z
- At U_{c2} transition: Z→0 (~ Brinkman-Rice)
- Heavy quasiparticles:

m*/m=1/Z diverges at U_{c2}

(divergence reflects large entropy of insulator with fluctuating local moments)

Near the transition:

B ~ $1/Z^2$ (Kadowaki-Woods)

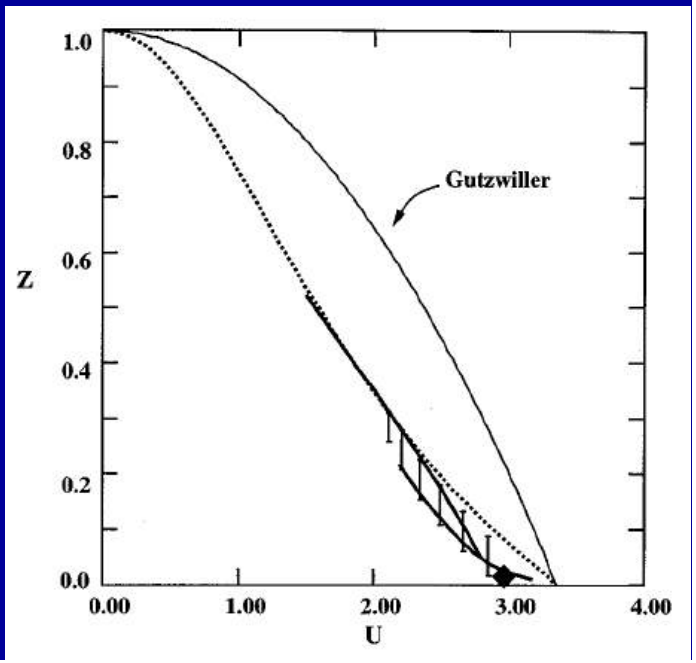

LaTiO3: AF Mott insulator

AF persists up to ~ 5% hole-doping

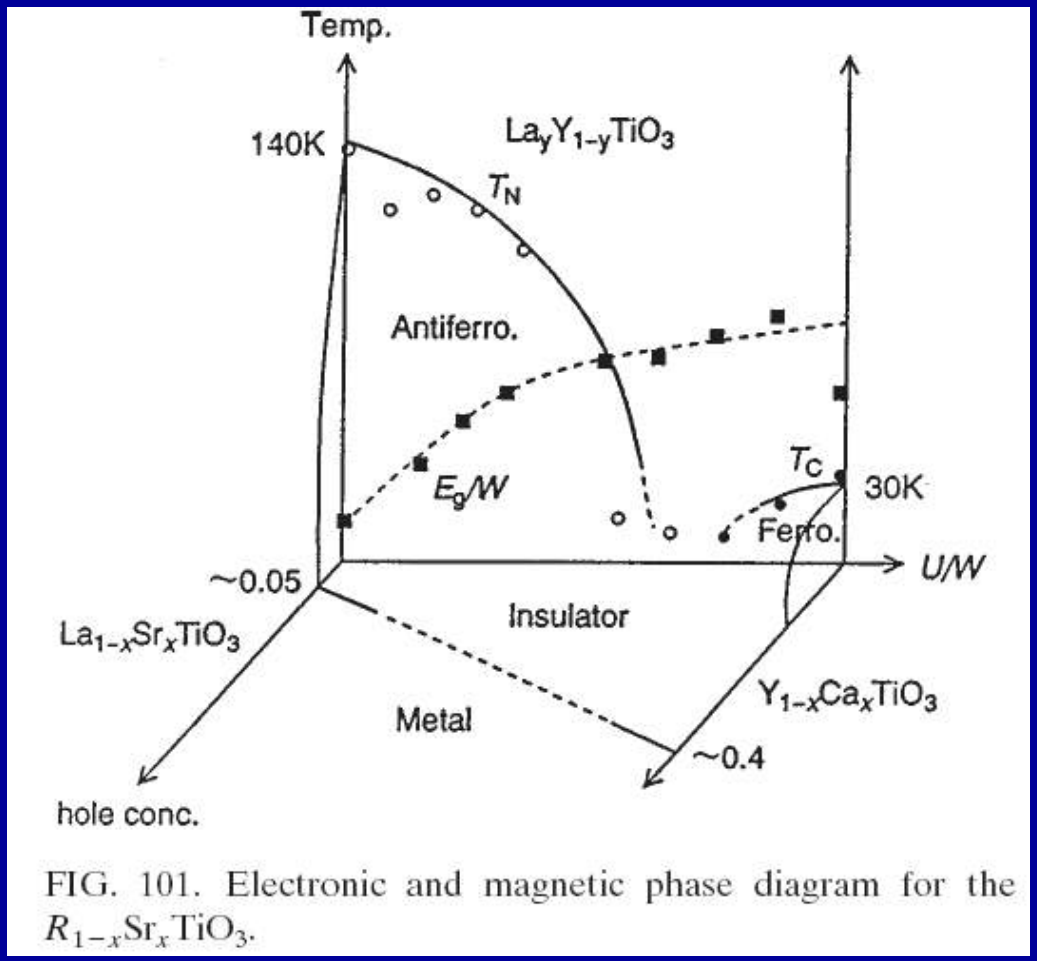

FIG. 101. Electronic and magnetic phase diagram for the $R_{1-x}Sr_xTiO_3$.

Photoemission spectrum: definitely a Mott insulator

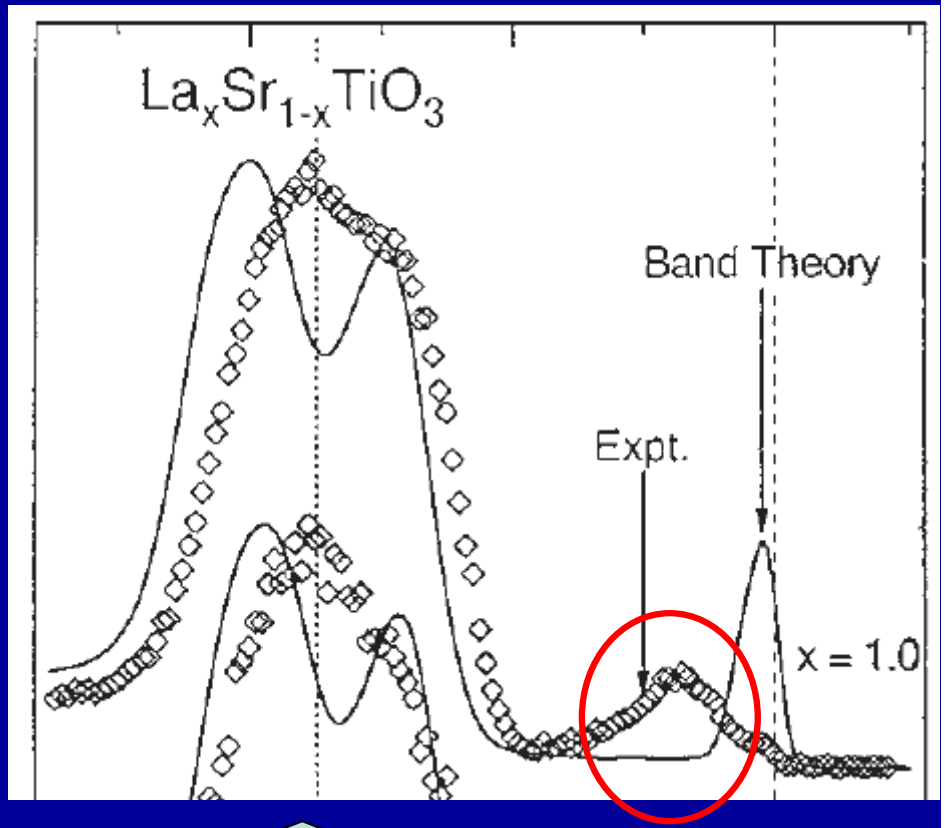

Oxygen states

Lower Hubbard band d1→d0

Approach to the Mott state in titanates

Saturation of m* in AF regime

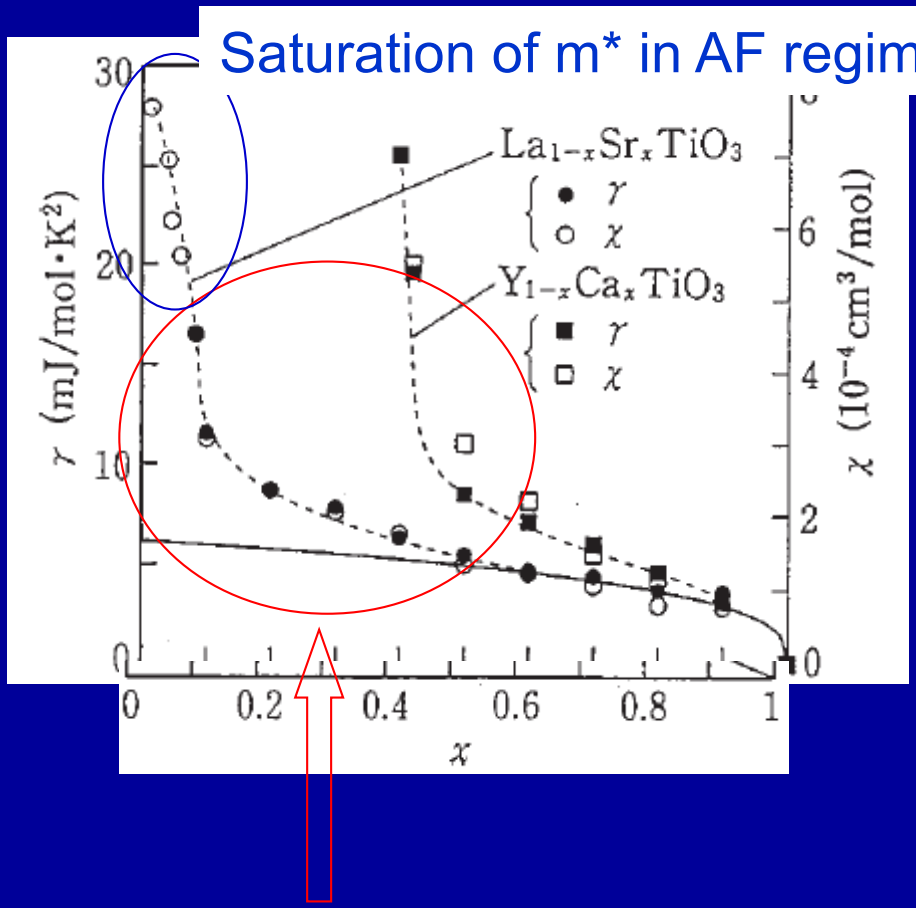

Increase of effective mass

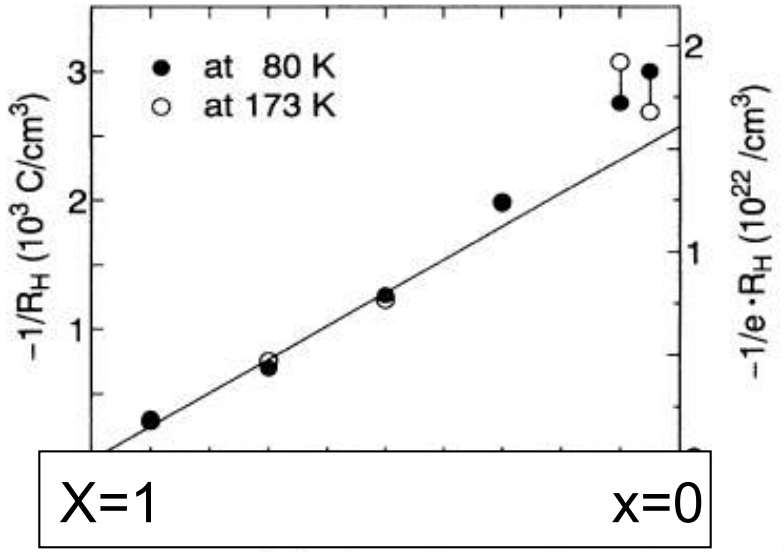

FIG. 2. The filling (x) dependence of the inverse of Hall coefficient (R_H^{-1}) in $Sr_{1-x}La_xTiO_3$. Open and closed circles represent the values measured at 80 K and 173 K, respectively. A solid line indicates the calculated one based on the assumption that each substitution of a Sr^{2+} site with La^{3+} supplies the compound with one electron-type carrier per Ti site.

R_H reported as ~ T-independent and consistent w/ large Fermi surface

Tokura et al.
PRL, 1993

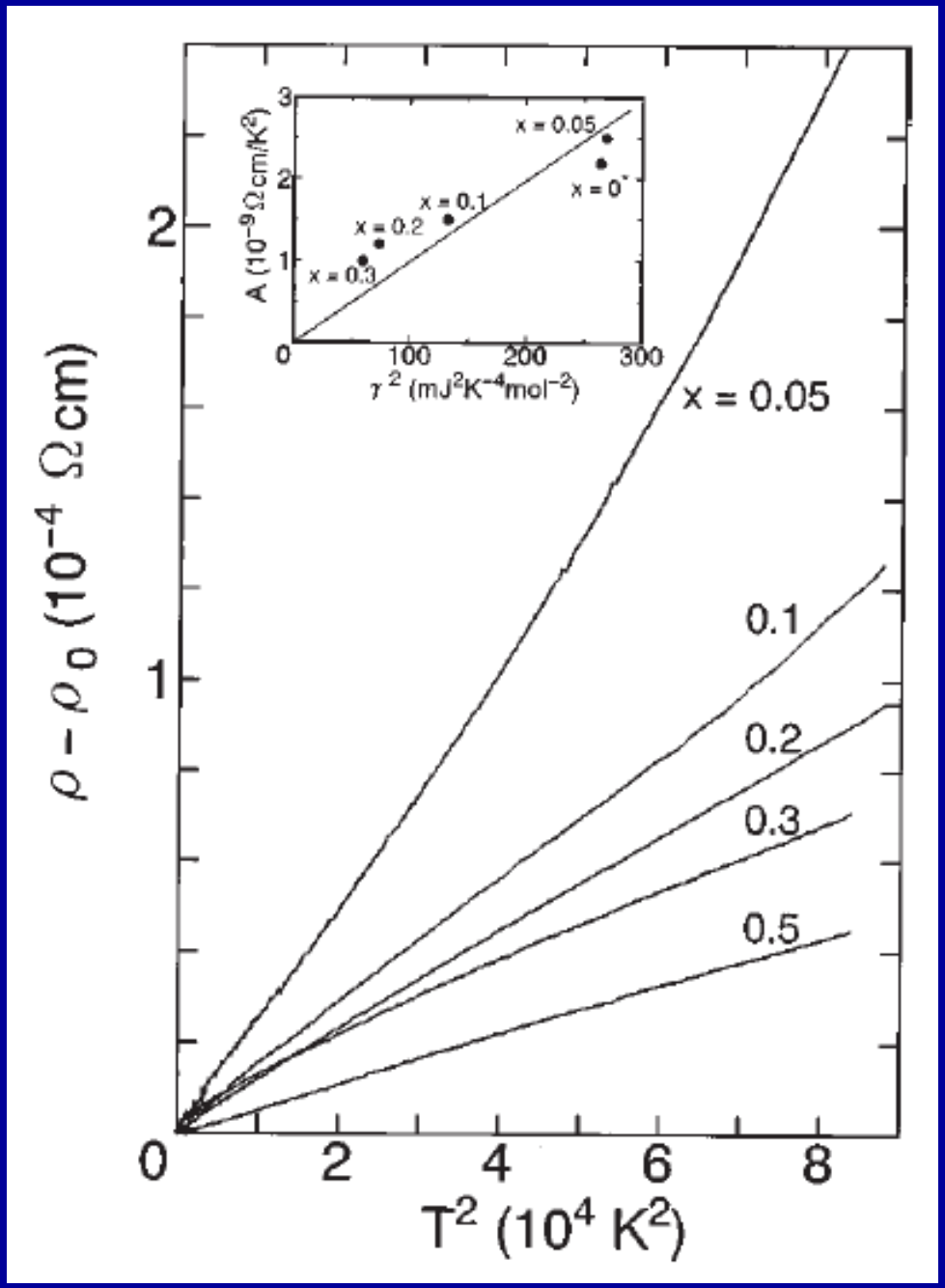

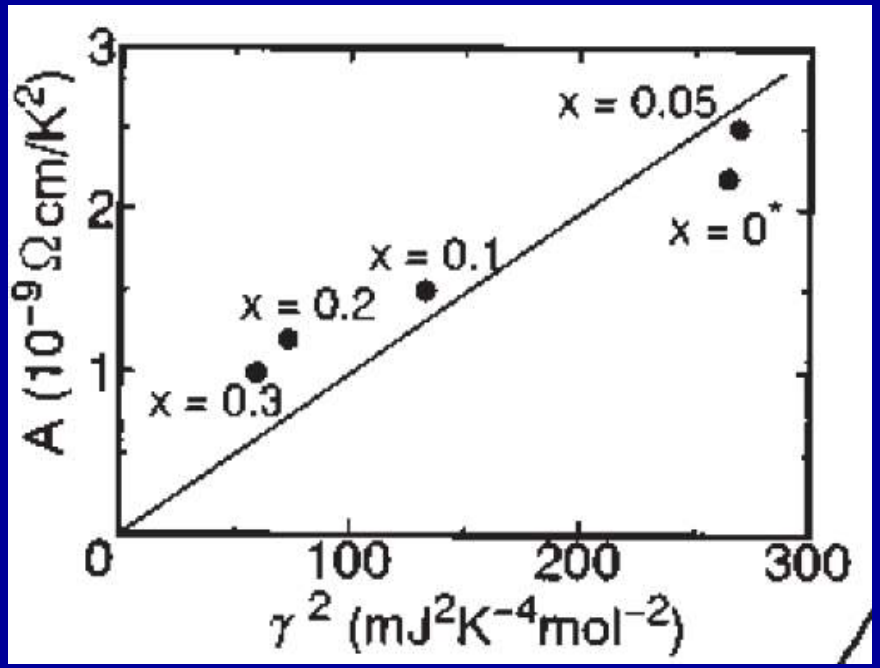

Titanates/transport:

$$\rho_{dc} = AT^2 + \cdots$$

$$A/\gamma^2 \sim \text{const.}$$

Fermi liquid behavior observed
Below ~ 100K @ 5% doping

But… there is (plenty of) life beyond the Fermi-liquid regime

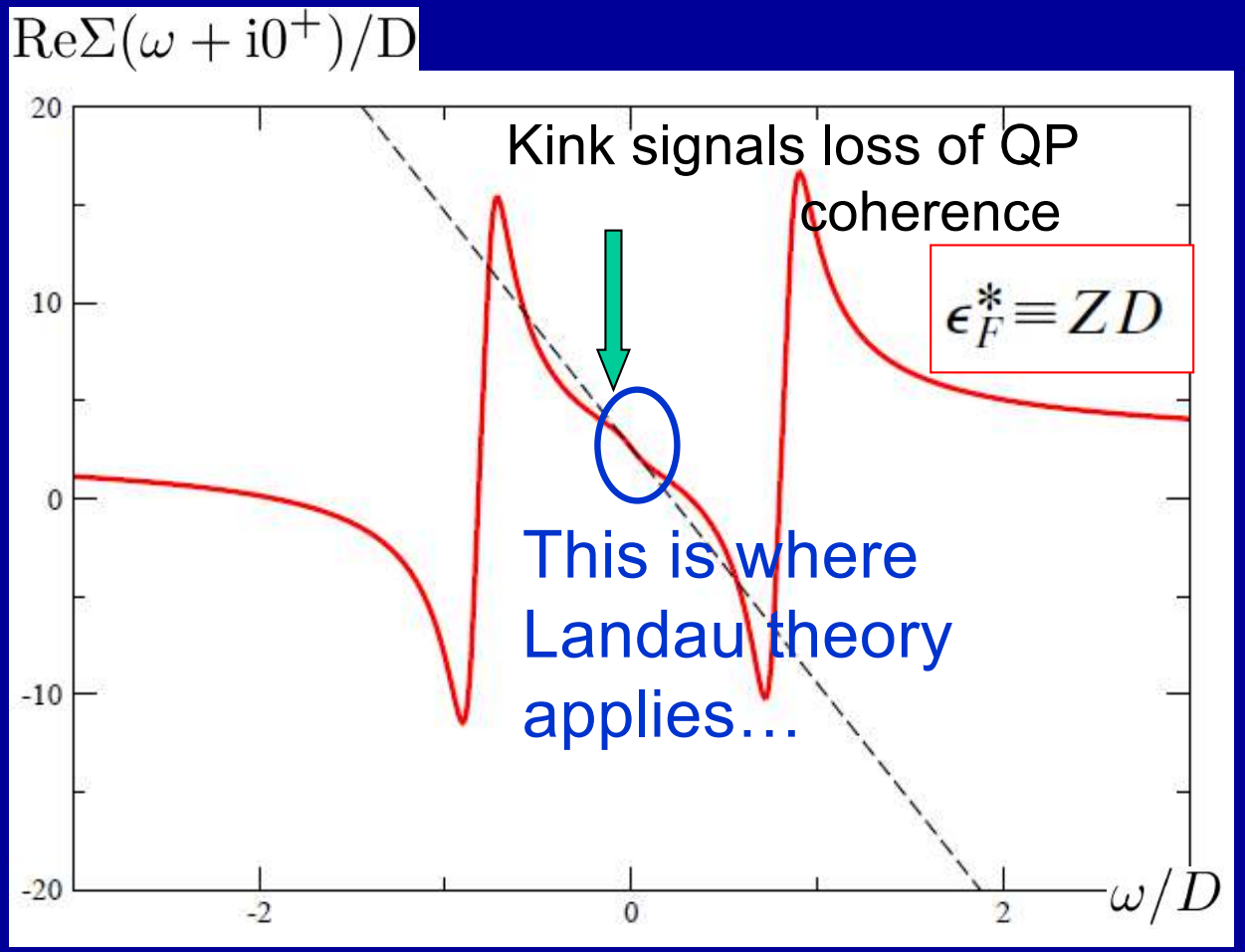

CTQMC+Analytical continuation (Pade),
courtesy M.Ferrero, compares perfectly to NRG

$B\omega^2$ applies only below coherence scale
B-coefficient is enhanced ~ $1/Z^2$

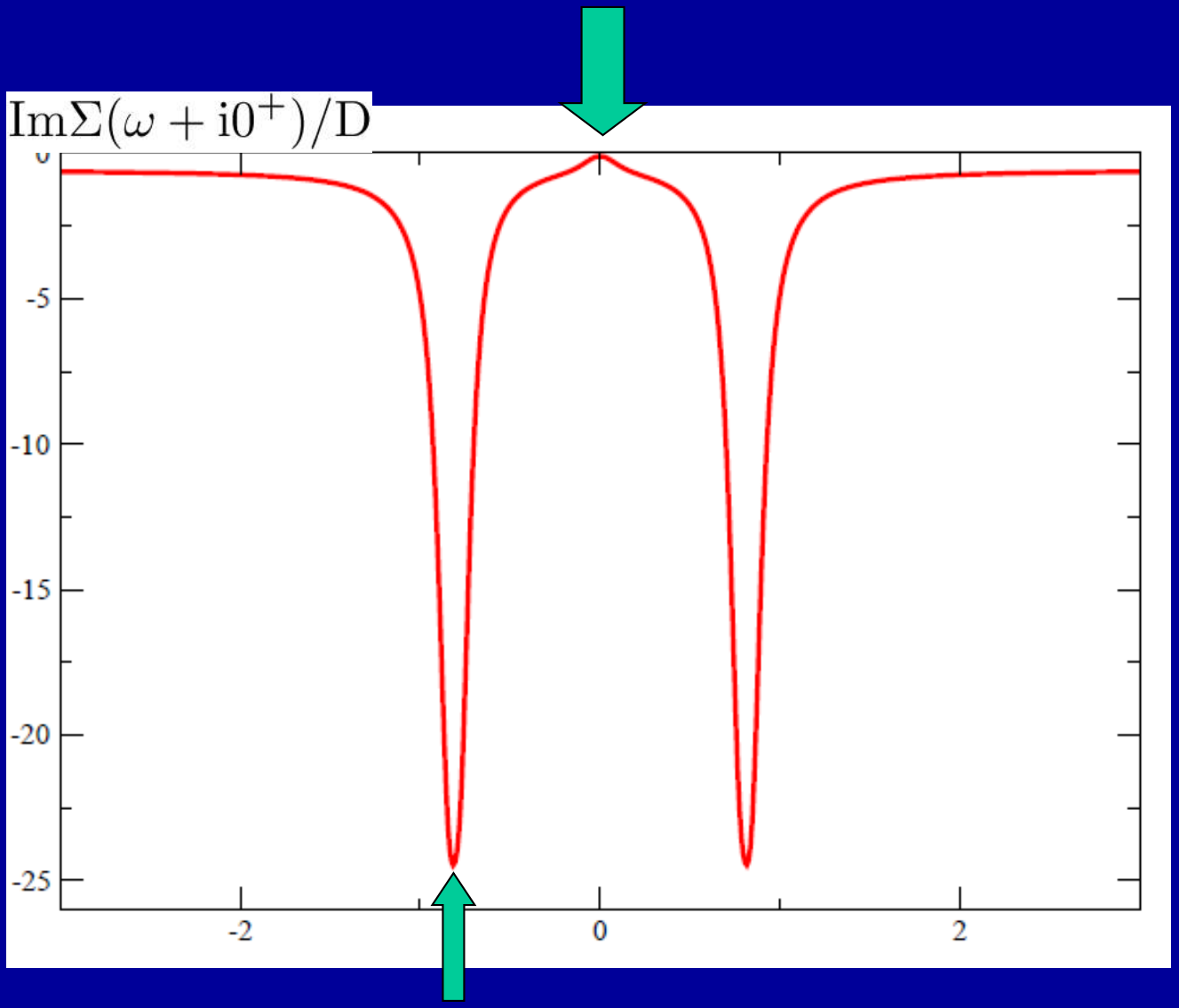

These 2 peaks will coalesce into a pole at ω=0
as insulator is reached

`Kinks' of purely electronic origin in quasiparticle dispersion

LETTERS

Nature Physics 3 (2007) 168

Kinks in the dispersion of strongly correlated electrons

K. BYCZUK[1,2]*, M. KOLLAR[1]*, K. HELD[3], Y.-F. YANG[3], I. A. NEKRASOV[4], TH. PRUSCHKE[5] AND D. VOLLHARDT[1]

PRL **110,** 246402 (2013) PHYSICAL REVIEW LETTERS week ending 14 JUNE 2013

Poor Man's Understanding of Kinks Originating from Strong Electronic Correlations

K. Held,[1] R. Peters,[2] and A. Toschi[1]

[1]*Institute of Solid State Physics, Vienna University of Technology, A-1040 Vienna, Austria*

[2]*Department of Physics, Kyoto University, Kyoto 606-8502, Japan*

(Received 25 February 2013; published 11 June 2013)

By means of dynamical mean field theory calculations, it was recently discovered that kinks generically arise in strongly correlated systems, even in the absence of external bosonic degrees of freedoms such as phonons. However, the physical mechanism behind these kinks remained unclear. On the basis of the perturbative and numerical renormalization group theory, we herewith identify these kinks as the effective Kondo energy scale of the interacting lattice system which is shown to be smaller than the width of the central peak.

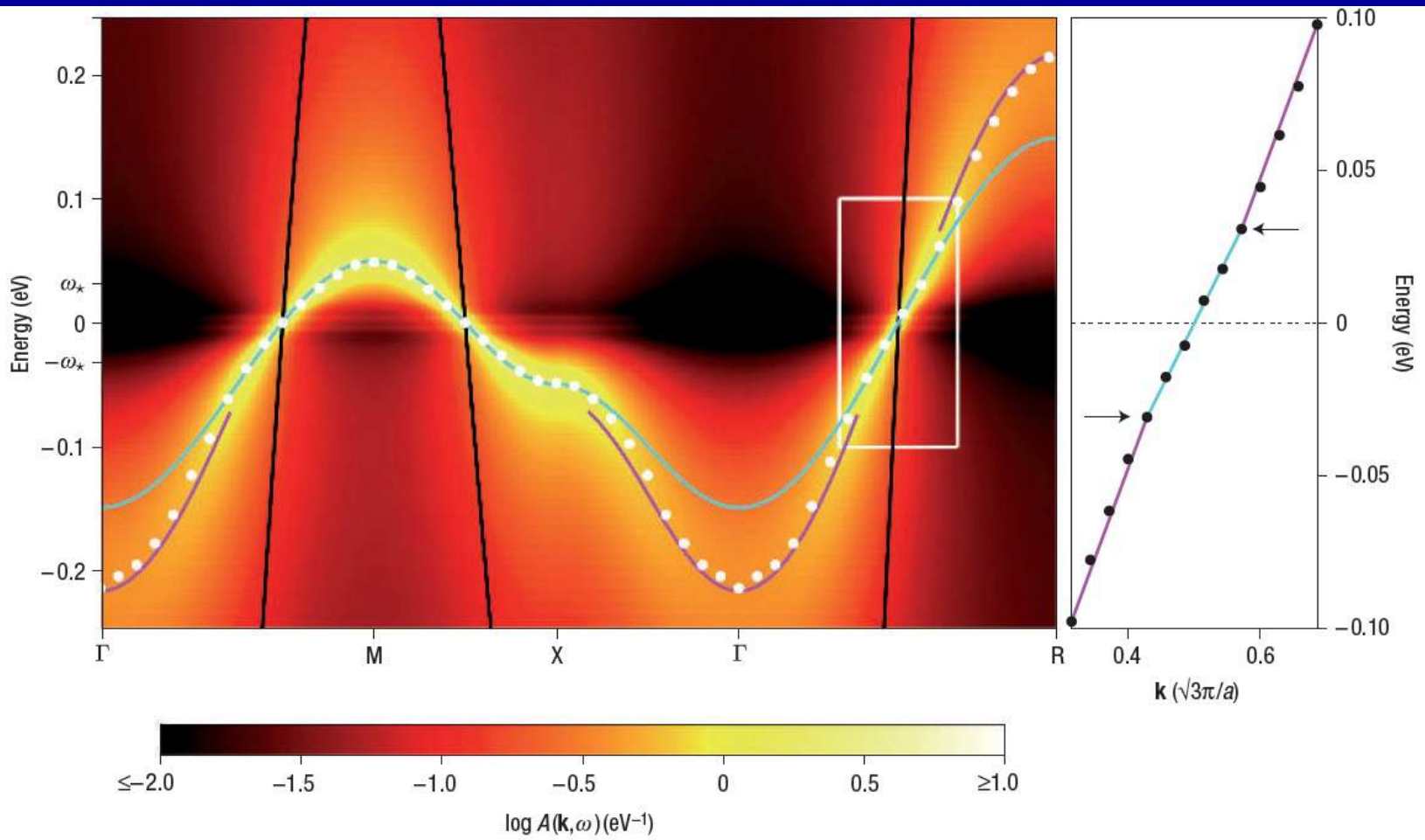

Figure 1 Kinks in the dispersion relation, $E_{\mathbf{k}}$, for a strongly correlated system. The intensity plot represents the spectral function $A(\mathbf{k}, \omega)$ (Hubbard model in DMFT, cubic lattice, interaction $U = 3.5$ eV, bandwidth $W = 3.46$ eV, $n = 1$, $Z_{\mathrm{FL}} = 0.086$, $T = 5$ K). Close to the Fermi energy, the effective dispersion (white circles) follows the renormalized band structure, $E_{\mathbf{k}} = Z_{\mathrm{FL}}\epsilon_{\mathbf{k}}$ (blue line). For $|\omega| > \omega_\star$, the dispersion has the same shape but with a different renormalization, $E_{\mathbf{k}} = Z_{\mathrm{CP}}\epsilon_{\mathbf{k}} - c\,\mathrm{sgn}(E_{\mathbf{k}})$ (pink line). Here, $\omega_\star = 0.03$ eV, $Z_{\mathrm{CP}} = 0.135$ and $c = 0.018$ eV are all calculated (see the Supplementary Information) from Z_{FL} and $\epsilon_{\mathbf{k}}$ (black line). A subinterval of Γ–R (white frame) is plotted on the right, showing kinks at $\pm\omega_\star$ (arrows).

Byczuk et al. Nat. Phys 2007

Near U_{c2}:
Effective Kondo problem
with FINITE coupling.

(Fisher, Kotliar, Moeller
PRB 52 (1995) 17112;Moeller et al. PRL 74 (1995) 2082)

The kink is associated with the effective Kondo scale, which is smaller than the width of the QP peak

(Held et al., PRL 2013 →)

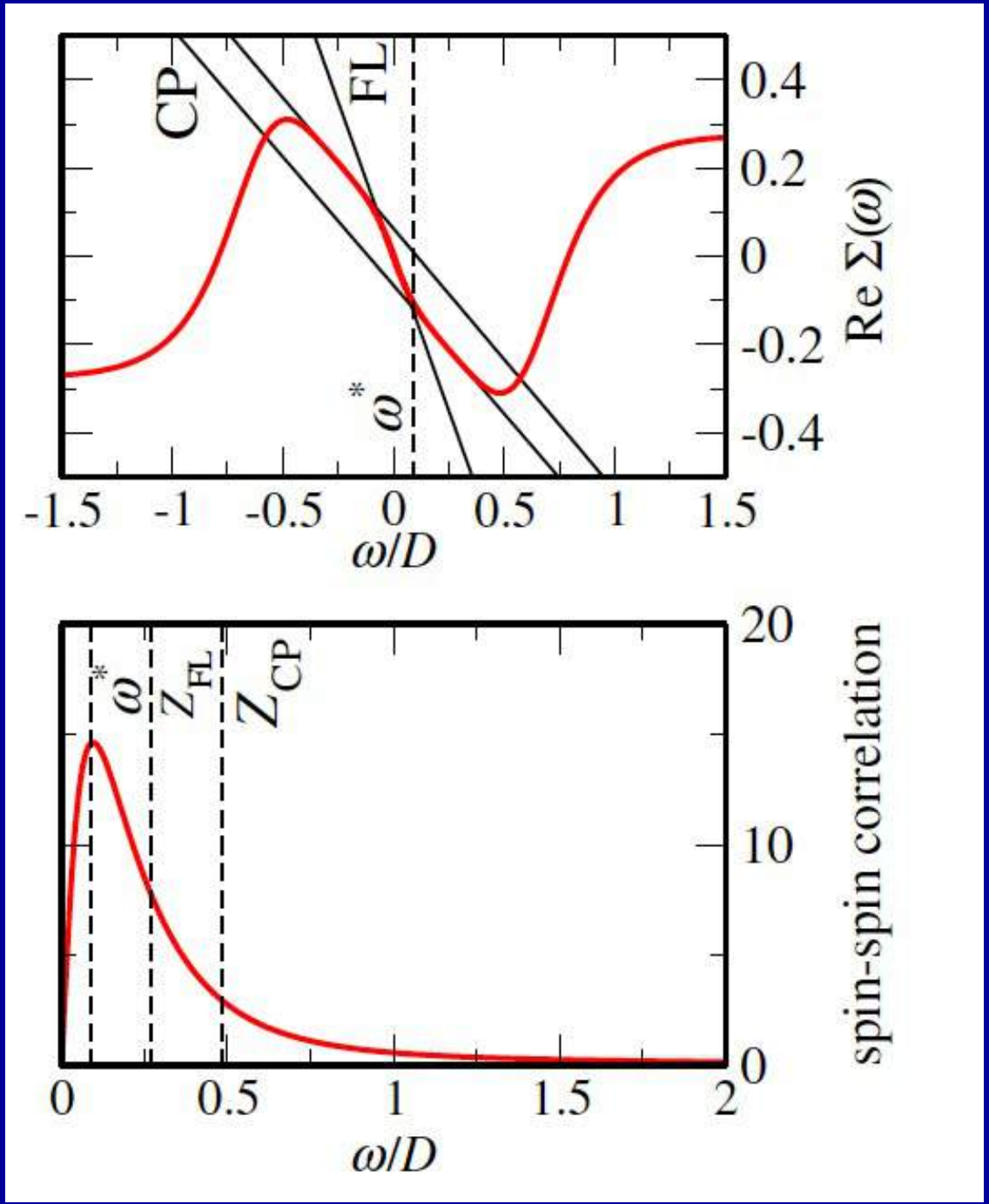

CT-HYB QMC and NRG allow for a high-accuracy exploration of the FL

(M.Ferrero, J.Mravlje, R.Zitko, X.Deng, AG)

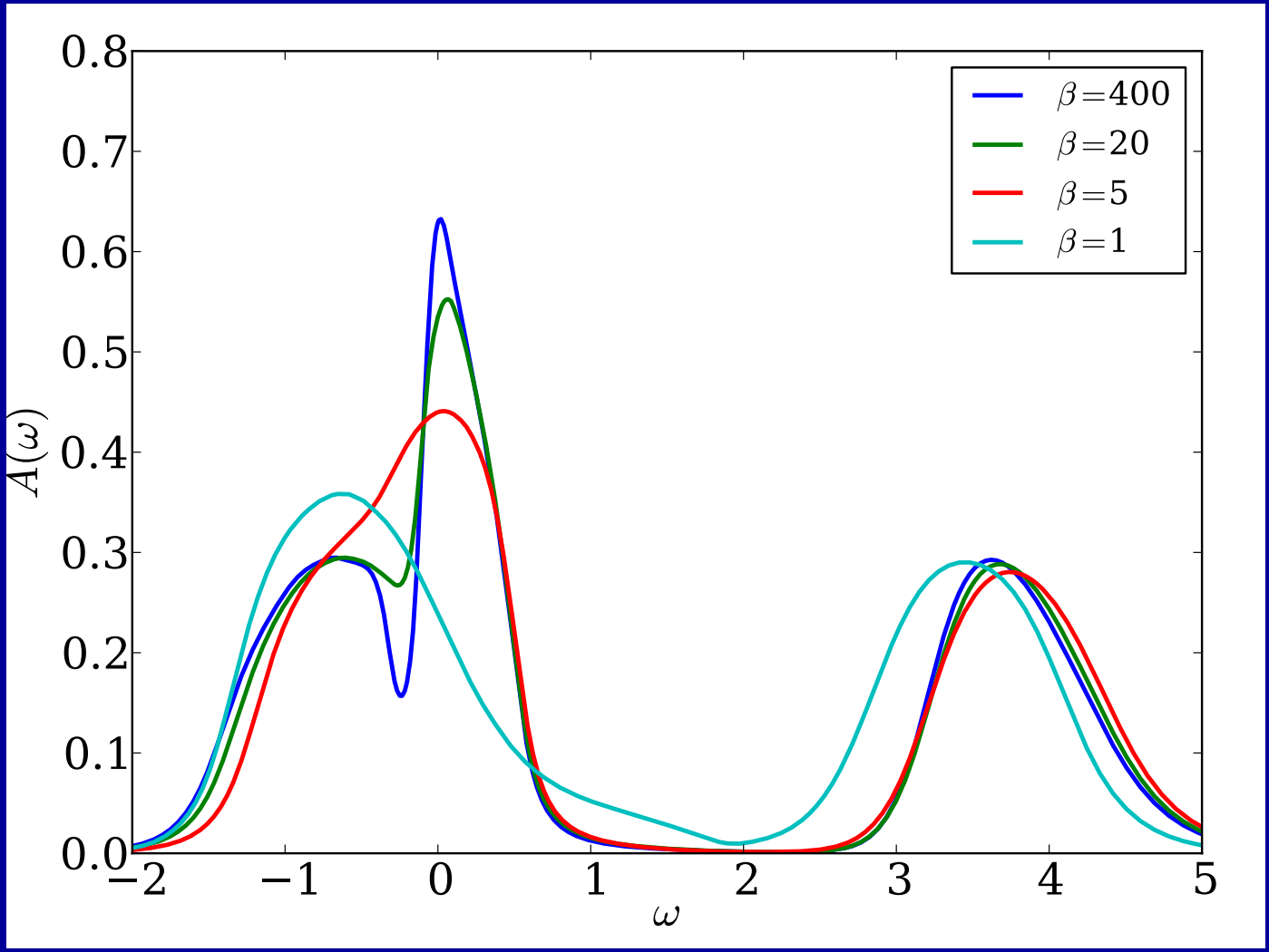

Bethe Lattice; U/D=4, 20%doping; NRG

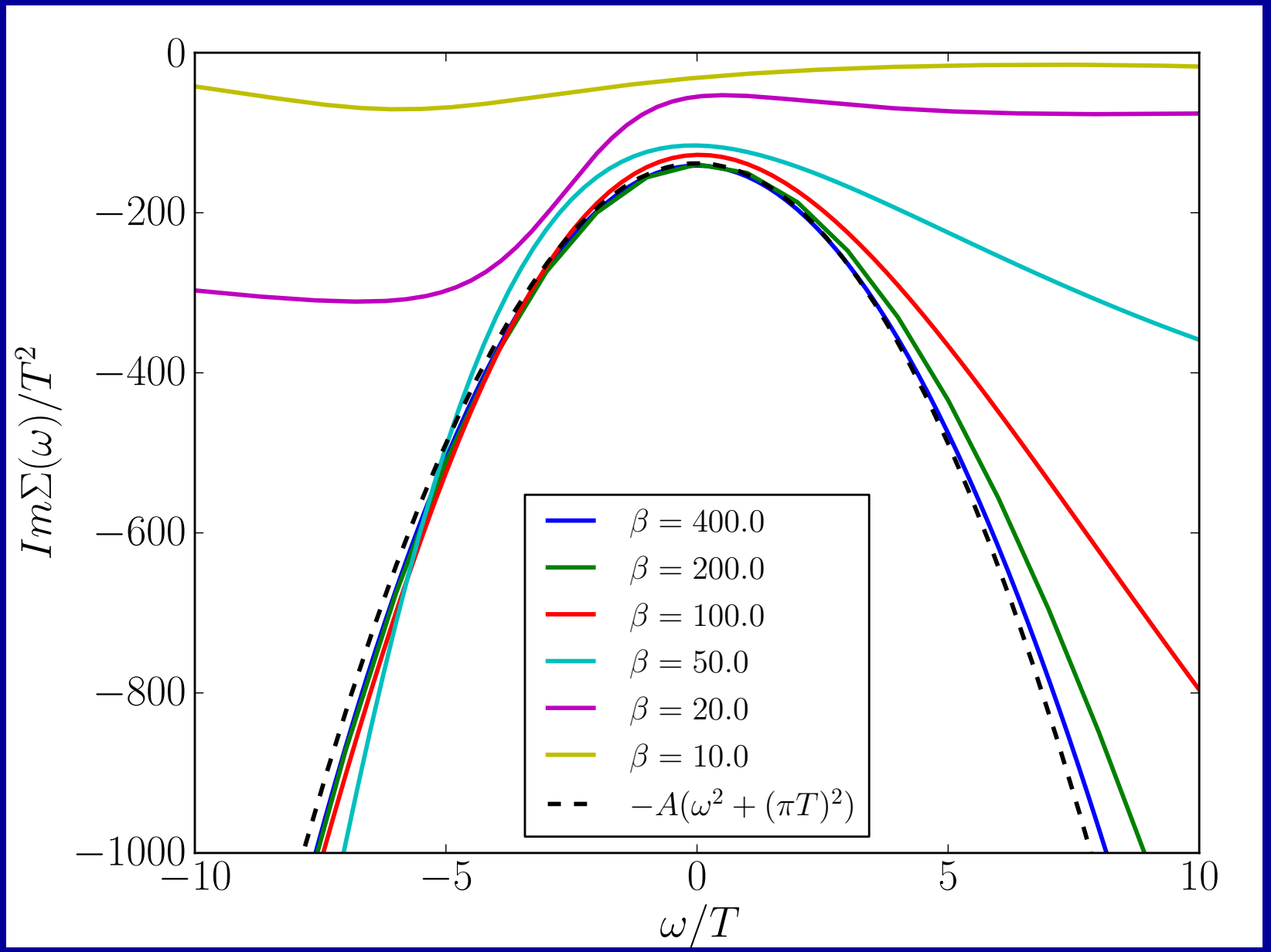
0
−200
−400
−600
−800
−1000
−10
−5
0
5
10
$Im\Sigma(\omega)/T^2$
ω/T
$\beta = 400.0$
$\beta = 200.0$
$\beta = 100.0$
$\beta = 50.0$
$\beta = 20.0$
$\beta = 10.0$
$-A(\omega^2 + (\pi T)^2)$

Momentum (energy) resolved spectral function

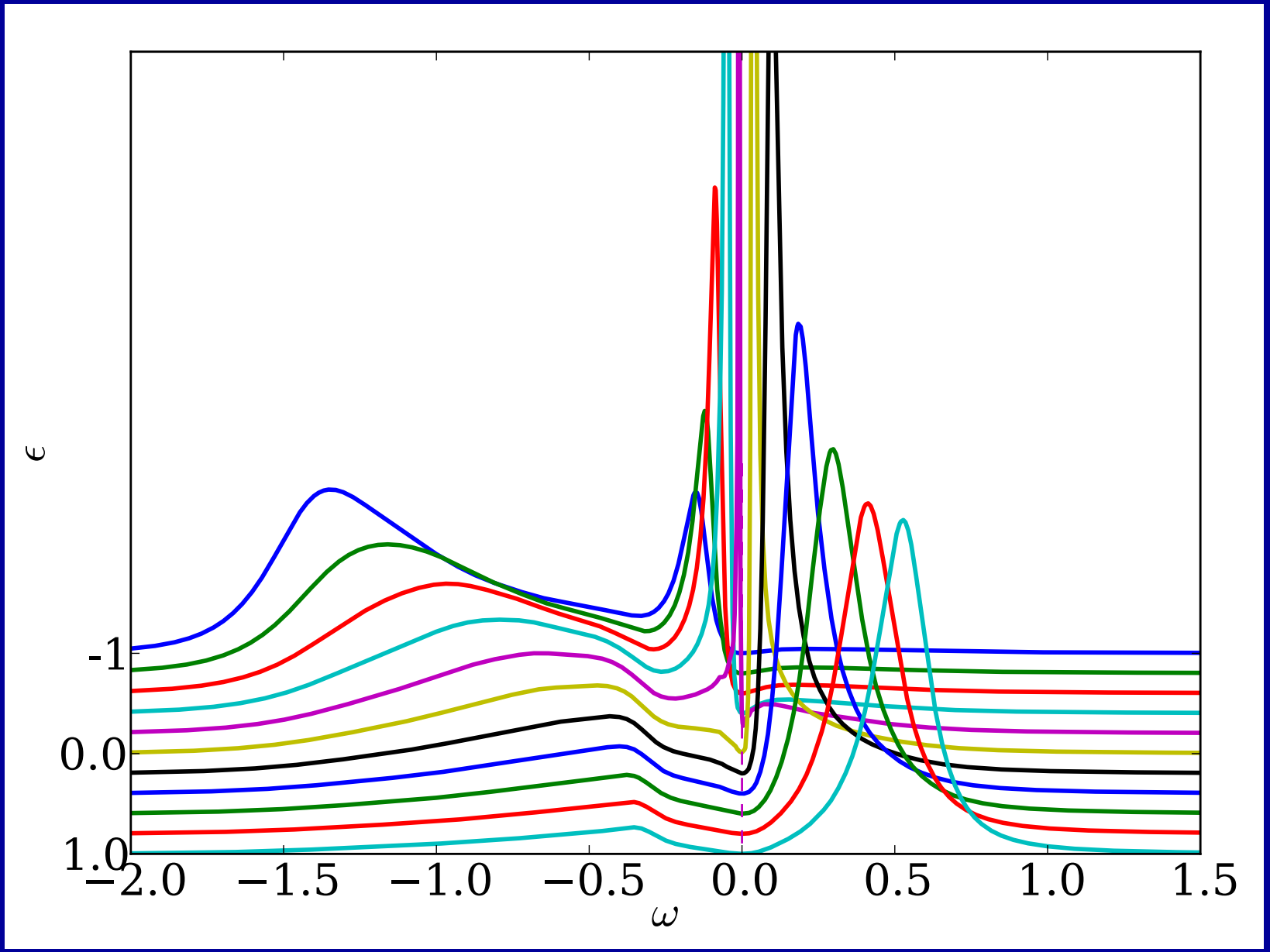

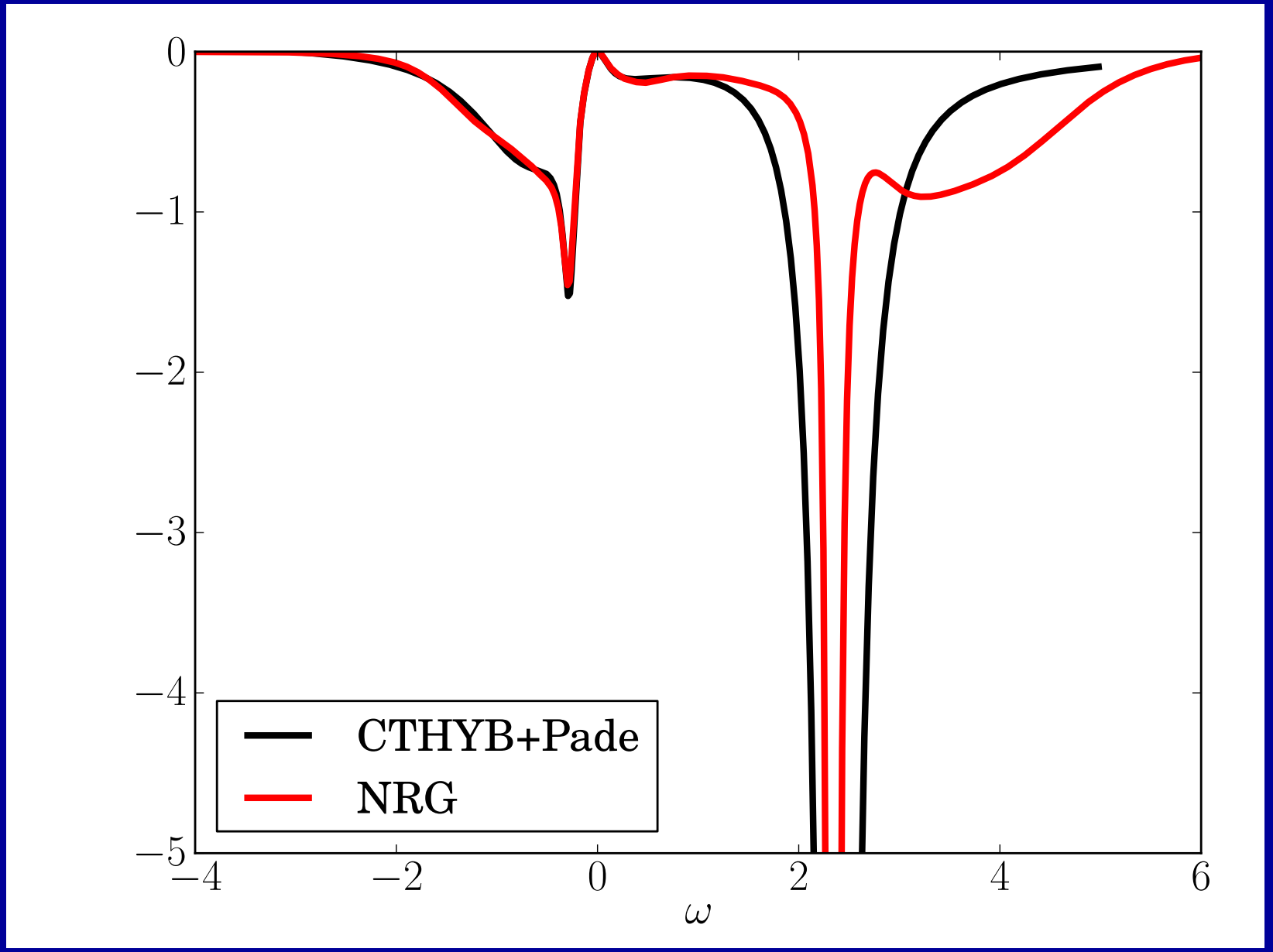
0
−1
−2
−3
−4
−5
−4
−2
0
2
4
6
ω
CTHYB+Pade
NRG

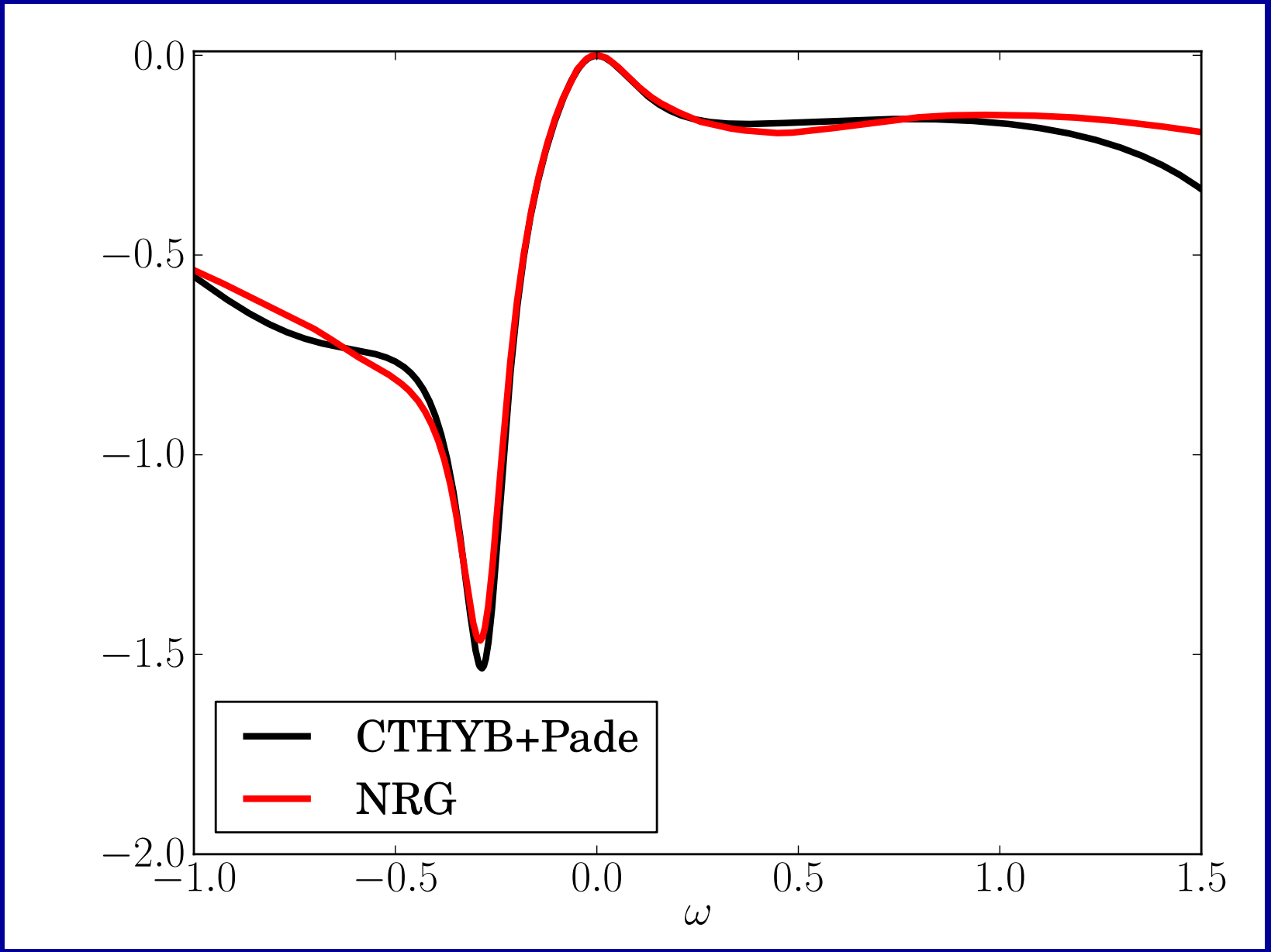
0.0
−0.5
−1.0
−1.5
−2.0
−1.0
−0.5
0.0
0.5
1.0
1.5
ω
CTHYB+Pade
NRG

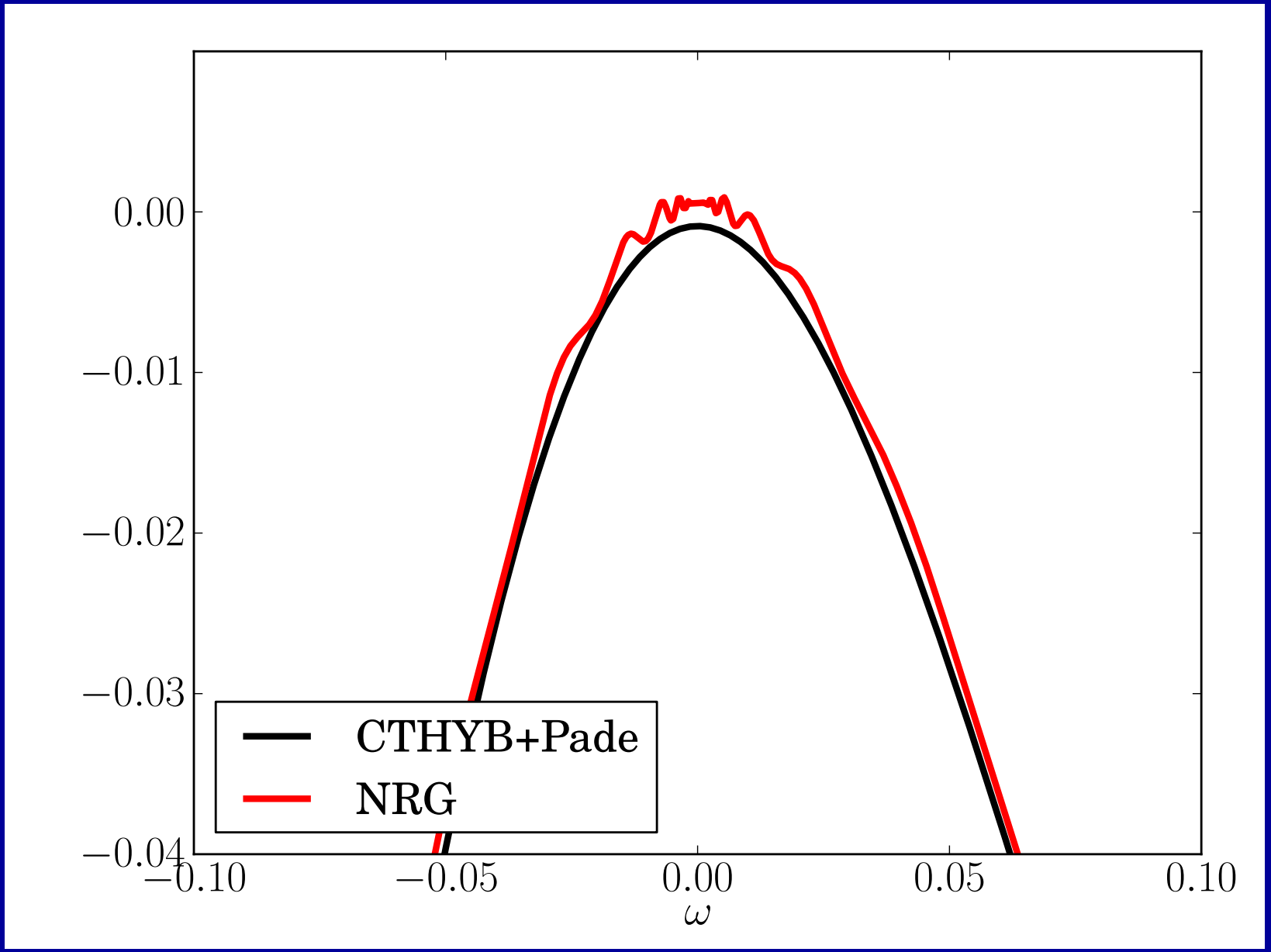
0.00
−0.01
−0.02
−0.03
−0.04
−0.10
−0.05
0.00
0.05
0.10
ω
CTHYB+Pade
NRG

DMFT insight into an old problem: "How bad metals become good"

`Resilient' *quasiparticles* *beyond Landau Theory*

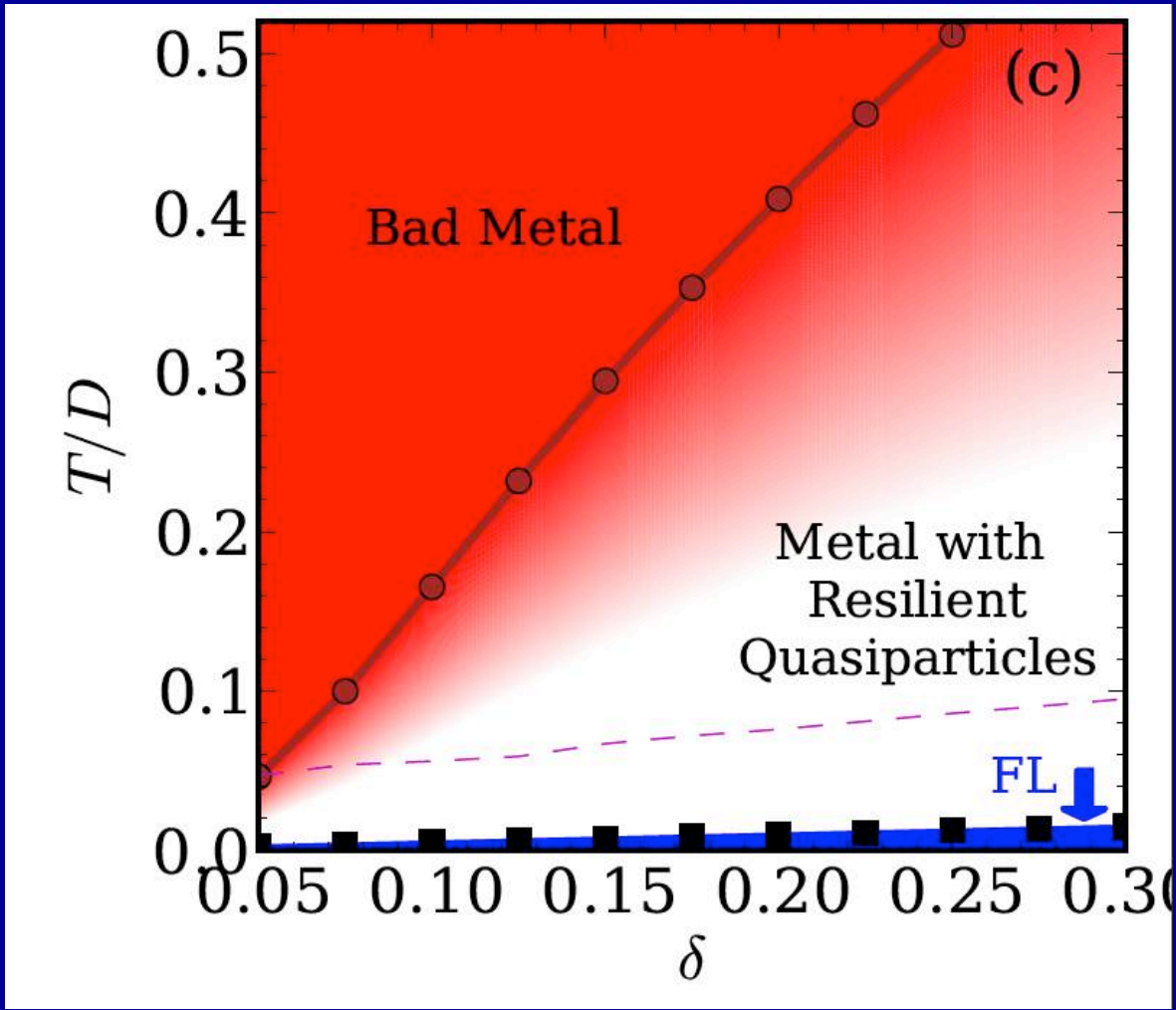

Deng et al.
PRL 110 (2013) 086401

Overview of calculated resistivity vs. T

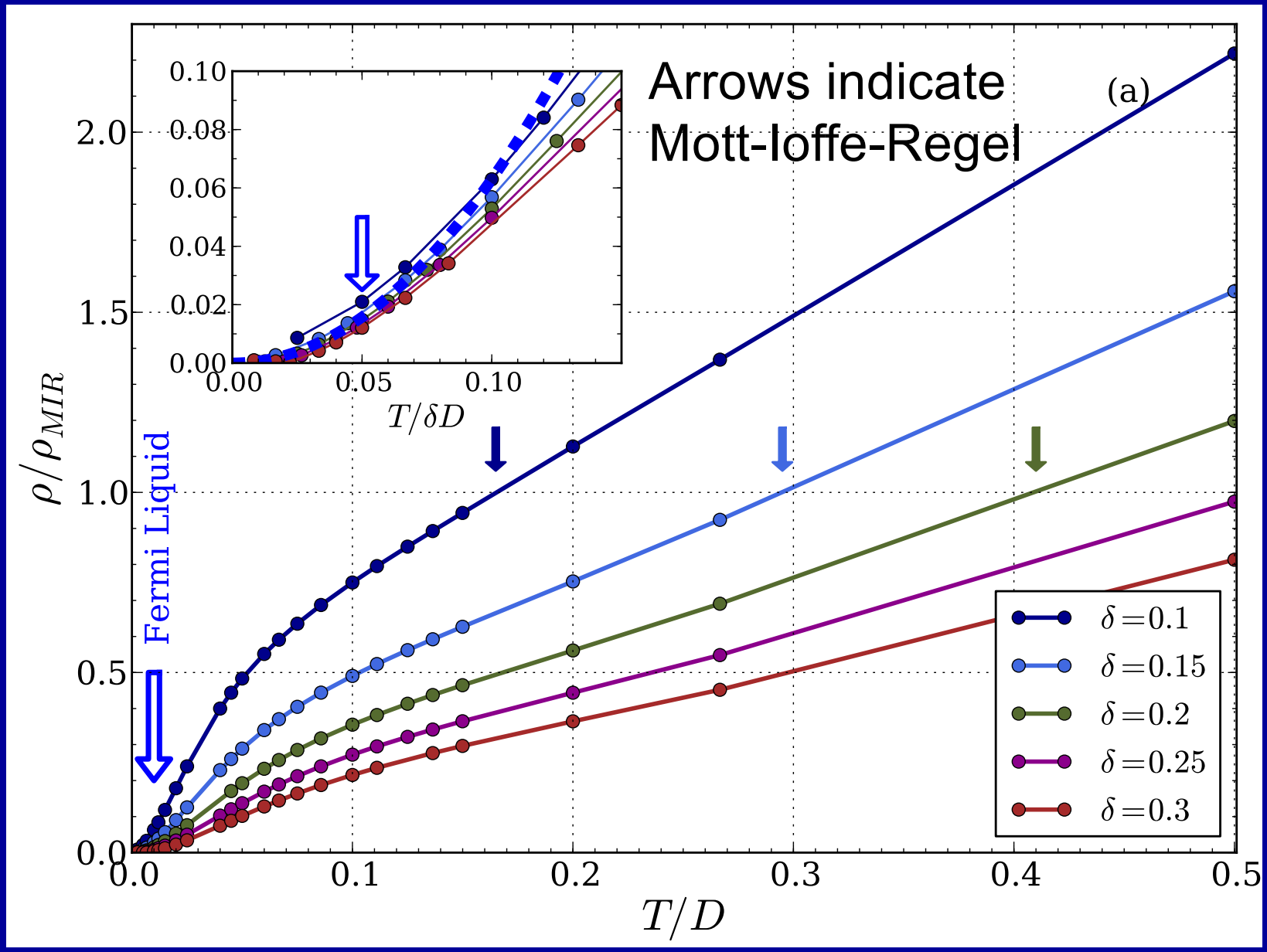

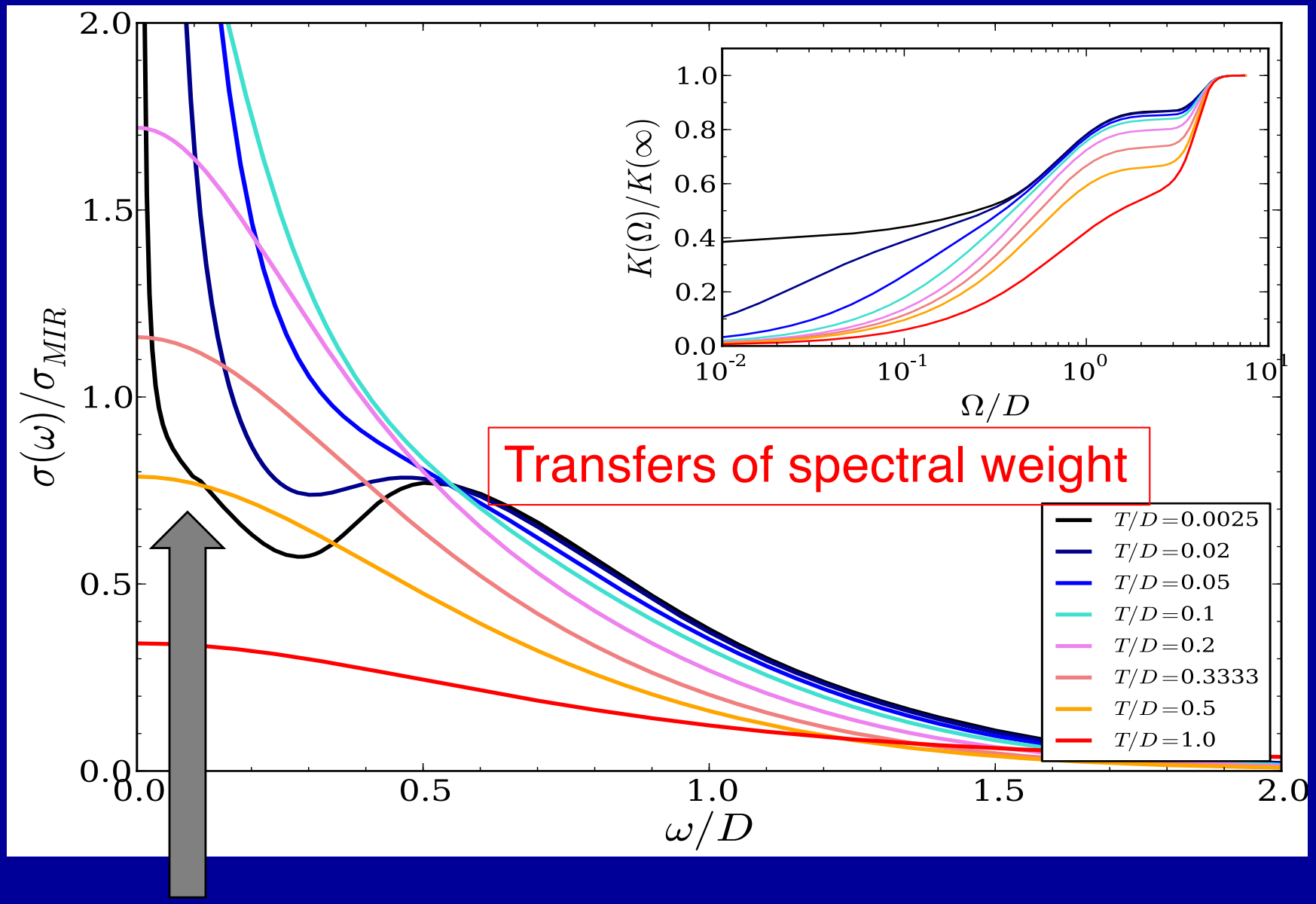

This non-Drude ``foot" is actually the signature of Landau's Fermi liquid in the optical spectrum !

Signature of the two crossovers (FL, MIR) in optical spectroscopy:

1. Merging of Drude peak and mid-infrared into broad peak at T_{FL}
2. Merging of QP band and LHB at T_{MIR}
3. Redistribution of sp.weight over very high energies at MIR, but involving only Drude+mid-infrared below T_{MIR}

cf. Hussey, Takenaka et al. LSCO PRB 2003
Hussey, Phil Mag
Gunnarsson RMP

Optical conductivity

Drude weight ~ doping

FIG. 108. N_D to N_{D0} as a function of δ (Katsufuji, Okimoto, and Tokura, 1995) for $La_{1-x}Sr_xTiO_3$.

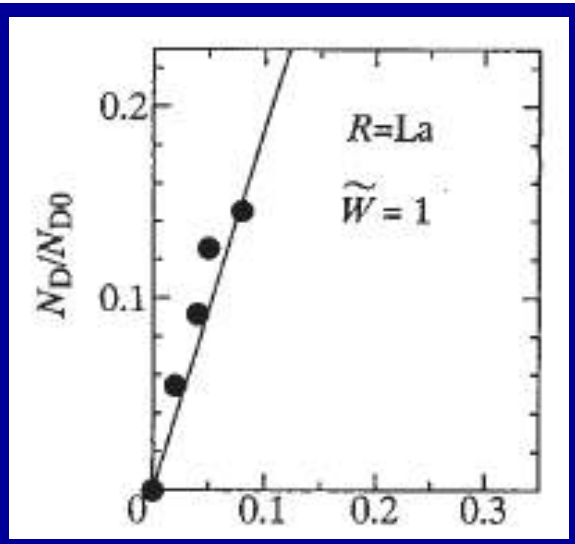

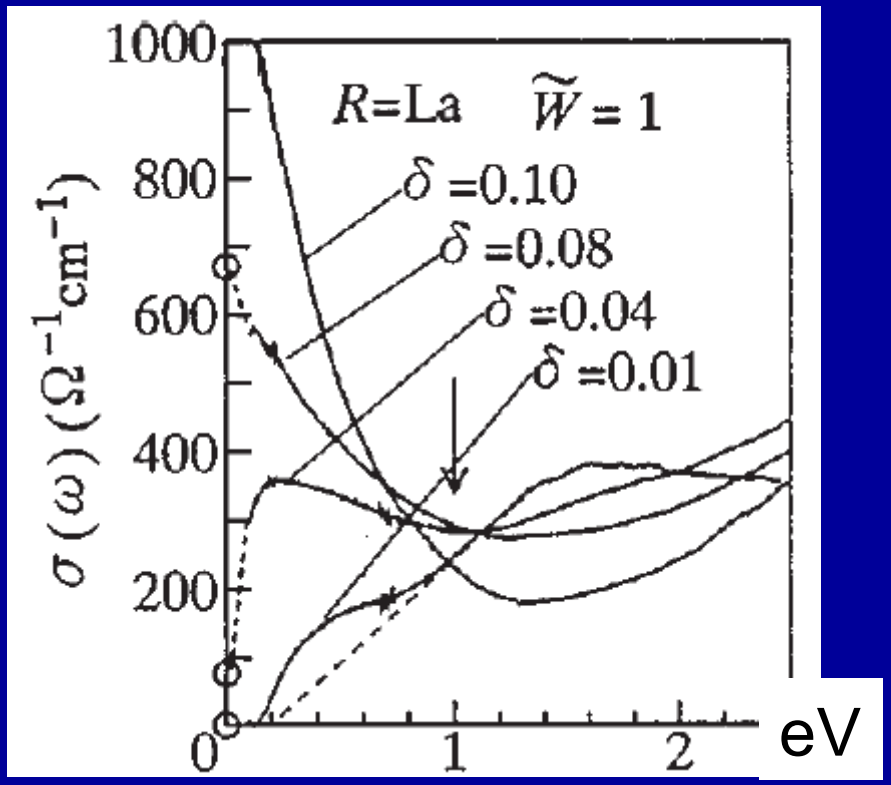

Large transfers of spectral weight

FIG. 107. Optical conductivity spectra in $R_{1-x}Sr_xTiO_{3+y}$ or $R_{1-x}Ca_xTiO_{3+y}$ (R=La, Nd, Sm, and Y). From Katsufuji, Okimoto, and Tokura, 1995.

The Mott critical endpoint: a liquid-gas like (Ising) transition

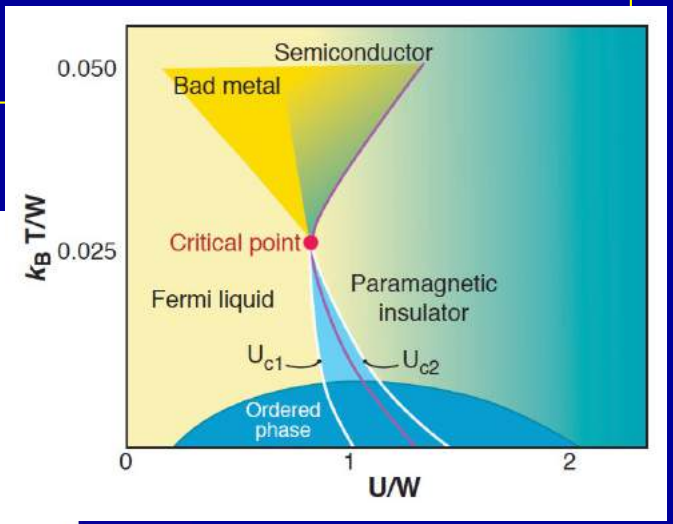

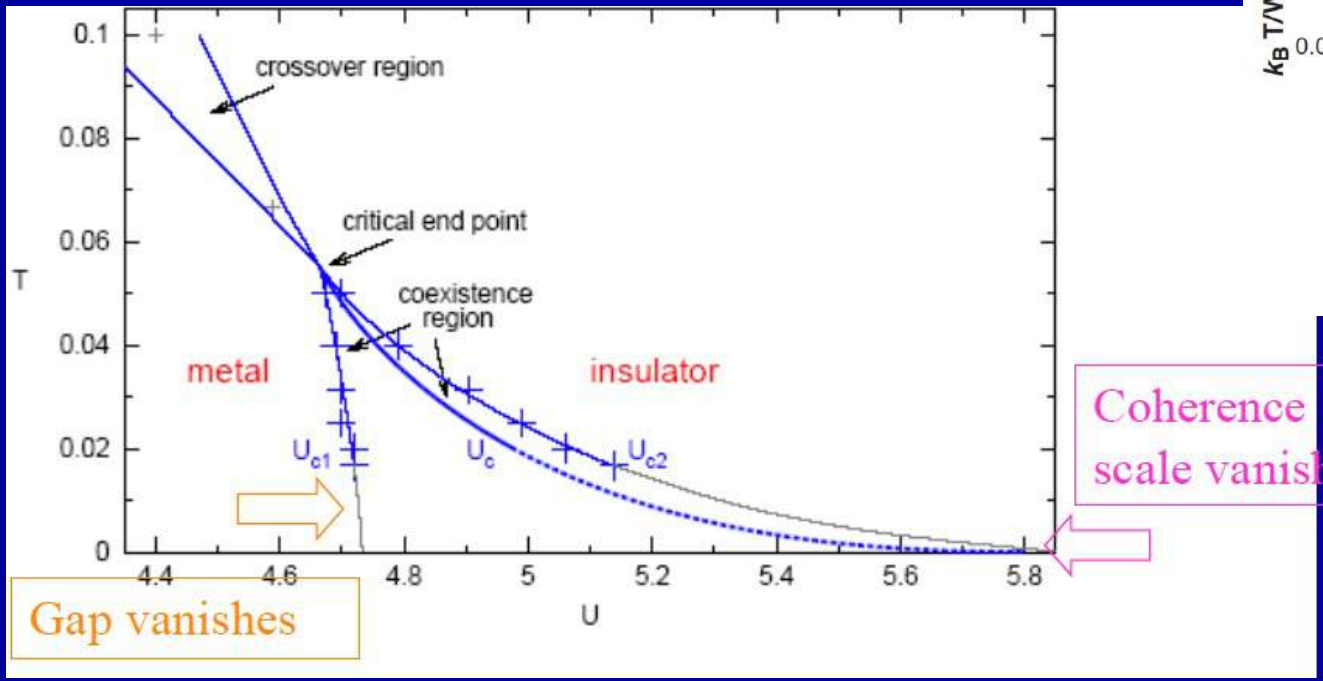

Unit here is bandwidth 2D

Critical behaviour at the Mott critical endpoint

A liquid-gas transition

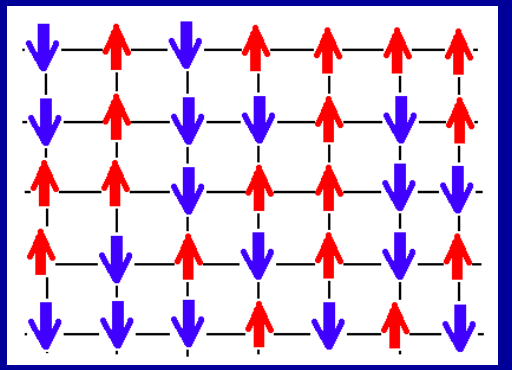

Insulator:
low-density of doubly occupied sites ➡ GAS

Metal:
High-density ➡ LIQUID

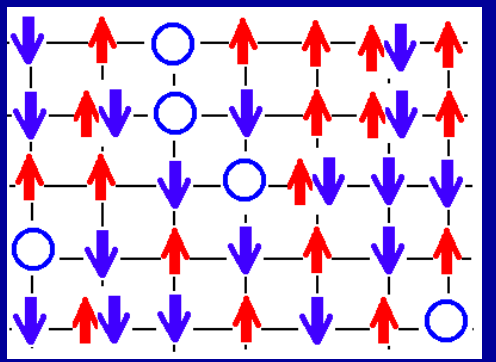

+ cf. early ideas of Castellani et al.
+ DMFT/Landau theory approach: **scalar** order parameter

New Model Hamiltonian for the Metal-Insulator Transition

C. Castellani
Istituto di Fisica, Università dell'Aquila, Aquila, Italy, and Istituto di Fisica "G. Marconi," Università di Roma, Roma, Italy, and Gruppo Nazionale di Struttura della Materia del Consiglio Nazionale delle Ricerche, Sezione dell'Aquila, Italy

and

C. Di Castro
Istituto di Fisica "G. Marconi," Università di Roma, Roma, Italy, and Gruppo Nazionale di Struttura della Materia del Consiglio Nazionale delle Ricerche, Sezione di Roma, Italy

and

D. Feinberg and J. Ranninger
Groupe des Transitions de Phases, Centre National de la Recherche Scientifique, Laboratoire Associée à l'Université Scientifique et Médicale de Grenoble, Grenoble, France

(Received 28 June 1979)

With use of the symmetry properties of the half-filled single-band Hubbard Hamiltonian, there is derived an effective Hamiltonian on a decimated lattice in which the spin and charge operators occur explicitly. Being a generalization of the Blume-Emery-Griffiths Hamiltonian for He^3-He^4 mixtures, this new statistical mechanical model permits one to give a preliminary discussion of the phase diagram of the correlated electron gas by establishing analogies with their results.

PRL 43 (1979) 1957

VOLUME 84, NUMBER 22 PHYSICAL REVIEW LETTERS 29 MAY 2000

Landau Theory of the Finite Temperature Mott Transition

G. Kotliar,[1] E. Lange,[1] and M. J. Rozenberg[2]
[1]*Serin Physics Laboratory, Rutgers University, 136 Frelinghuysen Road, Piscataway, New Jersey 08854*
[2]*Departamento de Física, FCEN, Universidad de Buenos Aires, Ciudad Universitaria Pabellón I, (1428) Buenos Aires, Argentina*

(Received 30 September 1999)

In the context of the dynamical mean-field theory of the Hubbard model, we identify microscopically an order parameter for the finite temperature Mott end point. We derive a Landau functional of the order parameter. We then use the order parameter theory to elucidate the singular behavior of various physical quantities which are experimentally accessible.

Universality and Critical Behavior at the Mott Transition

P. Limelette,[1*] A. Georges,[1,2] D. Jérome,[1] P. Wzietek,[1]
P. Metcalf,[3] J. M. Honig[3]

We report conductivity measurements of Cr-doped V_2O_3 using a variable pressure technique. The critical behavior of the conductivity near the Mott insulator to metal critical endpoint is investigated in detail as a function of pressure and temperature. The critical exponents are determined, as well as the scaling function associated with the equation of state. The universal properties of a liquid-gas transition are found. This is potentially a generic description of the Mott critical endpoint in correlated electron materials.

Science
302 (2003) 89

PHYSICAL REVIEW B **69**, 064511 (2004)

Transport criticality of the first-order Mott transition in the quasi-two-dimensional organic conductor κ-(BEDT-TTF)$_2$Cu[N(CN)$_2$]Cl

F. Kagawa,[1] T. Itou,[2] K. Miyagawa,[1,2] and K. Kanoda[1,2]
[1]*Department of Applied Physics, University of Tokyo, Bunkyo-ku, Tokyo 113-8656, Japan*
[2]*CREST, Japan Science and Technology Corporation, Kawaguchi 332-0012, Japan*
(Received 24 October 2003; published 27 February 2004)

nature Vol 436|28 July 2005|doi:10.1038/nature03806

LETTERS

Unconventional critical behaviour in a quasi-two-dimensional organic conductor

F. Kagawa[1], K. Miyagawa[1,2] & K. Kanoda[1,2]

V_2O_3

pressure / substitutions on V-site

Time-honoured example: V_2O_3 under pressure or chemical substitution on V-site

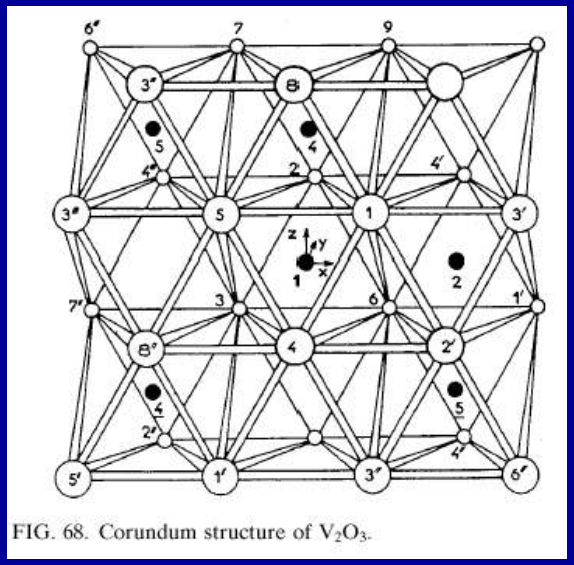

FIG. 68. Corundum structure of V_2O_3.

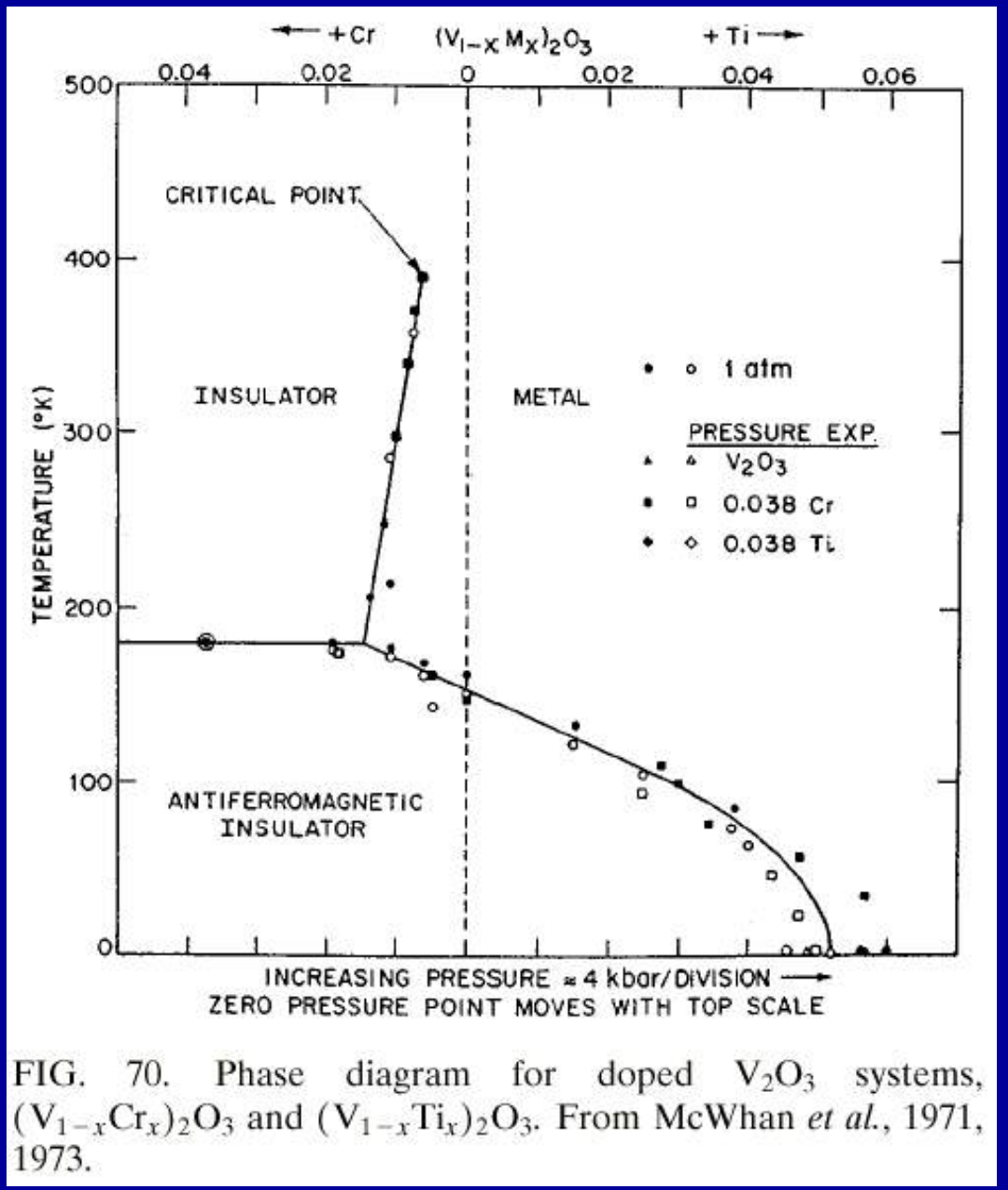

FIG. 70. Phase diagram for doped V_2O_3 systems, $(V_{1-x}Cr_x)_2O_3$ and $(V_{1-x}Ti_x)_2O_3$. From McWhan *et al.*, 1971, 1973.

Mc Whan et al. , 1971

Cartoons of the different phases

- ~ Free spins in paramagnetic insulator
>>> large entropy
>>> slope of Tc(p)
(cf Pomeranchuk)

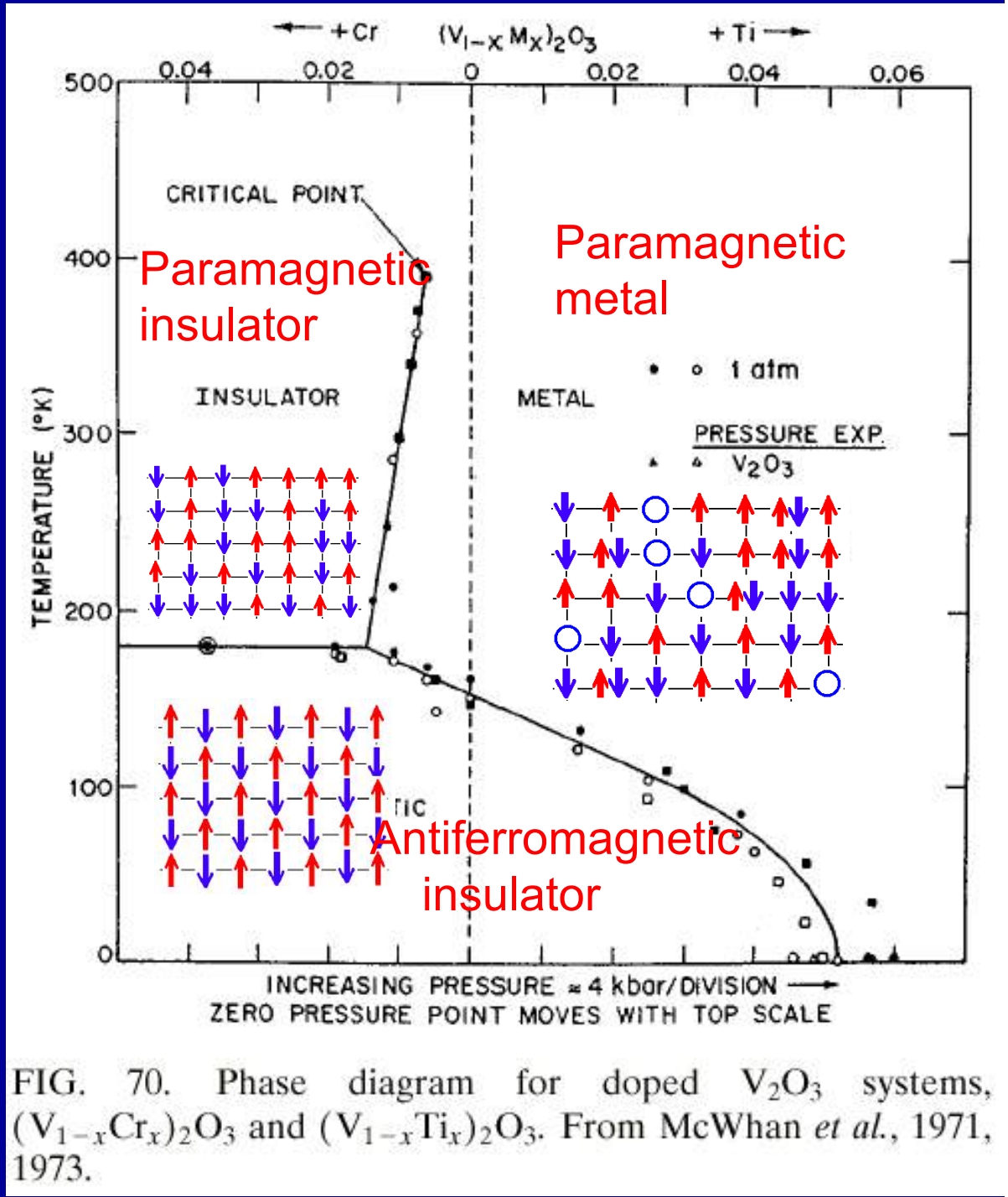

FIG. 70. Phase diagram for doped V_2O_3 systems, $(V_{1-x}Cr_x)_2O_3$ and $(V_{1-x}Ti_x)_2O_3$. From McWhan *et al.*, 1971, 1973.

Quasi-2D molecular conductors κ-(BEDT-TTF)$_2$X

BEDT-TTF :

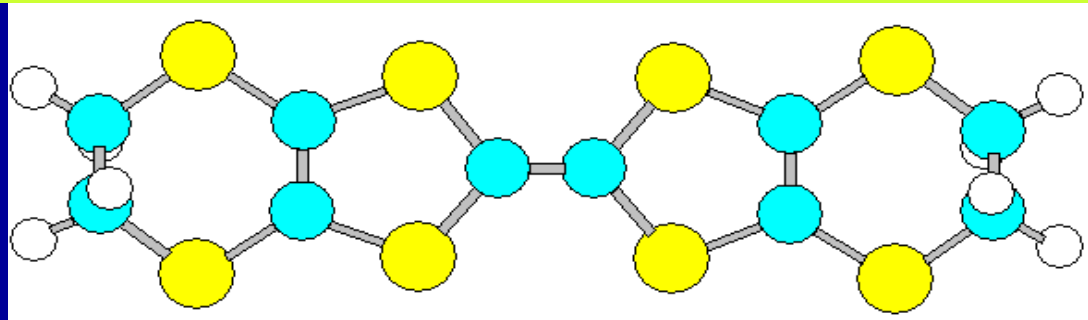

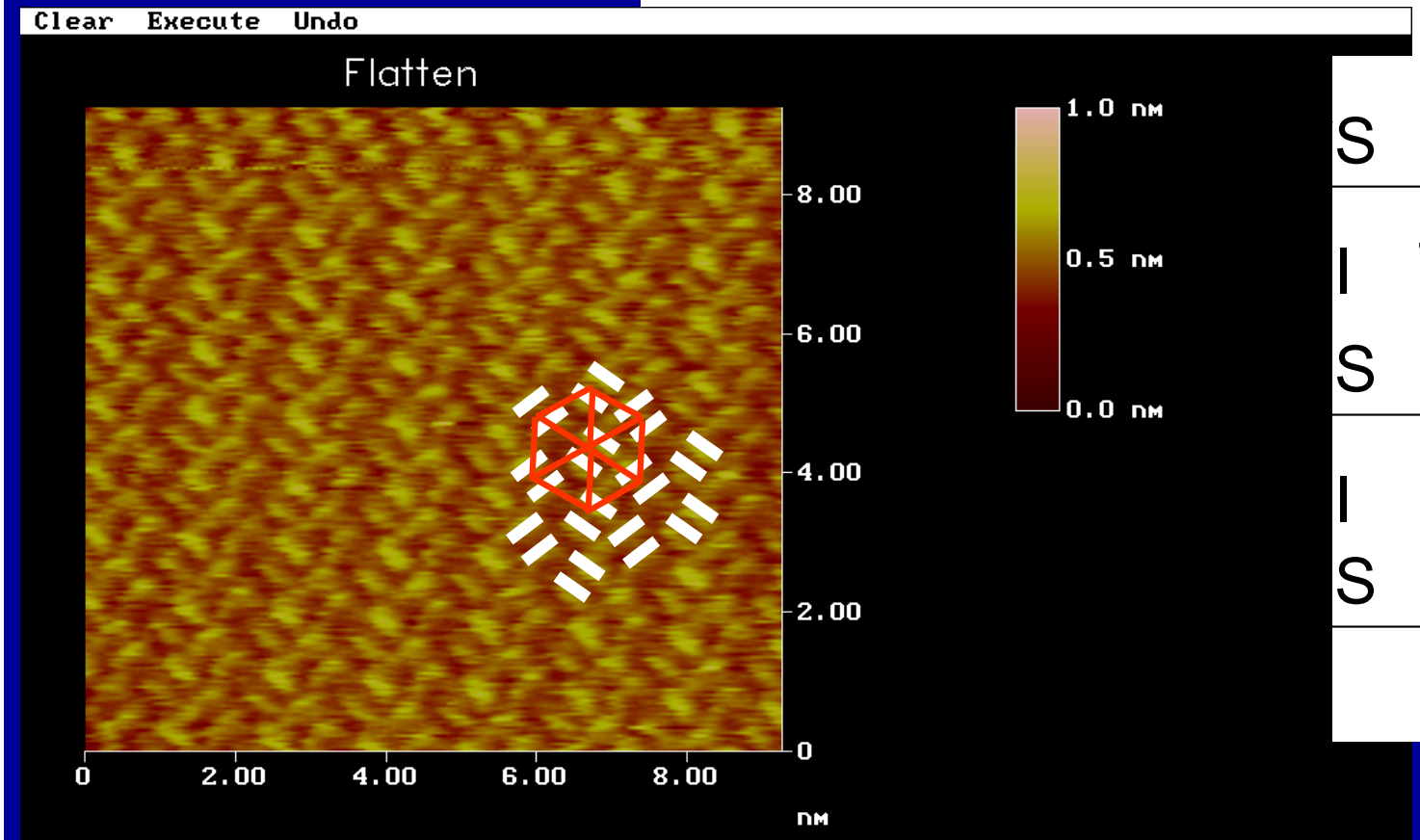

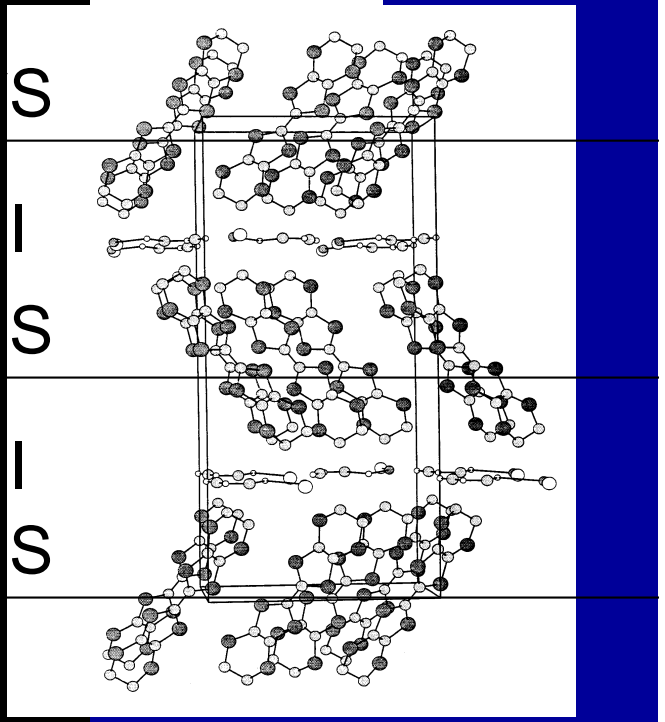

Z.Z.Wang, C.David, **L2M Bagneux**, P.Limelette, C.P.
résultats préliminaires

κ-$(ET)_2Cu[N(CN)_2]Cl$

Quasi 2D organic conductors: A rich phase diagram

From NMR experiments
Sherbrooke/Orsay
S.Lefebvre et al. :
Phys. Rev. Lett. **85** (2000) p. 5420

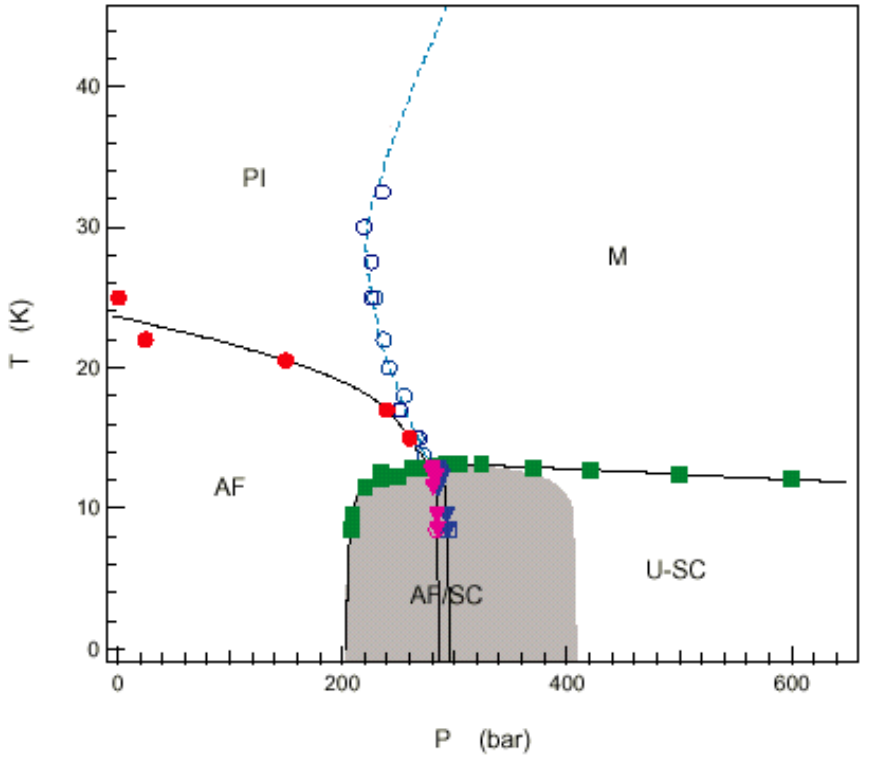

FIG. 1. Temperature *vs* pressure phase diagram of $\kappa-$Cl. The antiferromagnetic (AF) critical line $T_N(P)$ (dark circles) was determined from NMR relaxation rate while $T_c(P)$ for unconventional superconductivity (U-SC: squares) and the metal-insulator $T_{MI}(P)$ (MI: open circles) lines were obtained from the AC susceptibility. The AF-SC boundary (double dashed line) is determined from the inflexion point of χ'(P) and, for 8.5K, from sublattice magnetization. This boundary line separates two regions of inhomogeneous phase coexistence (shaded area).

Another beautiful system in which to study the Mott transition: Cs_3C_{60}

PRL 118, 237601 (2017) PHYSICAL REVIEW LETTERS week ending 9 JUNE 2017

Mott Transition in the *A*15 Phase of Cs_3C_{60}: Absence of a Pseudogap and Charge Order

H. Alloul,[1] P. Wzietek,[1] T. Mito,[1] D. Pontiroli,[2] M. Aramini,[3,2] M. Riccò,[2] J. P. Itie,[4] and E. Elkaim[4]

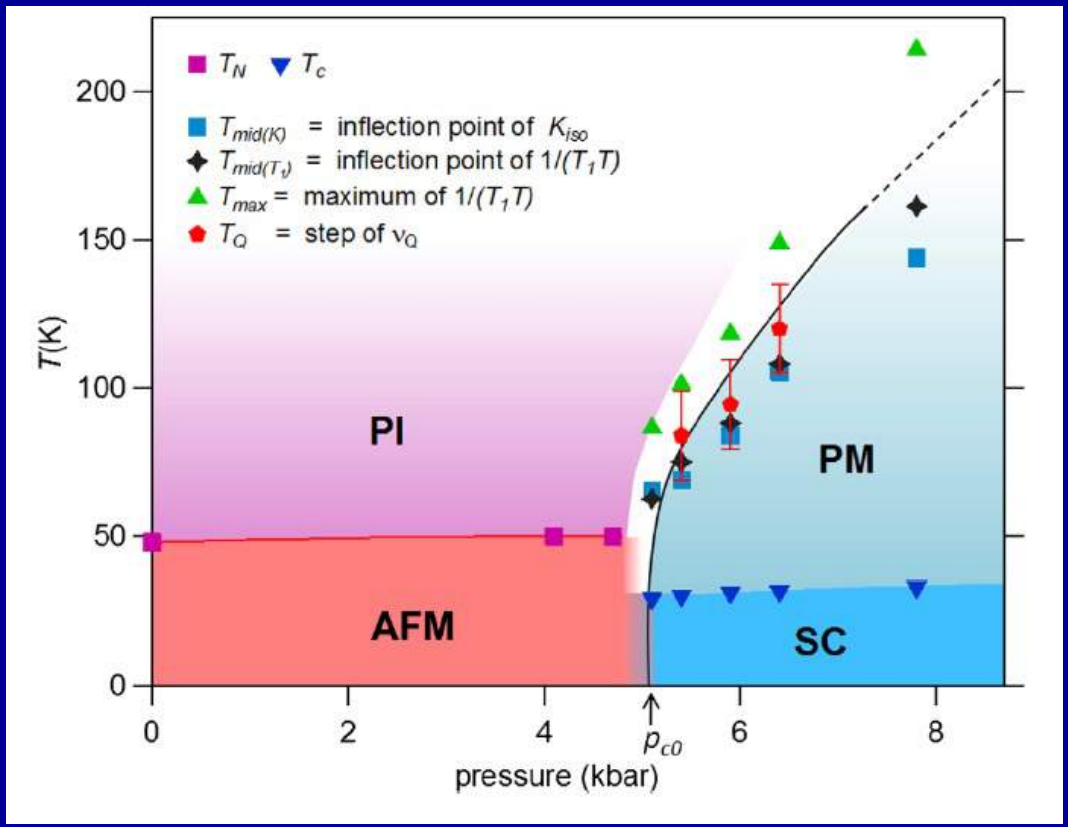

FIG. 4. MIT transition temperatures T_Q, $T_{\mathrm{mid}(T_1)}$, $T_{\mathrm{mid}(K)}$, and $T_{\max}$ deduced from ^{133}Cs NMR data for $p > 5.4$ kbar. The T_Q data mark the weak first-order regime (solid line), while $T_{\max}$ delineates the apparent upper half width of the transition given as the blank zone. This suggests that the transition becomes a crossover (dotted line) at high (T, p) beyond a critical point $p_c \simeq 7$ kbar (see the text). The AFM and SC fractions measured in Fig. 1(b) yielded $p_{c0} = 5.1 \pm 0.3$ kbar below 35 K. The phase diagram is completed by the horizontal T_N line below 5.1 kbar, and the T_c dome above 5.1 kbar.

Tuning the transition with pressure in V_2O_3

P. Limelette et al. (Orsay)
Science, 2003

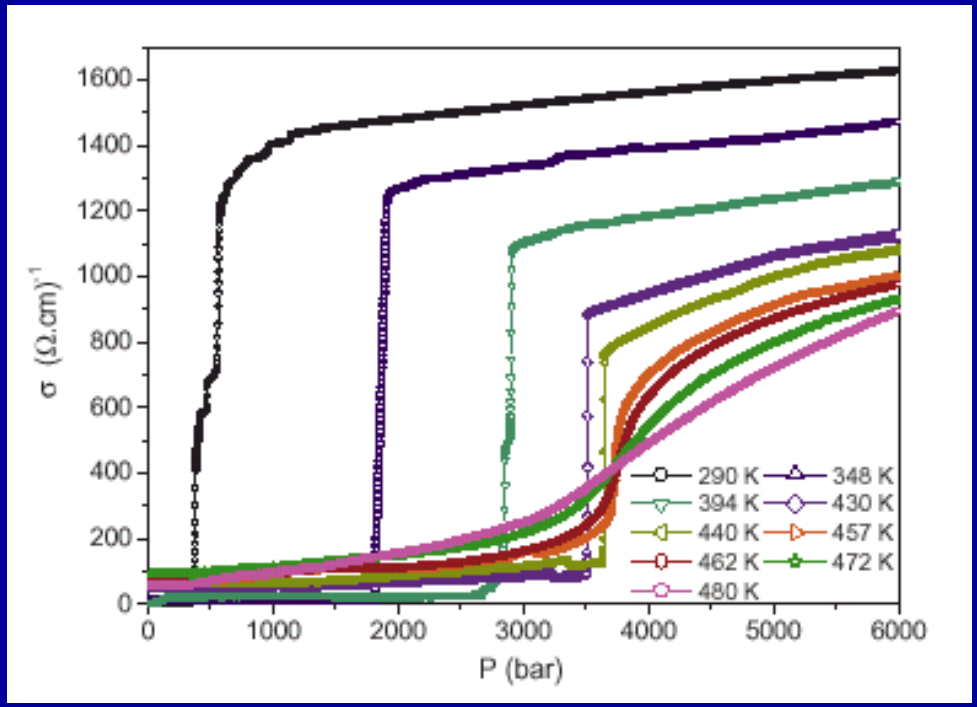

Fig. S1: Conductivity as a function of decreasing pressure, for temperatures ranging from T=485 K ($>T_c$=457.5 K) down to T=290 K ($<<T_c$). Only a selected set of values of T has been displayed for clarity (from the top at high pressure: 290, 348, 394, 430, 440, 457, 462, 472 and 480 K).

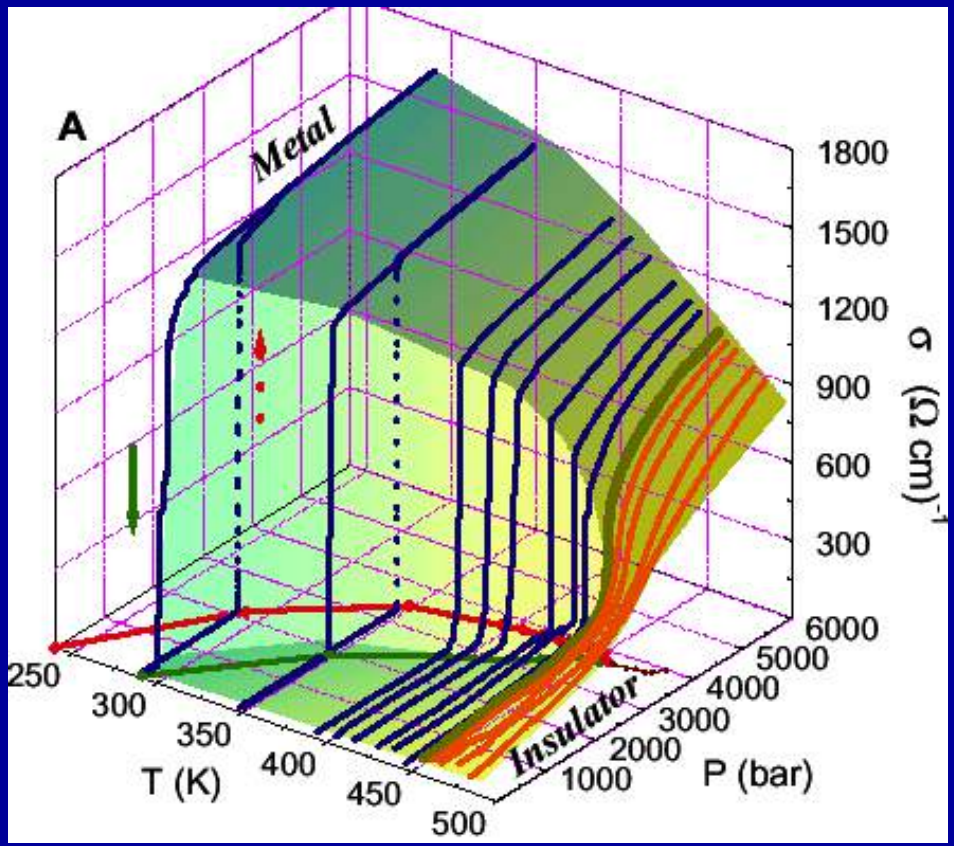

Analogy between the liquid-gas transition and the Mott transition

Hubbard model	Mott MIT	Liquid-gas	Ising model
$W - W_c$	$p - p_c$	$p - p_c$	Field h
$T - T_c$	$T - T_c$	$T - T_c$	Distance to cr. pt.
Low-ω spectral weight	id.	$v_g - v_L$	Order parameter (scalar)

In fact: $p-p_c$ and $T-T_c$ are linear combineations of h and $T-T_c$ for the Ising model

Critical exponent: Ising-like

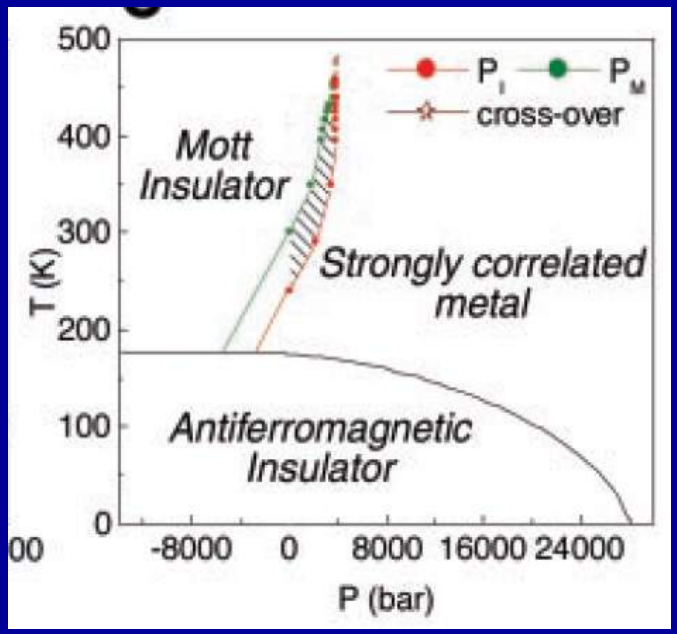

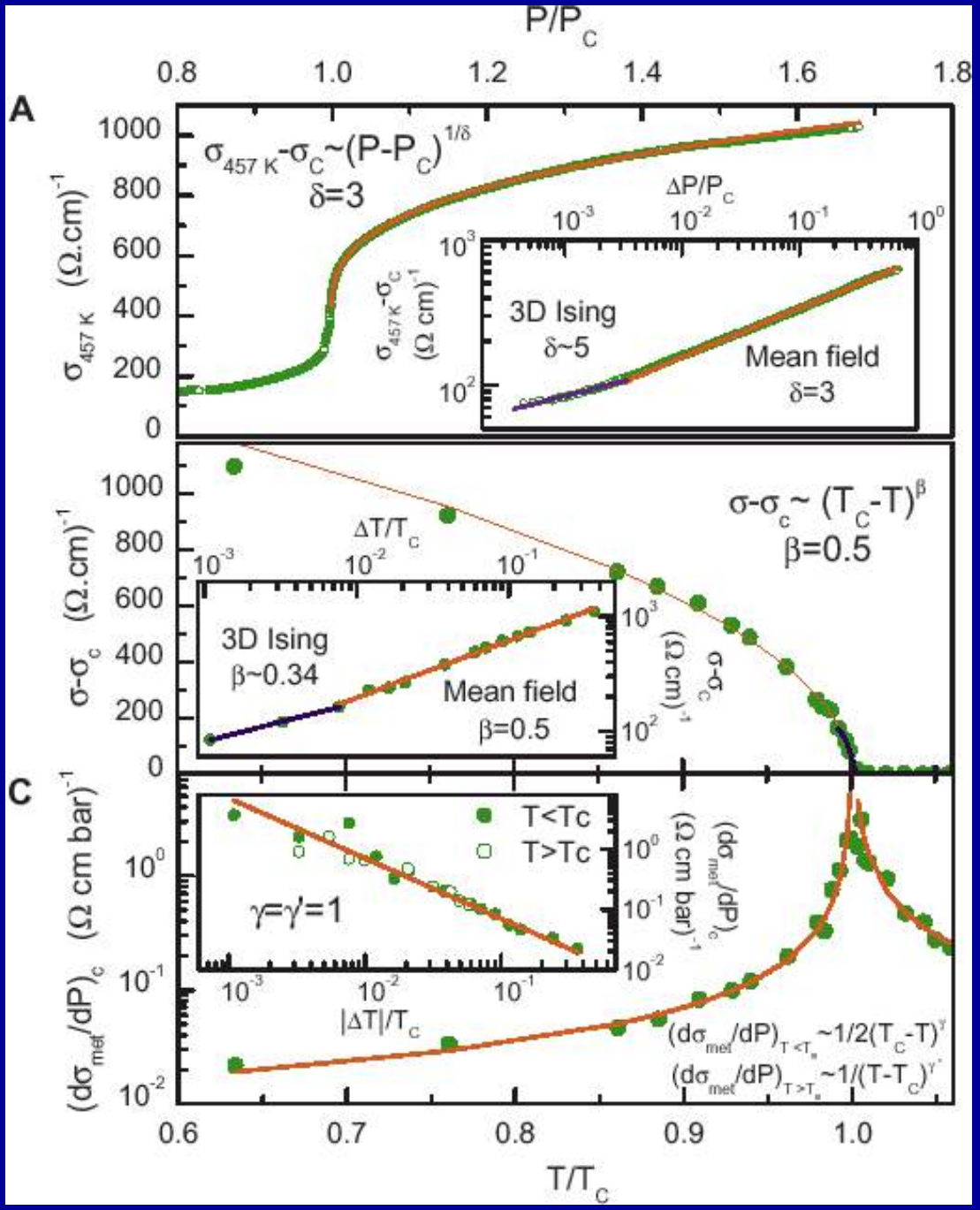

Scaling: Universal form of the ``equation of state''

$$\sigma_{met}(P,T) - \sigma_c = (\delta h)^{1/\delta} f_{\pm}\left(\frac{\delta h}{|r|^{\gamma\delta/(\delta-1)}}\right)$$

Cf also: Kagawa et al. (Kanoda's group) on the BEDT organics

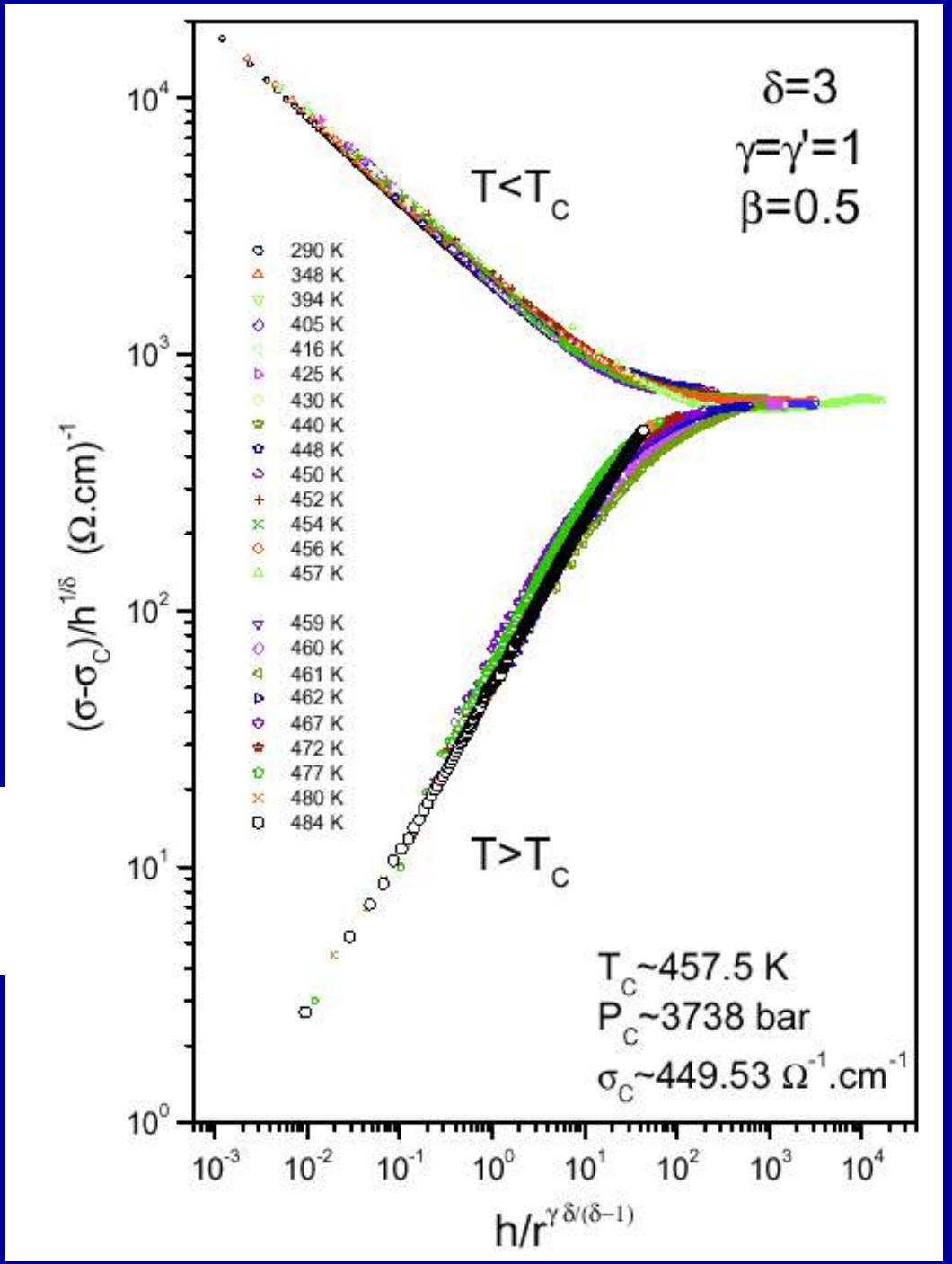

Is there something quantum about the observed scaling <u>above</u> (T_c,U_c) ?

PRL 107, 026401 (2011) PHYSICAL REVIEW LETTERS week ending 8 JULY 2011

Quantum Critical Transport near the Mott Transition

H. Terletska,[1] J. Vučičević,[2] D. Tanasković,[2] and V. Dobrosavljević[1]

[1]*Department of Physics and National High Magnetic Field Laboratory, Florida State University, Tallahassee, Florida 32306, USA*
[2]*Scientific Computing Laboratory, Institute of Physics Belgrade, University of Belgrade, Pregrevica 118, 11080 Belgrade, Serbia*

(Received 26 January 2011; published 5 July 2011)

We perform a systematic study of incoherent transport in the high temperature crossover region of the half filled one-band Hubbard model. We demonstrate that the family of resistivity curves displays characteristic quantum critical scaling of the form $\rho(T, \delta U) = \rho_c(T) f(T/T_0(\delta U))$, with $T_0(\delta U) \sim |\delta U|^{z\nu}$, and $\rho_c(T) \sim T$. The corresponding β function displays a "strong coupling" form $\beta \sim \ln(\rho_c/\rho)$, reflecting the peculiar mirror symmetry of the scaling curves. This behavior, which is surprisingly similar to some experimental findings, indicates that Mott quantum criticality may be acting as the fundamental mechanism behind the unusual transport phenomena in many systems near the metal-insulator transition.

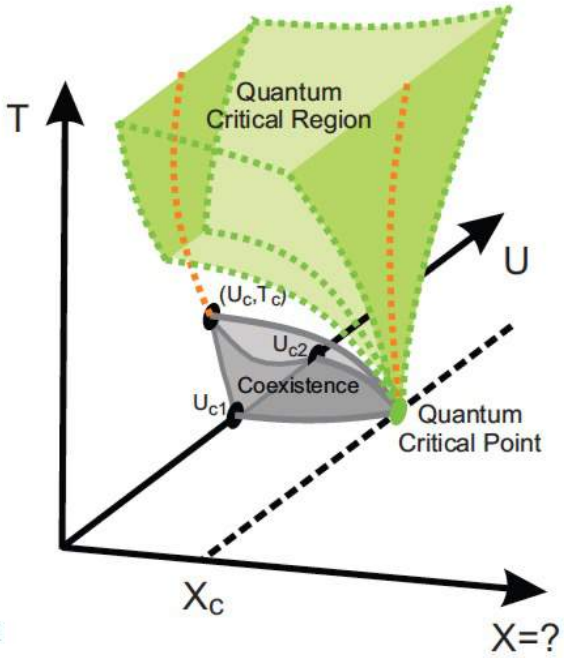

PHYSICAL REVIEW B 88, 075143 (2013)

Finite-temperature crossover and the quantum Widom line near the Mott transition

J. Vučičević,[1] H. Terletska,[2] D. Tanasković,[1] and V. Dobrosavljević[3]

nature materials LETTERS
https://doi.org/10.1038/s41563-018-0140-3

Quantum spin liquids unveil the genuine Mott state

A. Pustogow[1*], M. Bories[1], A. Löhle[1], R. Rösslhuber[1], E. Zhukova[2], B. Gorshunov[2], S. Tomić[3], J. A. Schlueter[4,5], R. Hübner[1,6], T. Hiramatsu[7], Y. Yoshida[7,8], G. Saito[7,9], R. Kato[10], T.-H. Lee[11], V. Dobrosavljević[11], S. Fratini[12] and M. Dressel[1]

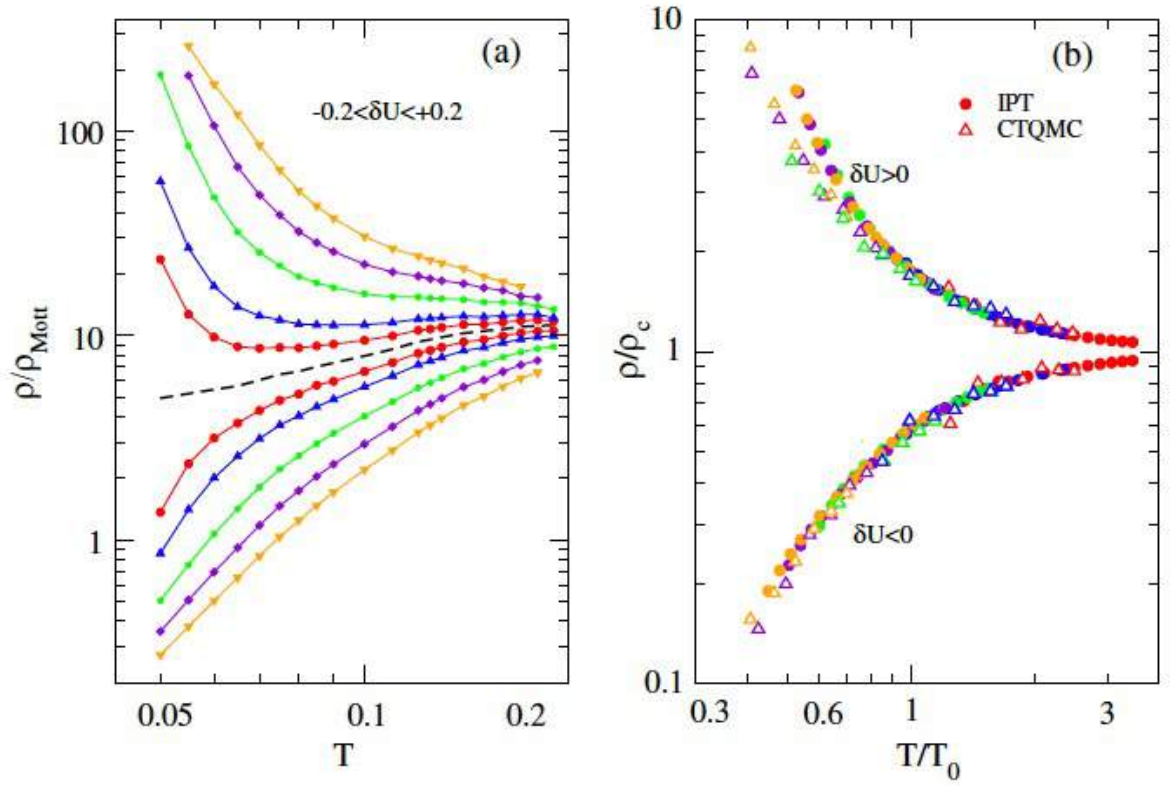

FIG. 1 (color online). (a) DMFT resistivity curves as a function of temperature along different trajectories $-0.2 \leq \delta U \leq +0.2$ with respect to the instability line $\delta U = 0$ (black dashed line; see the text). Data are obtained by using IPT impurity solver. (b) Resistivity scaling; essentially identical scaling functions are found from CTQMC (open symbols) and from IPT (closed symbols).

Terletska et al. PRL 2011

Unified Phase Diagram

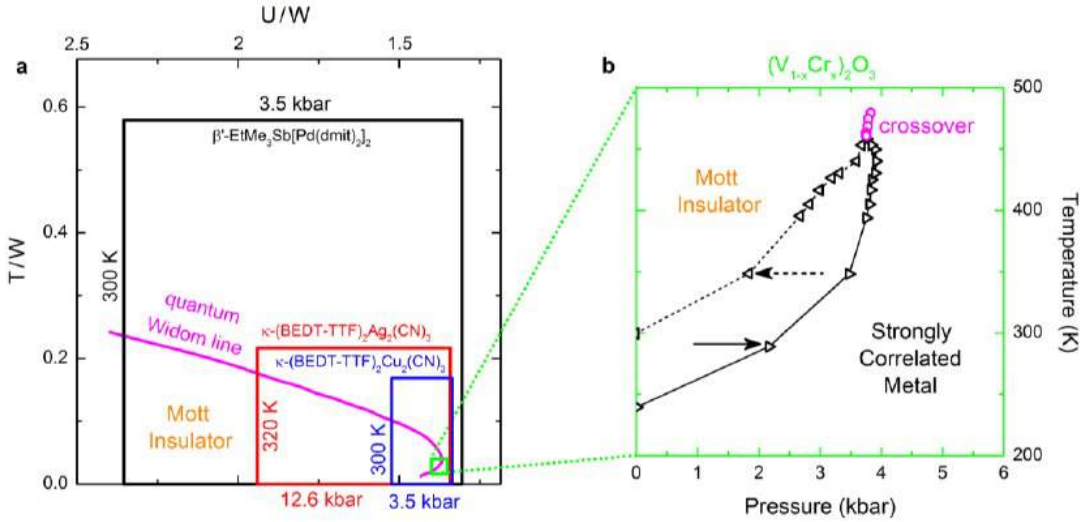

transition-metal oxide V_2O_3

- similar shape of QWL
- comparable *p*, *T* scales
- smaller *T*/*W* – *U*/*W* range (larger bandwidth)

Unified Phase Diagram Valid for *all* Mott insulators!

Limelette *et al.*, *Science* **302**, 89-92 (2003)

Courtesy A.Pustogow – APD March Meeting, 2019

Beyond (single-site) DMFT: taking better account of spatial correlations

To what extent does DMFT take spatial correlations into account ?

- Key point: $J_{ij} = O(\frac{1}{d}) \ , \ \sum_j J_{ij} = O(1)$

- → Ordered Phases have Tc = O(1)
- 2-particle correlation functions know about ordering and critical behavior: non-trivial $\chi(\vec{Q}, \omega)$
- BUT NO FEEDBACK OF SPATIAL CORRELATIONS/FLUCTUATIONS INTO 1-PARTICLE PROPERTIES

We expect:

- The divergence of the effective mass to be cutoff by (spin) correlations
- e.g. large-N t-J: $Z \propto \delta \quad , \quad m^*/m \sim \left[\delta + \frac{J}{td}\right]^{-1}$
- cf. finite entropy of low-T insulator

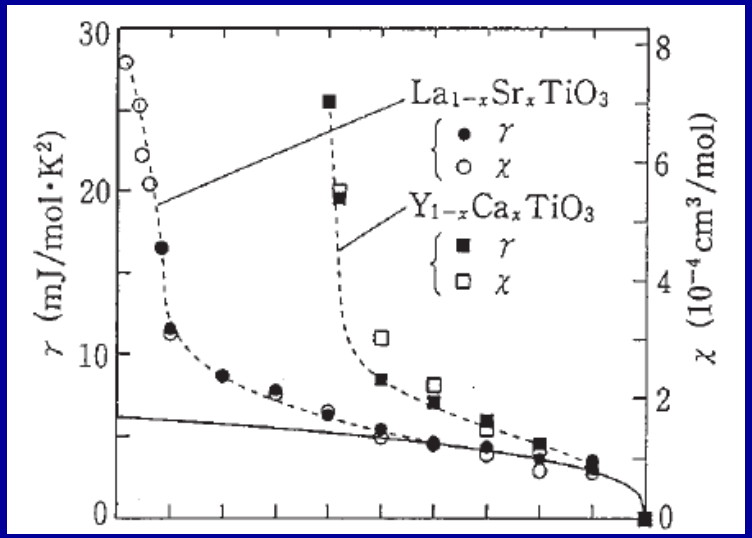

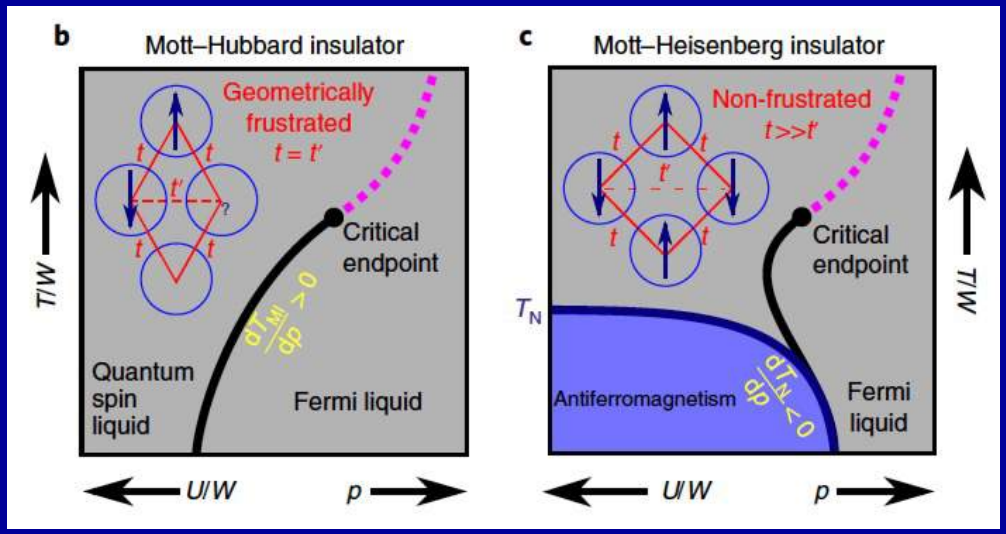

Suppression of Pomeranchuk effect at low T

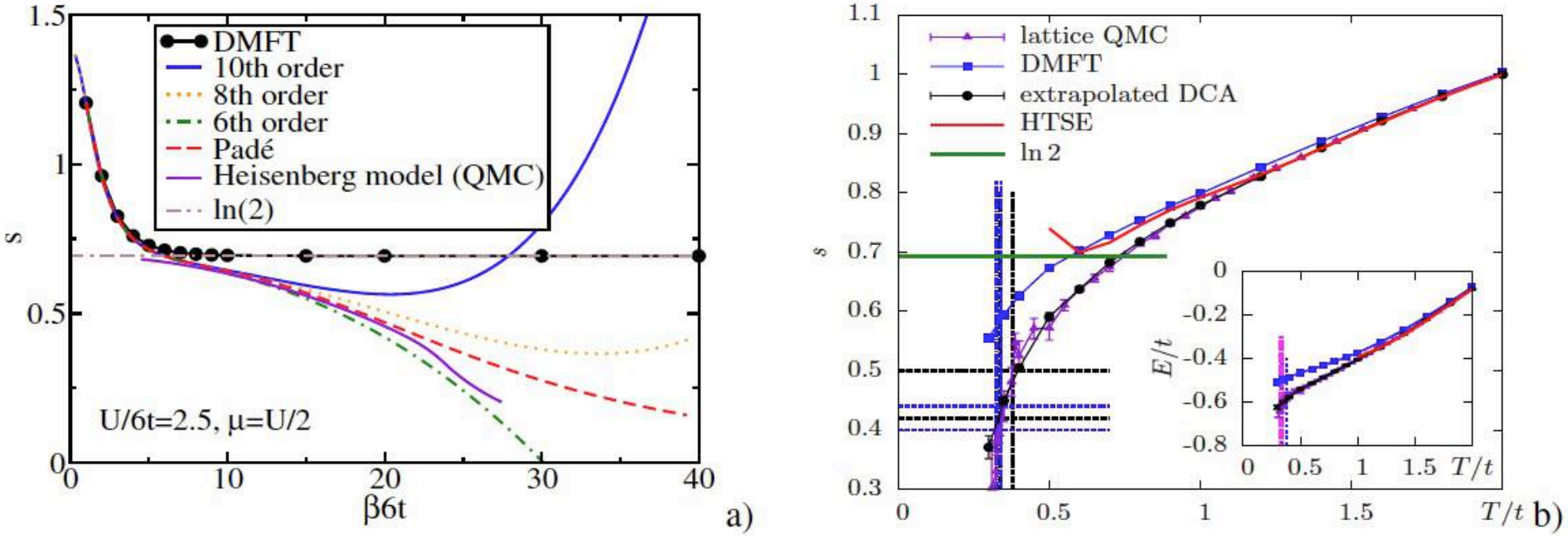

Fig. 3 (online colour at: www.ann-phys.org) Entropy per site of the half-filled Hubbard model on a cubic lattice. a) At $U/t = 15$, from single-site DMFT and high-temperature series at various orders (reproduced from [10]). For comparison, the QMC result of [20] for the Heisenberg model is also displayed. b) At $U/t = 8$, from single-site DMFT, extrapolations of cluster (DCA) methods, and direct lattice Monte-Carlo (reproduced from [17]).

The most extreme influence of J on quasiparticles: cuprates and the d=2 1-band Hubbard model

- Fate of quasiparticles in the 2D Hubbard model as the Mott transition is approached: selective destruction in k-space

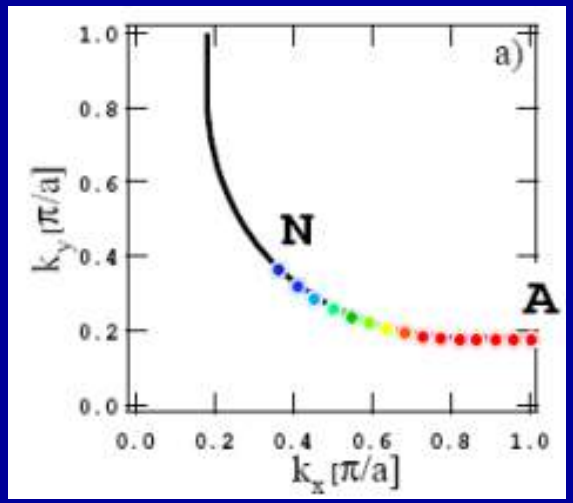

ARPES- Kaminski et al., 2004
Bi2212
Tc=90K@T=140K

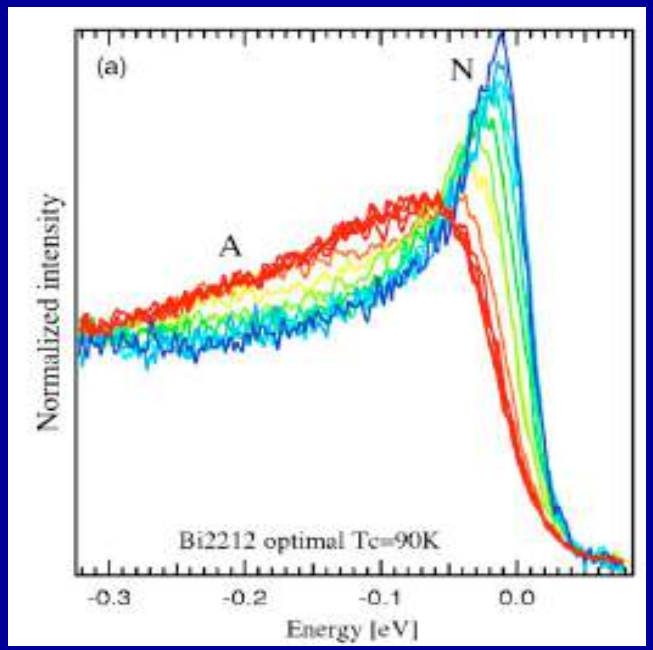

`Fluctuation Diagnostics':
AF correlations are responsible for the pseudogap

PRL 114, 236402 (2015) PHYSICAL REVIEW LETTERS week ending 12 JUNE 2015

Fluctuation Diagnostics of the Electron Self-Energy: Origin of the Pseudogap Physics

O. Gunnarsson,[1] T. Schäfer,[2] J. P. F. LeBlanc,[3,4] E. Gull,[4] J. Merino,[5] G. Sangiovanni,[6] G. Rohringer,[2] and A. Toschi[2]
[1]*Max-Planck-Institut für Festkörperforschung, Heisenbergstraße 1, D-70569 Stuttgart, Germany*
[2]*Institute of Solid State Physics, Vienna University of Technology, A-1040 Vienna, Austria*
[3]*Max-Planck-Institute for the Physics of Complex Systems, D-01187 Dresden, Germany*
[4]*Department of Physics, University of Michigan, Ann Arbor, Michigan 48109, USA*
[5]*Departamento de Física Teórica de la Materia Condensada, IFIMAC Universidad Autónoma de Madrid, Madrid 28049, Spain*
[6]*Institute of Physics and Astrophysics, University of Würzburg, D-97070 Würzburg, Germany*
(Received 25 November 2014; published 10 June 2015)

RAPID COMMUNICATIONS

PHYSICAL REVIEW B 96, 041105(R) (2017)

Controlling Feynman diagrammatic expansions: Physical nature of the pseudogap in the two-dimensional Hubbard model

Wei Wu,[1,2] Michel Ferrero,[1,2] Antoine Georges,[2,1,3] and Evgeny Kozik[4]

See Alessandro Toschi's talk at workshop this afternoon

From the mean-field picture… … to fluctuations

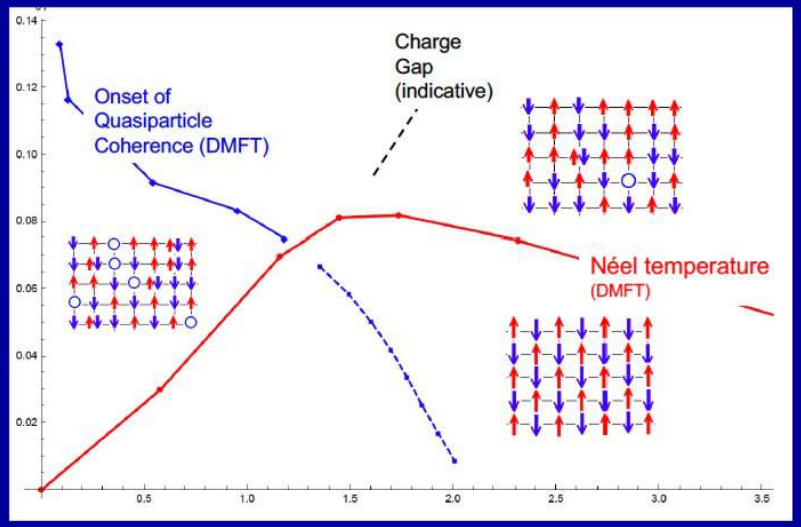

Courtesy T.Schäfer

See also recent work using diagMC/CDET
F.Simkovic et al.

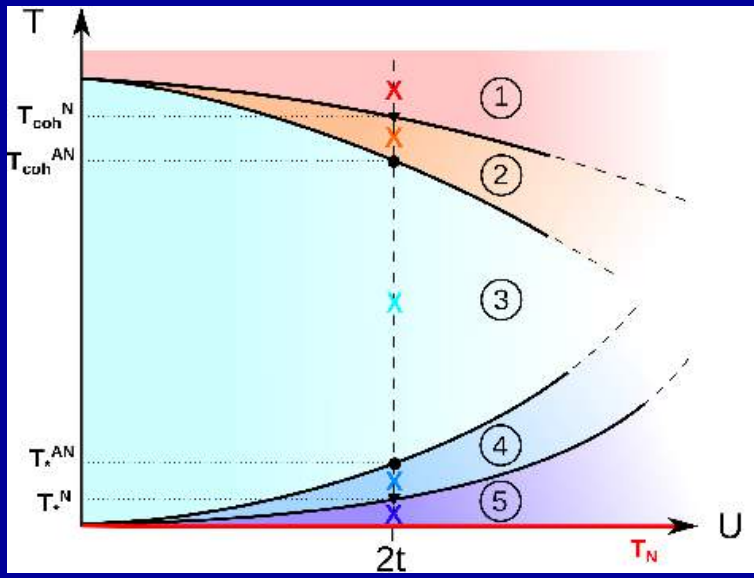

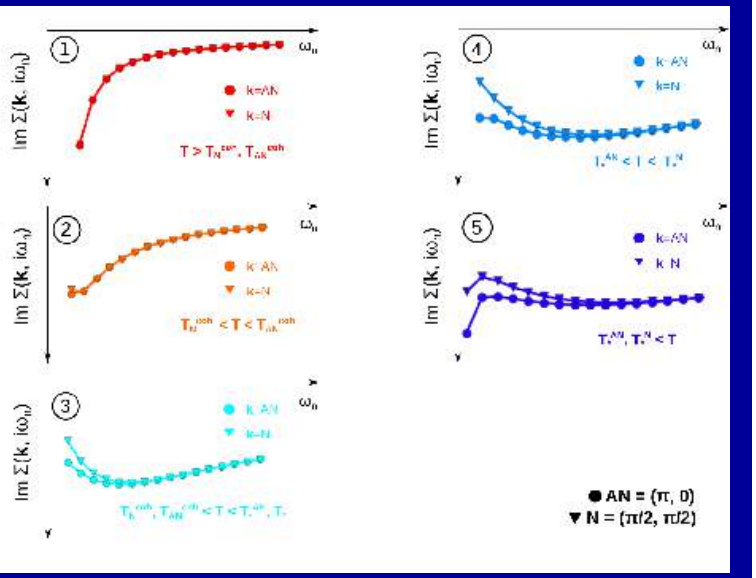

The three main routes beyond DMFT

- Cluster Embedding Methods: cDMFT, DCA…

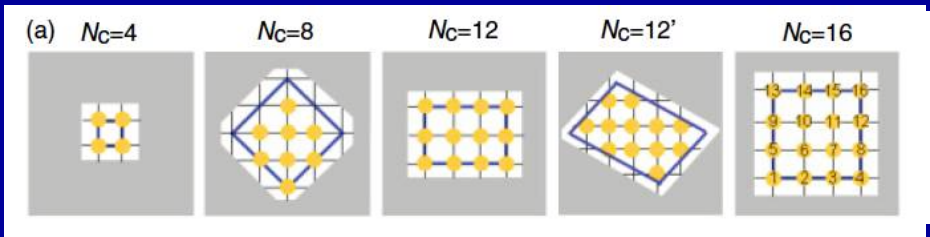

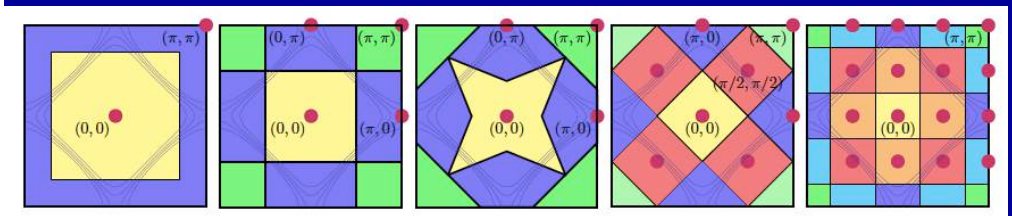

- Expansions involving higher-order correlator/vertex functions: DΓA, TRILEX, dual Fermions/Bosons, etc…
- Using DMFT as a booster for diagrammatice Monte Carlo, or fRG etc..,

As we flow down from high energy to lower energy, range of spatial correlations will grow and 1-site DMFT may become increasingly inaccurate

Starting from:
- High-temperature /
- High-energy /
- High-doping level /
- Large frustration t'/t, etc.

All these can be viewed as control parameters
~ range of spatial correlations

DMFT is a compass to orient oursleves when flowing down in energy

cf. A.G Ann. Phys. 523, 672 (2011)
arXiv:1112.5212

Following the flow to low energy…

Atomic configurations:
Intra-shell interactions+crystal fields

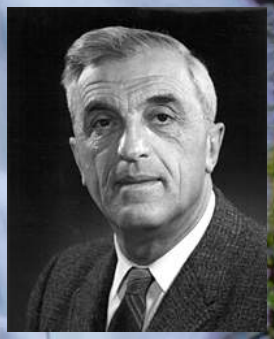

Insulators:
Kugel-Khomskii
Low-energy models
Magnons, Orbitons etc.

Metals
Fermi liquids
Quasiparticles
Collective modes

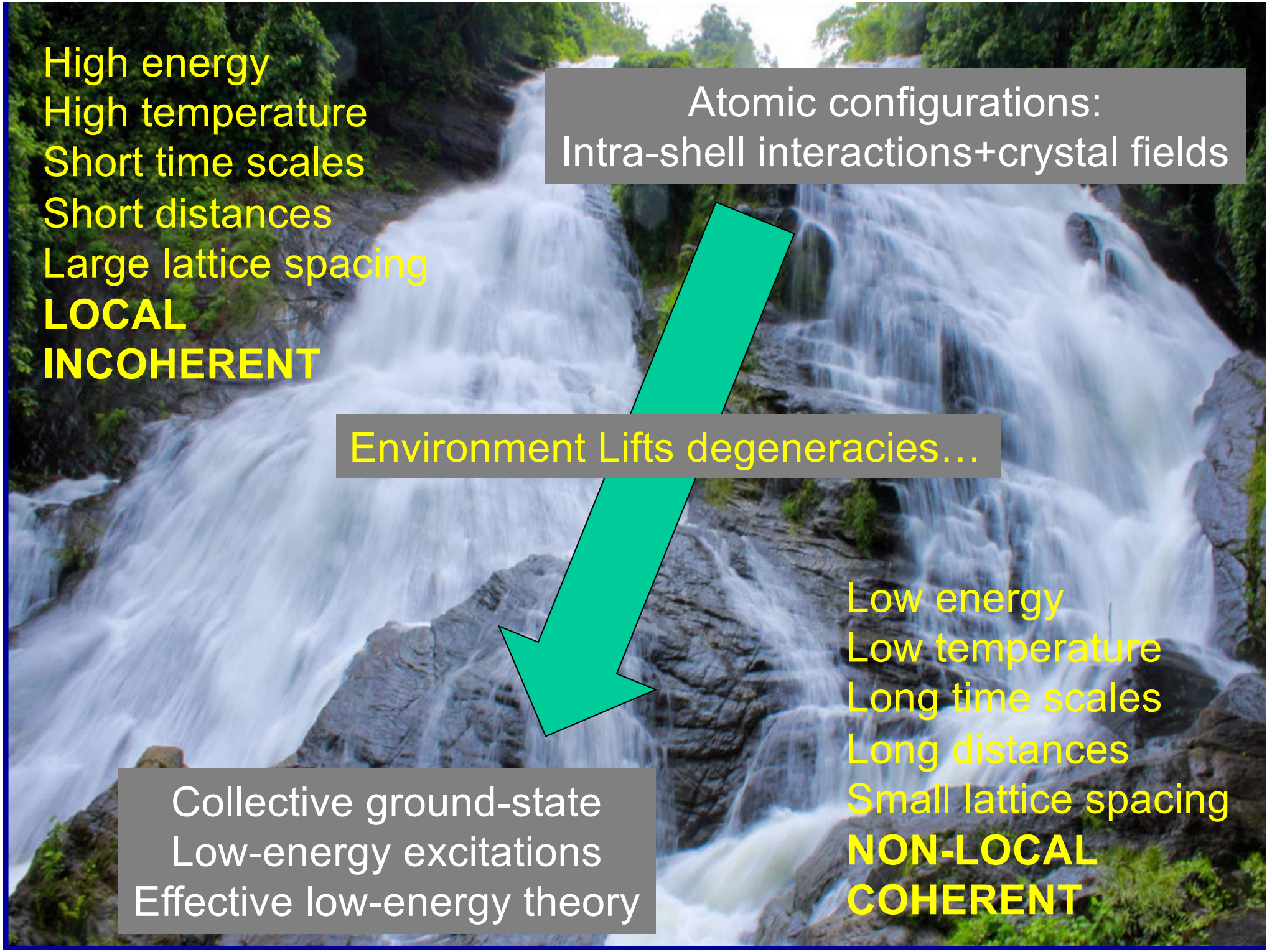
High energy
High temperature
Short time scales
Short distances
Large lattice spacing
LOCAL
INCOHERENT
Atomic configurations:
Intra-shell interactions+crystal fields
Environment Lifts degeneracies…
Low energy
Low temperature
Long time scales
Long distances
Small lattice spacing
NON-LOCAL
COHERENT
Collective ground-state
Low-energy excitations
Effective low-energy theory

This is very much how we think about materials
In DMFT:
Start from local atomic configurations
and follow the flow down into collective behaviour
Initially, spatial correlations are short-range
At lower energy, spatial correlations build up
→ Cluster extensions of DMFT

Atomic configurations:
Intra-shell interactions+crystal fields

?

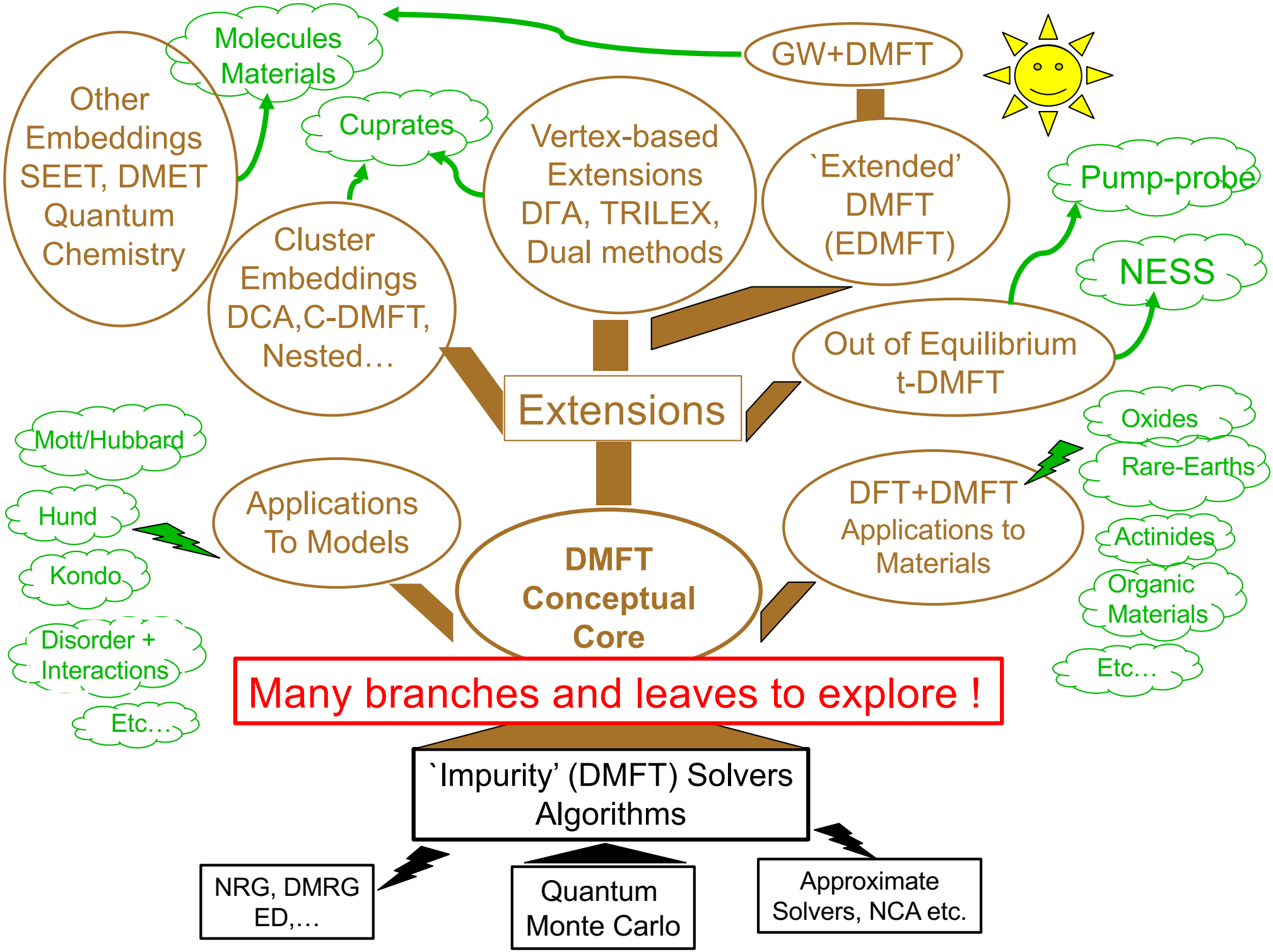
Molecules
Materials
GW+DMFT
Other
Embeddings
SEET, DMET
Quantum
Chemistry
Cuprates
Vertex-based
Extensions
DΓA, TRILEX,
Dual methods
`Extended'
DMFT
(EDMFT)
Pump-probe
NESS
Cluster
Embeddings
DCA,C-DMFT,
Nested…
Out of Equilibrium
t-DMFT
Extensions
Mott/Hubbard
Hund
Kondo
Disorder +
Interactions
Etc…
Applications
To Models
DMFT
Conceptual
Core
DFT+DMFT
Applications to
Materials
Oxides
Rare-Earths
Actinides
Organic
Materials
Etc…
Many branches and leaves to explore !
`Impurity' (DMFT) Solvers
Algorithms
NRG, DMRG
ED,…
Quantum
Monte Carlo
Approximate
Solvers, NCA etc.